EXPERIMENTAL INVESTIGATIONS ON WELDING AND CORROSION BEHAVIOR OF LOW NICKEL AUSTENITIC AND SUPERFERRITIC STAINLESS STEELS

Thesis Submitted for the Award of the Degree of

DOCTOR OF PHILOSOPHY

in

Mechanical Engineering

By

Prashant Kumar Pandey

Registration Number: 41700244

Supervised By

Dr. Mahipal

(Associate Professor)

Mechanical Engineering

Lovely Professional University

Co-Supervised By

Dr. Rajeev Rathi

(Assistant Professor Grade-I)

Mechanical Engineering

NIT, Kurukshetra, Haryana

Dr. Jagesvar Verma

(Assistant Professor)

Mechanical and Manufacturing Engineering

NIAMT, Ranchi, Jharkhand

LOVELY PROFESSIONAL UNIVERSITY, PUNJAB

2024

DECLARATION

I, hereby declare that the presented work in the thesis entitled "**Experimental Investigations on Welding and Corrosion Behavior of Low Nickel Austenitic and Superferritic Stainless Steels**" in fulfillment of my degree of **Doctor of Philosophy (Ph.D)** is the outcome of research work carried out by me under the supervision of Dr. Mahipal (17711), working as Associate Professor, in the School of Mechanical Engineering of Lovely Professional University, Punjab, India. In keeping with the general practice of reporting scientific observations, due acknowledgments have been made whenever the work described here has been based on the findings of other investigators. This work has not been submitted in part or full to any other University or Institute for the award of any degree.

Prashant Kumar Pandey

Registration No.: 41700244

School of Mechanical Engineering

Lovely Professional University,

Punjab, India

CERTIFICATE

This is to certify that the work reported in the Ph. D. thesis entitled "**Experimental Investigations on Welding and Corrosion Behavior of Low Nickel Austenitic and Superferritic Stainless Steels**" submitted in fulfillment of the requirement for the reward of the degree of **Doctor of Philosophy (Ph.D.)** in the School of Mechanical Engineering, is a research work carried out by Prashant Kumar Pandey (41700244), is a bonafide record of his/her original work carried out under my supervision and that no part of thesis has been submitted for any other degree, diploma or equivalent course.

(Signature of Supervisor)
Dr. Mahipal
Associate Professor
School of Mechanical Engineering
Lovely Professional University

(Signature of Co-Supervisor)
Dr. Rajeev Rathi
Assistant Professor
Department of Mechanical Engineering
NIT, Kurukshetra

(Signature of Co-Supervisor)
Dr. Jagesvar Verma
Assistant Professor
Department of Mechanical and Manufacturing Engineering
NIAMT, Ranchi

ACKNOWLEDGEMENT

First, I would like to make some sincere remarks about those who supported my research and provided significant assistance from its very beginning, including those who supported it and helped out immensely while the research was in the stages of determining its main subject. This word of acknowledgement is to express my deep sense of gratitude to all those luminaries and unseen hands without their support the completion of this detailed discourse would not have materialized.

I would like to express my deepest gratitude to my supervisors, Dr. Mahipal, Dr. Rajeev Rathi, and Dr. Jagesvar Verma, for their unwavering support, guidance, and mentorship throughout my doctoral journey. Your dedication to my academic and personal growth has been instrumental in the successful completion of this Ph.D. thesis.

With great pleasure, I take this opportunity to express my sincere gratitude to my supervisor Dr. Mahipal, Associate Professor, School of Mechanical Engineering, LPU, Punjab, who has been a constant source of inspiration. Your insightful feedback, constructive criticism, and the countless hours you spent reviewing and refining my work have been invaluable. Your commitment to pushing the boundaries of knowledge and your passion for research has motivated me to strive for excellence in my work.

I am immensely grateful for the guidance and mentorship of Dr. Jagesvar Verma, Assistant Professor, Department of Mechanical and Manufacturing Engineering, NIAMT, Ranchi. Your ability to provide a different perspective and your profound knowledge in the area of materials and metallurgy enriched the depth and breadth of my research. Your patience, encouragement, and unwavering support during the challenging phases of my thesis have been instrumental in my academic growth.

I would like to acknowledge my co-supervisor Dr. Rajeev Rathi, Assistant Professor, Department of Mechanical Engineering, NIT, Kurukshetra, Haryana. I express my gratitude and sincere thanks to his constant support and guidance without which this

research work would not be possible. The spirit and cooperation he gave me during the research were key to achieving the goal.

I would also like to extend my appreciation to the entire School of Mechanical Engineering, Lovely Professional University, Punjab for fostering an intellectually stimulating environment that has nurtured my research endeavors. The collaboration, discussions, and exchange of ideas with fellow researchers have been invaluable in shaping my research.

I sincerely thank Dr. A. P. Patil, Professor, Metallurgical and Materials Engineering Department, VNIT, Nagpur for permitting the use of the corrosion laboratory to perform the various tests.

I am thankful to my family, my mother Mrs. Kamala Pandey, my wife Mrs. Purnima Pandey, my daughter Prisha, and my son Prashiv who stood behind me and gave me much-needed support every step of the way and friends for their unending support, love, and encouragement throughout this journey. Your belief in me has been a constant source of motivation.

This thesis is a testament to the collective effort of many individuals, and I am deeply indebted to each one of you. Thank you for being an integral part of this journey.

Finally, I want to dedicate this thesis to the loving memory of my dear father, the Late Mr. Vikramaditya Pandey. Even though he is no longer physically present with me, his constant encouragement, support, and knowledge still serve as a daily guide for me. Throughout this difficult road of earning a Ph.D., he was my greatest supporter, my inspiration, and my pillar of strength. His sacrifices and unwavering determination instilled in me the qualities of resilience and dedication, pulling me ahead even in the darkest of moments. This thesis demonstrates his long-term influence on who I am today. Thank you for inspiring in me a desire to learn, a thirst for information, and an unyielding commitment to excellence. His memory will be appreciated and remembered for the contributions I make in my field.

ABBREVIATIONS

AC	Alternating Current
ASS	Austenitic Stainless Steel
ASTM	American Society for Testing and Materials
AWS	American Welding Society
BCC	Body-Centered Cubic
BM	Base Metal
CCGTAW	Continuous Current Gas Tungsten Arc Welding
CPP	Cyclic Potentiodynamic Polarization
DC	Direct Current
DCEN	Direct Current Electrode Negative
DLEPR	Double Loop Electrochemical Potentiokinetic Reactivation
DOS	Degree of Sensitization
DSS	Duplex Stainless Steel
EBSD	Electron Backscatter Diffraction
EBW	Electron Beam Welding
EDM	Electric Discharge Machining
EDS	Energy Dispersive Spectroscopy
FCAW	Flux-Cored Arc Welding
FCC	Face Centered Cubic
FSS	Ferritic Stainless Steel
FSW	Friction Stir Welding
GMAW	Gas Metal Arc Welding
GRA	Grey Relational Analysis
GRG	Grey relational Grades
GTAW	Gas Tungsten Arc Welding
HAZ	Heat Affected Zone
HCL	Hydrochloric Acid

IGC	Intergranular Corrosion
LBW	Laser Beam Welding
MCDM	Multi-Criteria Decision Making
MSS	Martensitic Stainless Steel
OCP	Open Circuit Potential
PAW	Plasma Arc Welding
PCGTAW	Pulsed Current Gas Tungsten Arc Welding
PDP	Potentiodynamic Polarization
PHSS	Precipitation Hardening Stainless Steel
PWHT	Post-Weld Heat Treatment
SAW	Submerged Arc Welding
SCC	Stress Corrosion Cracking
SCE	Saturated Calomel Electrode
SEM	Scanning Electron Microscopy
SMAW	Shielded Metal Arc Welding
SS	Stainless Steel
TEM	Transmission electron microscopy
TIG	Tungsten Inert Gas
UTM	Universal testing machine
UTS	Ultimate Tensile Strength
WM	Weld Metal
XRD	X-ray diffraction

ABSTRACT

Stainless steels (SS) have always been the grade that is used the most often for a variety of applications within the industrial sector. The superior resistance to corrosion, excellent mechanical properties at elevated temperatures, and improved weldability of this material make it highly desirable for a wide range of applications. According to the World Stainless Steel Forum and considering the stainless-steel production data till 2020-21, the steel demand is cumulative day by day at the rate of nearly 5% per annum. The data available also indicates that stainless-steel production increased by almost about 15% from 2020 to 2021. This increasing demand needs the production of these steels worldwide. The major production of steel takes place in countries like China, India, Japan, the United States, etc.

Stainless steel is known as an iron-based alloy that primarily contains corrosion-resistant alloying elements such as chromium (Cr) (min approximately 11%). It also delivers better heat resistance properties. The various grades of SS mainly comprise constituents like carbon (not greater than 1.2%), chromium (Cr), nickel (Ni), nitrogen, molybdenum, titanium, silicon, copper, sulfur, and manganese. Cr and Ni are the two elements that make up the majority of these steels. These alloying elements boost the resistance of steels to corrosion while making them endure longer at higher temperatures. Additionally, they enhance a variety of other properties. The precise composition of SS varies depending on the desired properties and applications. The presence of Cr is the distinguishing characteristic between SS and other varieties of steel. It creates a passive oxide layer on the surface, referred to as the "stainless" or "corrosion-resistant" layer, which gives the material exceptional corrosion resistance. Furthermore, Nickel improves SS's corrosion resistance. The incorporation of nickel enhances the material's resistance to pitting, crevice corrosion, and SCC. Nickel strengthens SS alloys, thereby enhancing their mechanical properties. This enhanced durability enables SS to withstand greater loads and impacts without deforming or breaking. This characteristic is crucial for applications requiring complex shapes,

intricate designs, or deep-drawing processes. It aids in maintaining the material's strength and structural integrity at elevated temperatures, hence making it best-suitable for industrial applications where high temperatures are a major question. On the other hand, the challenges associated with the availability of nickel and the fluctuations in its price make it possible for the development of other alternate grades. Once analyze the fluctuations in nickel's price that have happened on the London Metal Exchange over the past five years, it has been identified that 2018 marked the year when prices dipped to their lowest, hovering around USD 10,400 per tonne, only to soar to dazzling heights, nearing USD 48,500 per tonne in the exhilarating first quarter of 2022.

Nickel is mined predominantly in a few countries, and its availability is susceptible to geopolitical and economic factors. The production of low-nickel SS reduces reliance on nickel as a basic material, diversifies the supply chain, and improves the manufacturing stability of SS. It reduces industries' susceptibility to nickel price fluctuations and potential supply disruptions. Nickel mining and extraction processes can have environmental impacts such as deforestation, water contamination, and greenhouse gas emissions. By decreasing the nickel content in SS production, the environmental impact of nickel mining and subsequent processing can be reduced. Low nickel SS aligns with sustainability objectives and promotes a greener approach to SS production. A small percentage of the population is allergic or sensitive to nickel. By producing low-nickel SS or nickel-free alternatives, industries can accommodate individuals with nickel allergies, ensuring that their products are safe and comfortable for a greater number of consumers.

Considering the above facts, consumer preferences and market demands for nickel-reduced or nickel-free SS have increased. Therefore, it becomes desirable to give special attention to developing and using low-nickel SS and hence potentially provide consumers with more affordable stainless-steel products. This can also be especially beneficial for industries such as construction and infrastructure that require significant quantities of this material.

It is crucial to observe that the production of low-nickel SS entails some compromises.

Nickel provides SS with specific advantageous properties, such as corrosion resistance and high-temperature strength. To compensate for the reduced nickel content and preserve desirable properties in low nickel SS, alternative alloying elements or processing techniques are frequently employed. Manufacturers must strike a delicate balance between reducing nickel content and ensuring that the resulting SS fulfills the performance requirements of the intended applications.

Among the available alternatives of low nickel SSs, grades J204 Cu and AISI 444 offer numerous benefits in terms of cost-effectiveness, supply chain stability, environmental sustainability, allergenic considerations, regulatory compliance, and market demand. These stainless-steel grades present an attractive alternative for industries seeking SS solutions with reduced nickel content. Both AISI 444 and J204 Cu exhibit outstanding corrosion resistance. They are resistant to acidic, alkaline, and chloride environments, among others. This makes them suitable for applications in chemical processing, marine, and food processing industries, where corrosion resistance is crucial for long-term durability and dependability. These grades provide fabrication and processing versatility since they are easily formable, weldable, and fabricated using standard methods. This makes them suitable for a vast array of applications in industries such as construction, automotive, manufacturing, and infrastructure.

Considering the suitability of the above SS grades i.e. AISI444 and J204 Cu for various industrial applications and their potential to replace SS grades containing a comparatively high amount of nickel as an alloying element, it may be necessary to join these two distinct grades of SS, either to achieve a joint of similar materials or may be of dissimilar characteristics.

Some applications require specific material properties that cannot be met by a single SS grade and by combining two different grades, it may become possible to create a material that seamlessly blends a perfect harmony of properties, tailored precisely to meet the unique demands of any application. For instance, an application may require high strength and corrosion resistance, which can be achieved by combining two

grades with these respective properties. In certain situations, to enhance compatibility with the operating conditions of a particular application joining of different grades of SS may be required. Depending on the application, various sections of a component may have varying properties. Combining various grades of SS permits the material's performance to be tailored to specific applications. For instance, areas of a component subjected to varying mechanical stresses may require a higher-strength grade, whereas areas exposed to corrosive environments may require a grade with superior corrosion resistance. Above all, while joining different classes of SS for particular applications, it is essential to consider material compatibility, joint design, welding techniques, and potential problems such as galvanic corrosion. Consultation with materials engineers or specialists can aid in the successful implementation of these joints successfully.

To ensure a strong and reliable bond when joining two distinct materials, specific techniques are required. Several methods exist for joining AISI 444 SS and J204 like mechanical fastening, welding, hybrid joining, etc. each with its advantages and disadvantages. Welding is frequently regarded as the superior method for joining various grades of SS since it creates a metallurgical bond between the base materials, resulting in joints that are robust and durable. During welding, the fusion of the materials permits the formation of a continuous and seamless connection. This ensures that the joint retains its integrity and strength even when subjected to significant pressures or stresses. Welding is compatible with a wide variety of SS grades, both similar and dissimilar. It permits the joining of distinct classifications with distinct properties or characteristics. By selecting appropriate welding procedures and infill materials, it is possible to create joints between different grades of SS that are both reliable and effective. Welding permits localized joining, minimizing HAZs and preserving the material properties of the joined SS grades. By controlling the heat input and employing appropriate welding techniques, the risk of compromising the mechanical, corrosion-resistant, or other essential properties of SS can be minimized. For SS alloys, welding can be a cost-effective joining method. It eliminates the requirement for additional fasteners or connectors, thereby reducing material and labor

expenses. Additionally, welded joints typically require less maintenance than other joining methods, resulting in potential long-term cost reductions. Welding provides versatility in terms of the types of connections that can be formed. It can be used to join SS components of various shapes and sizes, allowing for complex structures and assemblies. The selection of the appropriate welding method hinges on factors like the thickness of the SS, the desired weld quality, and the specific demands of the project, with each technique having its own set of advantages and restrictions.

Gag tungsten arc welding (GTAW) is regarded as the preferred method for joining SS due to its many advantages. GTAW offers precise control over the heat input and welding parameters, including the travel speed. This precision enables welders to produce welds of superior quality with minimal distortion. It is especially advantageous when welding thin sections or conducting precise, critical welds. It produces flawless, high-quality welds that are also aesthetically pleasing. The inert gas safeguards the SS joint from atmospheric contamination, ensuring its integrity and resistance to corrosion. GTAW is effective for joining dissimilar metals, such as various grades of SS or SS with other materials such as carbon steels (CS) or nickel alloys. The precise control over heat input and infill metal selection permits the proper fusion of dissimilar materials and the formation of a strong bond. Unlike other welding methods, GTAW does not require the use of flux, thereby reducing the danger of weld contamination and eliminating the need for post-weld cleaning. In addition, GTAW generates minimal spatter, resulting in a spotless welding environment and a decreased need for rework. GTAW is particularly advantageous for thin SS section welding. Its low heat input and precise control make fusion possible without excessive heating or deformation of the base material. In applications where maintaining the structural integrity of thin sections is crucial, this is crucial. It is also suitable for welding in all positions, including horizontal, vertical, overhead, and flat positions. This adaptability enables welders to work on a variety of joint configurations and produce consistent and dependable welds regardless of orientation.

Weld joints of SS must have sufficient strength to withstand the applied loads and

service conditions. The tensile strength, yield strength, and ultimate strength of a weld joint can be ascertained by analyzing its mechanical properties. This information is necessary for evaluating the structural integrity and dependability of welded components. Mechanical properties play a crucial role in the design of structures or equipment containing weld joints made from SS. Understanding the strength, hardness, and ductility of the weld joint enables engineers to determine the necessary dimensions, thickness, and reinforcement to ensure adequate performance under anticipated loading conditions. Stainless steel weld joints may be subjected to tensile, compressive, bending, or torsional stresses, among others. By evaluating the mechanical properties, the weld joint's capacity to withstand these stresses without failure or deformation can be determined. This analysis ensures that the weld joint meets the design requirements and performs well in service. The assessment of mechanical properties is used to estimate the superiority which can have a substantial impact on the mechanical strength and performance of the joint.

Stainless Steel is renowned for its superior corrosion resistance. However, the welding procedure can alter the microstructure and composition of the weld joint, thereby affecting its resistance to corrosion. Examining the corrosion behavior helps assess the susceptibility of the weld joint to various corrosive environments and ensures that it meets the standards for corrosion resistance. The corrosion behavior of SS weld joints is crucial in determining their service life. By analyzing corrosion resistance, the rate of material deterioration takes into account factors like pitting, crevice corrosion, intergranular corrosion, and SCC can be predicted. Analyzing corrosion behavior may lead to identifying factors that may contribute to accelerated corrosion in the weld joint. This information enables estimating the service life of the weld joint and the optimization of welding processes, such as the selection of suitable filler materials, the control of heat input, and post-weld therapies, to reduce corrosion susceptibility and improve the overall performance and durability of the weld joint.

CONTENTS

LIST OF FIGURES

LIST OF TABLES

CHAPTER 1

INTRODUCTION

1.1 Stainless Steels

Numerous global industries and applications have been revolutionized by stainless steel (SS); a remarkable alloy renowned for its extraordinary properties. Its unique combination of corrosion resistance, strength, durability, and aesthetic appeal has made it the preferred material in a variety of industries, from construction and automotive to aerospace and biomedical engineering (Baddoo, 2008). Stainless Steel's versatility and performance make it an intriguing subject of study, compelling researchers and engineers to investigate its fundamental properties and novel applications (Rossi, 2014). Stainless steel is distinguished by its composition, which consists predominantly of iron, chromium (Cr), and other alloying elements. The addition of Cr creates a passive, self-repairable oxide coating on the surface of SS, rendering it highly resistant to corrosion in aggressive environments. This quality makes it ideally suited for applications in which moisture, chemicals, and extreme temperatures are prevalent. In addition, SS's exceptional mechanical strength, combined with its excellent formability and weldability, enables intricate fabrication, thereby facilitating the creation of complex and structurally sound components (Schmitt and Iung, 2018) (Covert and Tuthill, 2000).

The corrosion resistance of SS is one of its most important characteristics. This characteristic is a result of the protective Cr oxide layer that forms on the surface and prevents the underlying metal from interacting with its surroundings (Mandal et al., 2018). Cr is essential for the formation of a passive film on SS, which is responsible for its superior corrosion and wear resistance. A minimum Cr content of 10.5 weight percent is required for this film to form as seen in Figure 1.1. Passive film is not permanent and can be damaged by scratches, dents, or exposure to harsh chemicals. However, it can be repaired by re-exposure to oxygen (Hilbert et al., 2003). Consequently, SS is widely used in the

construction of infrastructure, such as bridges, structures, and pipelines, where its resistance to severe climatic conditions and corrosive elements is of the utmost importance (Kurtis, 2015) (Hasan *et al.*, 2020). In addition, the food and beverage industry relies heavily on SS's hygienic properties, as it inhibits bacterial growth and ensures the safety and integrity of processed products (Goode *et al.*, 2013).

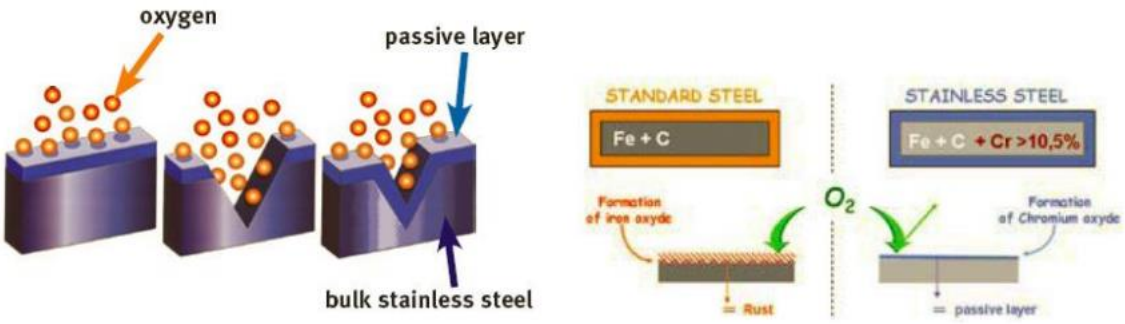

Figure 1.1: Schematic Representations of Stainless Steel (Lo *et al.*, 2009a)

Stainless steel is an indispensable material for the production of automotive components, such as exhaust systems, engine parts, and structural frameworks, due to its high strength and durability. Its capacity to withstand high burdens, resist deformation, and endure fatigue assures dependable and long-lasting performance, which contributes to increased safety and operational efficiency. In addition, the aviation and aerospace industries utilize SS's strength-to-weight ratio in the production of aircraft components, landing gear, and turbine blades, where lightweight, extreme-conditions-resistant materials are essential (Ghassemieh, 2011) (Schmitt and Iung, 2018). The aesthetic appeal and versatility of SS expand its applications. It is widely used in architectural design, interior adornment, and consumer goods due to its lustrous, polished surface and ability to retain its pristine appearance for extended periods. SS offers a streamlined, modern aesthetic that is both immutable and aesthetically pleasing and is utilized in a variety of environments, from iconic landmarks to commonplace domestic items.

Stainless steel is available in a wide range of grades, each with its unique properties. Some grades like duplex stainless steels are more resistant to corrosion, while austenitic stainless steels are stronger and more ductile due to the high composition of nickel and other alloying

elements. Stainless steel can also be finished in a variety of ways, such as polished, brushed, or satin. The choice of SS grade and finish depends on the specific application. For example, SS used in food processing equipment must be highly resistant to corrosion and stain, while SS used in architectural applications may need to be more aesthetically pleasing. The quantity of Cr that is contained in SS is what differentiates it from carbon steel (CS) (Sanders, 2004).

1.2 Brief History of Stainless Steel

In the year 1821, Pierre Berthier carried out revolutionary research, which is credited as being the first recorded instance of realizing the benefits of adding Cr into steel to strengthen the material's resistance to corrosion. The use of this innovation resulted in the creation of an alloy that had 1.5% Cr in it. At first, this alloy was thought to be suitable for use in cutlery; however, it was discovered that its high carbon concentration made it less malleable than other alloys. In June 1872, J.E.T. Woods and J. Clark acquired a British Provisional invention for a weather-resistant iron alloy having 30-35% Cr and 2% tungsten. This event marked the beginning of the development of what we now refer to as SS. In the year 1892, Robert A. Hadfield carried out research on high Cr steels at Sheffield, England, in the United Kingdom. On the other hand, these materials were declared unacceptable because of the high levels of carbon (up to 2%) and Cr (up to 16.74%) that they contained. During the accelerated corrosion experiments that used 50% sulfuric acid, these elements contributed to the formation of corrosion difficulties. During this period, there was a widespread misconception that this test accurately reflected real-world corrosion conditions (“The history of Stainless Steels”, 2011).

In 1912, Harry Brea looked into problems that were occurring with gun barrels, which was the beginning of his key involvement in the invention of the SS. In light of the facts he had obtained, he put up the idea of manufacturing steel with reduced carbon content and greater Cr levels. Brearley cast an alloy on August 20, 1913, that included 0.24% carbon and 12.8% Cr in it. Brearley attempted to etch the alloy to carry out a microstructural investigation,

but he ran into problems since the alloy either would not etch at all or was etched at an extremely sluggish rate (Guiraldenq and Hardouin Duparc, 2017).

During this period, many other researchers were investigating the same kinds of materials with a variety of Cr concentrations. Some people in the United States believe that Elwood Haynes was the first person to find SS and that Brearley is given credit for the invention because he was able to get a patent in the United States, despite the fact that he was unable to do so in England.

The Krupp Iron Works in Germany produced Cr-nickel steel in 1908 specifically for use in the building of yachts. This steel's exact chemical make-up has not been released to the public. Despite this, two of the employees determined that it was martensitic. During this period, Leon Guillet and Albert Portevin, two French scientists, were doing research on materials that had compositions that were very similar to martensitic grades. Even though other researchers from different parts of the globe contributed to the development of SS, Harry Brearley is usually recognized as a pivotal player in the history of the material. This is an important fact to keep in mind. This acknowledgment is mostly due to the efforts he made and the patent he was granted in the United States (Price *et al.*, 2014).

Even though SS has been used for a long time, several issues have not been fully overcome. There is undoubtedly plenty of space for more investigation given the availability of newer generations of SS with high nitrogen concentrations (Lo *et al.*, 2009a) (Backhouse and Baddoo, 2021).

Future research efforts should focus on developing ways to add even more nitrogen to SS ideally using already available processes and reasonably priced equipment (Balachandran *et al.*, 2000). Over a century has passed since the creation of the 200-series alternatives and nearly a century after the widespread usage of austenitic stainless steel (ASS), but fluctuations in the price of nickel still drive the quest for alternatives to nickel in these materials. The more significant impact of nickel replacement is on pitting corrosion resistance, where copper has a varied effect, manganese has a severely negative effect, and nitrogen increases pitting corrosion resistance (Muwila and Papo, 2007). The mechanical and processing characteristics are further impacted by nickel substitution, for instance by

the potent strengthening action of nitrogen and the possible adverse effect of copper alloying on hot workability. The conclusion is that nickel cannot simply be replaced; nevertheless, austenitic grades that are low in nickel or nickel-free can be utilized successfully, although this needs to be carefully considered under certain conditions (Pistorius and Du Toit, n.d.).

1.3 Key Mechanical Properties of Stainless Steel

Several important mechanical properties of SS contribute to its pervasive use in a variety of industries. Here are some of the SS's most important mechanical properties:

Strength: The high strength of SS enables it to withstand large loads and resist deformation. Depending on the grade and thermal treatment of the stainless-steel alloy, the specific strength can vary(Huang *et al.*, 2008).

Hardness: The hardness of SS varies depending on its composition and treatment. It can range in hardness from comparatively flexible to extremely firm, allowing it to satisfy the needs of a variety of applications (Huang *et al.*, 2008).

Ductility: It exhibits excellent ductility, which is the capacity to endure plastic deformation without fracture. This property facilitates fabrication and forming operations such as bending, rolling, and deep drawing (Haftlang *et al.*, 2021) (Obeid *et al.*, 2022)

Toughness: Stainless steel is renowned for its exceptional resilience, which is its capacity to absorb energy and resist fracture under impact or high-stress conditions. This characteristic makes the material suitable for applications requiring resistance to abrupt or repeated loading (Brnic *et al.*, 2011) (Tavares *et al.*, 2007).

Fatigue strength: Stainless steel has a high fatigue strength, which means that it can withstand cyclic loading without failing over time. This property is essential for applications subject to repeated or varying stress, such as structural and mechanical components (Morita *et al.*, 2012).

Creep resistance: Good creep resistance is exhibited by SS, which is the material's ability to resist deformation under protracted exposure to high temperatures and constant stress.

This characteristic is essential for applications operating in high-temperature environments, such as power facilities and exhaust systems (Gardner *et al.*, 2010).

Resistance against corrosion: Although corrosion resistance is predominantly a chemical property, it has a significant impact on the mechanical performance of SS. The corrosion resistance of SS allows it to maintain its mechanical integrity in hostile environments, such as those containing moisture, chemicals, or salinity (Moura *et al.*, 2008) (Peguet *et al.*, 2007).

Wear resistance: Certain stainless-steel alloys have exceptional wear resistance, making them suitable for applications involving abrasion, attrition, and sliding contact. This characteristic guarantees the durability and longevity of components subject to mechanical attrition ("Introduction to Surface Engineering for Corrosion and Wear Resistance", 2020).

Machinability: Depending on its composition and microstructure, SS exhibits varying degrees of machinability. The ease with which SS can be machined, pierced, or cut depends on factors including alloying elements, particle size, and hardness (Vinoth Jebaraj *et al.*, 2017).

Stainless steel is generally regarded as weldable, allowing for the joining of structures and components. However, weldability can vary depending on grade and welding technique (Woo and Kikuchi, 2002) ("Welding metallurgy and weldability of stainless steels", 2005).

The versatility and extensive utility of SS stem from its distinctive mechanical characteristics. Its amalgamation of robustness, malleability, tensile strength, and resistance to corrosion establishes it as a preferred material in sectors where mechanical excellence is paramount.

1.4 Applications of Stainless Steel

Numerous fields and businesses make heavy use of SS. It is widely used in the following applications:

- SS's corrosion resistance, visual appeal, and durability have made it a popular material in the construction and architecture industries. It is used in structural

components, bridges, building facades, handrails, roofing, and cladding (Baddoo, 2008) (Rossi, 2014) (Gardner, 2019).

- Due to its great strength, heat resistance, and corrosion resistance, SS is used in exhaust systems, engine components, fuel tanks, and chassis for automobiles. Additionally, it finds use in the construction of trains and ships (Saha Podder and Bhanja, 2013) (Schmitt and Iung, 2018).
- It is extensively used in the food and beverage industry for a wide variety of applications, including processing machinery, storage tanks, commercial kitchen appliances, and brewing apparatus. It prevents spoilage and keeps ingredients pure thanks to its sterility, cleanliness, and corrosion resistance.
- Its biocompatibility, stabilizability, and corrosion resistance make it ideal for use in medical and pharmaceutical applications such as medical instruments, surgical tools, implants, and dental equipment. Containers, reactors, and pipe systems are all made using it in the pharmaceutical industry (Teodorescu *et al.*, 2019).
- It is used in many different types of power plants, from nuclear to fossil fuel to renewable energy. Due to, and its excellent temperature resistance, corrosion resistance, and strength, it is used in turbines, heat exchangers, pipe systems storage tanks (Chen *et al.*, 2020).
- It is a vital component in both the onshore and offshore oil and gas industries. Its resistance to corrosion in hostile conditions and high temperatures makes it suitable for use in pipelines, storage tanks, valves, and processing equipment (Mourad *et al.*, 2021).
- It is widely used in the aerospace sector for structural elements, exhaust systems, fasteners, and landing gear on aircraft. Aerospace applications rely heavily on their great strength, low weight, and corrosion resistance (Mohanty *et al.*, 2016).
- Stainless steel finds widespread use in the chemical processing, refining, and petrochemical industries. Due to its resistance to corrosion from a broad variety of chemicals and hostile conditions, it is used in reactors, storage tanks, pipelines, and valves.

- Its attractiveness, durability, and low maintenance make it a popular material for usage in a variety of home and consumer goods, including refrigerators, stoves, sinks, faucets, and even ornamental pieces.
- It is used in water and wastewater treatment facilities, as well as desalination plants and water distribution networks. It is appropriate for various uses because of its durability, sanitary qualities, and corrosion resistance (Srikanth *et al.*, 2017).

Stainless steel is widely used; however, these are some of the most important applications. The growth and invention of many fields may be attributed to its use because of its adaptability, strength, corrosion resistance, and aesthetic appeal.

1.5 Classification of Stainless Steel

A variety of characteristics, such as the microstructure, composition, and qualities of the SS, may be used to place the material into one of many distinct groups. SSs are typically classified into five groups as demonstrated in Figure 1.2, based on their structural characteristics: austenitic (with a face-centered cubic structure, FCC), ferritic (featuring a body-centered cubic structure, BCC), duplex (a combination of both austenitic and ferritic structures), martensitic, and precipitation hardening groups.

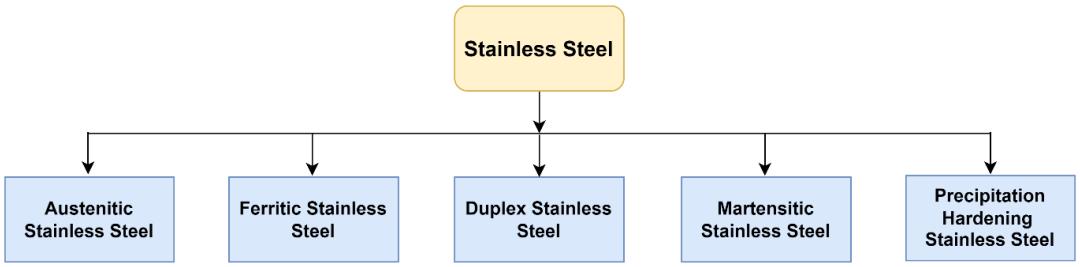

Figure 1.2: Classification of Stainless Steel (Source: Prepared by scholar)

1.5.1 Austenitic Stainless Steel (ASS)

Because of their superior formability, resistance to corrosion, and weldability, these are the most common SS. The austenitic category of SS is typically located within the AISI 300 series designations. These grades contain significant levels of the austenite phase and stabilizing components, primarily nickel and carbon, with additional elements like

manganese and nitrogen. As a result, austenite can persist even at room temperature. This form of SS, like the ferritic grades, is incapable of having its hardness increased by utilizing a heat treatment, regardless of how quickly it is cooled (Borgioli, 2020) (Kim *et al.*, 2004). Because ASS has a crystal structure known as face center cubic (FCC), they are less likely to experience a decrease in their toughness when subjected to low temperatures. Ferritic SS (FSS), on the other hand, has a body-centered cubic (BCC) crystal structure (Park and Kang, 2017)**.** ASSs have a crystal structure that is paramagnetic, meaning that they are weakly attracted to magnets, but not strongly enough to be considered magnetic. The non-magnetic properties of ASS make them ideal for applications where magnetic fields could interfere with the operation of equipment or devices. For example, ASS is often used in medical devices, aircraft, and electronic equipment (Lo *et al.*, 2009b).

The situations in which the materials are most often used include service conditions that are exposed to air corrosion, maritime environments, low temperatures, and high temperatures that exceed 650 degrees Celsius (Kratochvil *et al.*, 2019). Because of this, it is an excellent choice for use in applications that place a premium on corrosion resistance, such as those found in the processing of chemicals and nourishment, in maritime settings, and in medical equipment. In addition, ASS has exceptional mechanical qualities, including high tensile strength and good toughness, even when it is subjected to temperatures that are quite low. It is also famous for having extraordinary formability, which enables it can be readily molded into a variety of complicated shapes and produced into a variety of items (Plaut *et al.*, 2007).

A broad variety of fields, including construction, automobile manufacturing, aerospace engineering, the pharmaceutical industry, and even home appliance manufacturing, make extensive use of ASS. Pipes, fittings, tanks, heat exchangers, valves, cooking utensils, and ornamental components are all frequent places where they may be found being used in the production process. Because of its sanitary features, its simplicity of washing, and its visual appeal, it is also a popular option in business that deals with food and beverages (Talha *et al.*, 2013) (Lee *et al.*, 2009).

1.5.2 Ferritic Stainless Steel (FSS)

Ferritic stainless steel is characterized by its low carbon content and high Cr content (Dong *et al.,* 2022). High levels of Cr give them excellent corrosion resistance. Molybdenum is sometimes added to FSSs to further improve their resistance to chloride SCC. FSSs cannot be hardened by heat treatment, and they are always magnetic. This is because they have a BCC crystal structure, which is the same crystal structure as iron. FSSs are classified as members of the 400 series of SSs, along with Martensitic SSs (MSS) (Yan *et al.,* 2021) (Cashell and Baddoo, 2014).

The most used grades of FSS are:

- AISI 409: This grade has a low Cr content (10-12%), and it is relatively inexpensive. The common application areas include exhaust systems and electrical enclosures.
- AISI 430: This grade has a medium Cr content (16-18%), and it is more corrosion-resistant than AISI 409. It is commonly used in applications such as kitchenware, appliances, and architectural components.
- AISI 446: This grade has a high Cr content (29-32%), and it is the most corrosion-resistant of the FSS. It is commonly used in applications where exposure to harsh chemicals is likely, such as chemical processing plants and marine environments.

It is a versatile and economical material that is used in a wide variety of applications. They are particularly well-suited for applications where corrosion resistance is important, but where heat treatment is not possible or desired (Pandey *et al.,* 2022).

The FSS typically features a crystal structure known as BCC, and its microstructure remains ferritic from ambient temperature up to the point when the material melts. Carbon is often found in the form of Cr carbide precipitates since this structure can only contain very small quantities of carbon in solution (Tadepalli *et al.*, 2019).

The only time this is not the case is when the gamma loop, which can be seen on the iron–Cr equilibrium diagram as shown in Figure 1.3, extends into the area of the specific ferritic alloy that is being discussed. This will result in a change from ferrite to austenite when the material cools from its melting point, and then, if the rate of cooling is slow enough, it will

convert back into ferrite. If the transformation is not carried out at a slow enough rate, martensite will be produced (Venkatraman *et al.*, 2013). This is due to the fact that austenite is capable of holding a significant amount of carbon, and as a result, martensite occurs during rapid cooling since the carbon does not have enough time to come out of solution. Due to the large drop in ductility and toughness that results from the strengthening processes that may occur in FSSs as a result of heat treatment, these strengthening mechanisms are typically not desired (Sahu *et al.*, 2009).

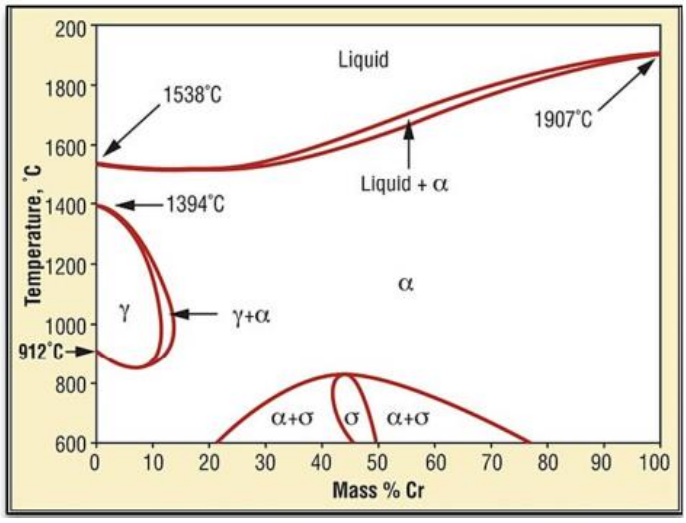

Figure 1.3: Iron-Cr Equilibrium Diagram (Venkatraman *et al.*, 2013)

Ferritic stainless steels are often suited in conditions exposed to temperatures that may reach up to 650 degrees Celsius. However, certain grades are employed inside catalytic convertors that operate at temperatures that are greater than 650 degrees Celsius, and some of the FSS grades that have a higher Cr concentration are used within the maritime sector (Lula, 1989).

1.5.3 Duplex Stainless Steel (DSS)

This grade of steel incorporates the advantageous qualities of austenitic and FSS. It is referred to as a "duplex" because its microstructure consists of austenite and ferrite elements in approximately equal proportions (Akisanya *et al.*, 2012). This unique combination of phases confers exceptional strength, corrosion resistance, and durability in

these steels (Vinoth Jebaraj *et al.*, 2017) (Kahar, 2017). The primary alloying elements in DSS are Cr, Ni, molybdenum (Mo), and sometimes nitrogen (N). Nickel helps to stabilize the austenite phase, which is important for maintaining the dual-phase microstructure. Molybdenum further enhances the corrosion resistance of DSS, especially SCC. Nitrogen can be added to DSS to further increase its strength and toughness.

In addition to the primary alloying elements, sometimes DSS contains elements like manganese (Mn), silicon (Si), and carbon (C). These elements enhance the weldability, machinability, or thermal stability (Francis and Byrne, 2021) (Karlsson, 2012). In duplex grades, the amount of carbon is maintained at a minimum value. The precise composition may differ depending on the material's grade and intended application. DSSs typically have a higher Cr which advances their corrosion resistance. The duplex microstructure offers several significant benefits. First, DSS has greater strength than ASS, making it suitable for applications requiring high mechanical strength. Secondly, the presence of ferrite contributes to making it perfect for marine and offshore applications where chloride-induced corrosion is a concern (Charles, 2008) (Vinoth Jebaraj *et al.*, 2017).

It is uniquely resistant to pitting and crevice corrosion, making it an ideal material for use in harsh environments such as chemical processing plants, oil and gas production facilities, and desalination plants. The addition of nitrogen to DSS further enhances its weldability and formability, making it easier to fabricate complex structures. Additionally, DSS retains its mechanical properties and corrosion resistance over a wide range of temperatures, from cryogenic to elevated temperatures. This makes it a versatile material with a wide range of applications (Verma and Taiwade, 2017).

Here are some specific examples of the advantages of DSS in harsh environments:

- Chemical processing plants: It is used in chemical processing plants to handle corrosive chemicals such as acids, bases, and salts.
- Oil and gas production facilities: This grade is used in oil and gas production facilities to handle corrosive fluids such as hydrocarbons and brines.
- Desalination plants: This is used in desalination plants to handle seawater and brines.

In addition to its excellent corrosion resistance, DSS also offers a number of other advantages, including:

- High strength: Duplex stainless steel is stronger, making it ideal for applications where high loads must be supported.
- Good toughness: It has good toughness, making it resistant to impact damage.
- Excellent weldability: It is easy to weld, making it a versatile material for a variety of applications.

There are various varieties of DSS, including 2205 (UNS S31803/S32205) and 2507 (UNS 32750). These grades contain differing amounts of alloying elements, which affects their specific properties and environmental suitability (Schulz *et al.*, 2014).

1.5.4 Martensitic Stainless Steel (MSS)

A procedure referred to as the martensitic transformation is responsible for the creation of the martensitic microstructure. This change takes place often by quenching it in oil or water. The quick cooling "freezes" the carbon and other constituents in a supersaturated state, and causes a shift in the crystal structure from the initial austenitic or ferritic form to a metastable martensitic structure. This change in structure is caused by the rapid cooling. The steel is improved in both its strength and its hardness as a result of this change (Sohrabi *et al.*, 2020). The percentage of Cr found in these alloys ranges from 11.5% to 18% by weight. They may also have molybdenum added to them, and their carbon content ranges from 0.15 to 1.2 weight percent when compared to that of other SSs (Barbosa and Abud, 2013). The hardenability of the steel and its ability to be heat-treated to improve its strength are both directly attributable to the amount of carbon present in the steel (Derazkola *et al.*, 2021). To improve the martensitic grades' resistance to corrosion while simultaneously lowering their carbon content, the updated grades incorporate nitrogen. These grades, similar to ordinary CSs, can have their hardness and strength increased by undergoing heat treatment in the form of quenching and tempering, respectively (Turnbull and Griffiths, 2003). Knife blades, shafts, and surgical tools are only some of the most prevalent applications.

Because of its exceptional strength, MSS is well suited for use in applications that need

structural integrity and the ability to withstand large loads. The excellent wear resistance of these steels may be attributed, in part, to the material's high hardness. Because of its resistance to abrasive and erosive pressures, it is well-suited for use in applications that involve friction, such as cutting tools, blades, and components that are wear-resistant (Kumar *et al.*, 2012). Due to its martensitic microstructure, MSS has magnetic properties. The magnetic response might be different for each sample due to the distinct composition and heat treatment (Chen *et al.*, 2017). Although it has strong overall corrosion resistance, MSS is not as resistant to corrosion as austenitic or DSS. It is vulnerable to localized corrosion in harsh conditions, especially when chlorides are present, and this vulnerability increases with the severity of the environment (Wang *et al.*, 2021).

1.5.5 Precipitation Hardening Stainless Steels (PHSS)

Heat treatment can be used to strengthen precipitation-hardening SS, also known as PHSS or age-hardening SS. It offers a unique combination of corrosion resistance, high strength, and excellent durability, making it suitable for a variety of applications where these characteristics are essential. The precipitate hardening procedure consists of a series of stages, including solution treatment, quenching, and aging (“Welding metallurgy and weldability of stainless steels”, 2005) (Lippold, 2014). The key advantages provided by this family are relatively high strength, somewhat good corrosion resistance, and an easy construction process. After undergoing a heat treatment at temperatures ranging from 500 to 800 degrees Celsius, these grades demonstrate exceptional strength. Because the temperature can be kept lower, there is less of a risk of the parts becoming warped, which enables them to be utilized for manufacturing high-precision components. The early microstructure of PHSS groups is composed of either austenite or martensite. Before precipitation hardening can take place, the austenitic phases must first undergo heat treatment in order to transform into martensitic phases. The heat aging treatment may induce a process known as precipitation hardening to take place. This happens when martensite is tempered. Aerospace and several other high-technology sectors are typical users of this material (Ravitej *et al.*, 2018).

1.6 Weldability of Stainless Steel

1.6.1 Austenitic Stainless Steel

- Carbide precipitation.
- Excellent toughness and ductility.
- Sensitive to embrittlement. (Mourad *et al.*, 2021) (Verma and Taiwade, 2016)

1.6.2 Ferritic Stainless Steel

- Vulnerable to embrittlement when heated over 1150 degrees Celsius due to grain coarsening.
- Adequate amounts of both toughness and ductility.
- Vulnerable to the development of intergranular corrosion.

1.6.3 Austenitic–Ferritic Duplex Stainless Steel

- Lack of sensitivity to hot cracking.
- Exceptional toughness and favorable ductility throughout 40°C to 275°C.
- Susceptibility to embrittlement caused by the formation of sigma phase when subjected to temperatures ranging from 500 to 900 °C. (Sahu *et al.*, 2009) (Vinoth Jebaraj *et al.*, 2017)

1.6.4 Martensitic Stainless Steel

- Susceptibility to cold cracking, which is influenced by factors such as carbon and hydrogen concentrations, as well as residual stress levels. It is advisable to use preheating and post-heating procedures, particularly when operating below about 400 °C.
- Outstanding tensile strength and hardness.
- Excellent toughness, especially in low carbon grades (Derazkola *et al.*, 2021).

1.7 Welding

Welding is a thermo-mechanical process that involves the localized heating and joining of metals. One of the most important effects of welding is the formation of a heat-affected

zone (HAZ) around the weld. The HAZ is the region of material that is affected by the heat of the weld but does not melt. The HAZ may become softer and more ductile, or it may become harder and more brittle. These changes can lead to a number of problems, such as reduced fatigue strength and increased susceptibility to cracking. Another important effect of welding is the introduction of residual stresses and distortions into the welded component. Residual stresses are stresses that are present in a material even when there is no external load applied. Distortions are changes in the shape of a material. Residual stresses and distortions can be caused by a number of factors, including the heating and cooling of the material during welding, the shrinkage of the weld metal, and the uneven cooling of the welded component. Residual stresses and distortions can lead to a number of problems, such as fatigue failure, cracking, and premature wear.

Arc welding: The electric arc is generated between a welding electrode and the base material. The molten metal from the electrode and the base material then fuse together to form the weld.

a) *Consumable electrode arc welding:* It uses a consumable electrode to melt the metals at the welding site. The consumable electrode is typically made of a metal alloy that is similar to the base material. As the electrode melts, it is deposited into the weld pool.
b) *Non-consumable electrode arc welding*: It uses a non-consumable electrode to melt the metals at the welding site. The non-consumable electrode is typically made of tungsten. As the electrode melts, it is not deposited into the weld pool.

It is important to be aware of the potential impact of welding on the thermo-mechanical behavior of components when designing and fabricating welded structures. By understanding the thermo-mechanical effects of welding, engineers can take steps to mitigate these effects (K Srivastava and Sharma, 2017) (Deyev and Deyev, 2005).

1.7.1 Shielded Metal Arc Welding (SMAW)

Shielded metal arc welding**,** also known as stick welding, is a manual arc welding procedure that uses a consumable electrode coated with a flux to join metals. The flux melts and forms a shielding gas and slag that protects the weld area from atmospheric

contamination. It is also relatively inexpensive and easy to learn, making it a popular choice for many welding applications. The SMAW process begins by striking an arc between the electrode and the workpiece. The arc melts the electrode and the base metal (BM), forming a weld pool. The flux coating on the electrode melts and forms a shielding gas and slag. The weld pool then cools and solidifies, forming a weld bead. The slag is removed from the weld bead after it has cooled. This welding process can be preferred in positions, including flat, horizontal, vertical, and overhead. It can also be used to weld thick or thin materials. The external layer of the electrode, referred to as flux, plays a role in the generation of a protective blanket that safeguards the weld. When the electrode travels along the specimen at its right speed, the metal accumulates in a consistent layer referred to as a bead due to its uniformity.

The electrode that is being used will determine whether the current coming from the Stick welding power source is alternating current (AC) or direct current (DC). The stick welding power source delivers continuous current. Using DC power sources is often necessary to get optimal welding properties. Voltage and current are the metrics that are used to evaluate the power output of a welding circuit. The voltage (in Volts) is determined by the length of the arc that extends between the electrode and the base, with the electrode diameter also playing a role. Current, which is measured in amperes (Amps), is a more practical way of determining the power in a welding circuit. The diameter of the electrode, the size, and thickness of the components that are going to be welded, as well as the location in which the welding is going to take place all play a role in determining the necessary welding amperage. It takes less amperage to power a tiny electrode than it does a big one, and similarly, thinner metals need less current than thicker metals. When welding, it is best to put the item to be welded in a horizontal or level position. However, if you find yourself having to weld in an above or vertical position, it is good to lower the amperage from what you would normally use while welding horizontally (Haider *et al.*, 2019) (Vimal *et al.*, 2015).

1.7.2 Gas Metal Arc Welding (GMAW/MIG/MAG)

This weld technique is practiced for the purpose of metal fusion by introducing the metals to an electric discharge, hence escalating their temperature to the point of melting. The arc is created via the interaction between a consumable, uninterrupted electrode wire and the metal undergoing the welding process. The arc remains protected from ambient contaminants by the application of a shielding gas. An electric discharge is created between the wire and the workpiece, melting the wire, and the molten metal is then transferred to the workpiece to produce the weld (Norrish, 2017).

The essential setup includes:

- A power source
- Wire feeders employed in welding, including constant-speed and voltage-sensing types

The Constant Speed Feeder: It is designed to be used only in conjunction with a constant voltage (CV) power supply. The power source will be connected to this kind of feeder by a control wire. On the conveyor, the wire feed speed (WFS) is fixed. Conveyors feed welding wire from spools to feeders. Control cable electricity drives the feeder motor, which controls the WFS. It delivers electricity to the feeder and allows remote welding voltage adjustment. These cables are usually heavy-duty sheathed and hence insulating and protecting the control cord is essential.

Voltage-Sensing Feeder - Direct current (DC) power sources may either provide CV or constant current (CC), and this product is compatible with both. This kind of feeder is powered by the voltage. The moment the switch is activated, the wire input pace is set by the voltage that is already there. The feeder will adjust the wire's input speed following any variations in voltage. It is not possible to exercise remote control over the voltage using a voltage-sensing feeder (Ibrahim *et al.*, 2012) (Miller Welds, 2018).

1.7.3 Submerged Arc Welding (SAW)

This is a semi-automatic or automatic welding process that uses a continuously fed electrode and a blanket of granular flux to join metal parts. The electrode is a tubular wire

that contains the filler metal and flux. The flux melts and forms a blanket around the weld area, shielding it from atmospheric contamination and providing a protective gas shield. The filler metal from the electrode melts and mixes with the molten BM to form the weld joint. The flux also melts and forms a slag that floats on top of the weld pool and protects it from oxidation.

It is a versatile process that can be used to weld a wide variety of metals in a variety of positions. It is particularly well-suited for welding thick sections of metal, such as those used in pressure vessels, pipelines, and structural members. This is also used to weld a variety of other metal products, such as tanks, boilers, and castings.

It has several advantages, including:

- High deposition rate: It has a very high deposition rate, which means that it can produce a lot of WM in a short amount of time. This makes it a very efficient welding process.
- Deep penetration: It can achieve very deep penetration, which can eliminate the need for joint preparation in some cases.
- Excellent mechanical properties: The welds typically have excellent mechanical properties, which meet or exceed code and X-ray specifications.
- Reduced welder fatigue: Being semi-automatic or automatic welding process, It can help reducing the welder fatigue.

Submerged Arc Welding employs CS in 80 percent of SS applications. The probability of carbide precipitation and distortion will rise if there is a substantial input (Arora *et al.*, 2015) (Chahal and Sharma, 2022). It is a versatile welding process with many advantages. However, it is important to be aware of some aspects of SAW when welding ASS. ASS has a lower thermal conductivity than CS. This means that it conducts heat less well, which can make it more difficult to control the heat input during welding.

1.7.4 Gas Tungsten Arc Welding (TIG/GTAW)

Gas tungsten arc welding, which is also known as tungsten inert gas welding (TIG), is one of the primary welding technologies that has been extensively utilized in industries for the welding of SS, titanium alloy, and other nonferrous metals due to its excellent weld quality

and reduced equipment investment (Kumar *et al.*, 2017). It is commonly used for welding thin sections of SS, aluminum, and other non-ferrous metals that require high-quality welds. Additionally, dissimilar metals may be joined using the GTAW technique, including copper and brass, as well as SS and mild steel. Additional advantages of GTAW welding include the following (Welding, 2003) (Kah *et al.*, 2013):

- Since this method does not include the use of flux, there is no slag produced, which makes it easier for the welder to see the molten weld pool.
- There is no metal transfer across the arc, thus there will be no sparks or scattering. If the material that is being welded does not include any impurities, there will be no need to deal with any dispersion, and there will be no flames created.
- Less smoke and vapor are produced by this method.

It creates an electromagnetic discharge between the electrode and the workpiece using a non-consumable tungsten electrode. A shielding gas, typically argon or helium, is delivered through a flame to safeguard the tungsten electrode from oxidation. The arc generates a high-temperature zone that dissolves both the BM and the manually inserted filler metal (Devakumar and Jabaraj, 2014).

In TIG welding, a non-consumable tungsten electrode with a diameter between 0.5 and 6.5 mm is used, and it is surrounded by a cover of inert gas shielding (such as argon). As a result of the fact that the process uses up a non-consumable electrode, additional filler material is often used. Both the tungsten electrode and the weld pool are protected from the potentially harmful effects of the gases in the surrounding environment by the shielding gas. When welding unalloyed steels, low-alloyed steels, and SSs, argon is the shielding gas that is most typically used. In this welding technique, either AC or direct current may be employed as the source of the power supply. In most cases, this method makes use of a direct current (DC) arc. Since the tungsten electrode has a negative polarity, it becomes the cathode throughout the process, while the workpiece becomes the anode. This kind of polarity is referred to as straight polarity or direct current electrode negative (DCEN). In contrast to other processes, which can only do one or a few types of welding positions, this one is capable of performing all welding positions (O'Brien, 2011) (Siddall, 2019).

The tungsten electrode, which is responsible for bringing welding current to the arc, is held in place by the welding torch, which also serves as a way of transporting shielding gas into the area around the arc. The maximum amount of welding current that may be applied to a torch without causing it to overheat is how torches are rated. One of the electrical terminals of the arc that supplies the heat necessary for welding is made of tungsten, and this electrode serves in this capacity. It is possible to work with or without a filler wire depending on the weld preparation and the thickness of the workpiece that has to be welded. In most cases, the material that is going to be welded will dictate how the shield gas is chosen.

1.7.4.1 Process Dynamics and Variables of GTAW

(a) *The geometry of the weld:* It is used throughout the process of choosing the welding procedure. Several other joints may be used, including butt, lap, fillet, and T-joints. The bevel may take the form of a single V, a double V, or a U. The geometry of the weld has a direct impact on the quality of the weld. Many different positions may be used for welding, including flat, horizontal, vertical, or above, among others. The most typical positions for welding are the horizontal and vertical orientations. If the welding position is tough, then it will be more difficult to get the appropriate weld quality. This will make the situation more complex. The angle at which the workpiece is held with the welding gun is another factor that might affect the shape of the weld bead that is produced.

(b) Shielding Gas (in lit/minute): It performs the function of a protective gas to prevent the pollution of the atmosphere. As a consequence of the fact that the TIG welding process is almost always carried out in the presence of shielding gas, the quality of the welds produced is also improved. The velocity at which the shielding gas flows has the most significant impact on the form of the weld bead, which in turn influences the degree of distortion, the amount of residual stress, the size of the HAZ, and the mechanical characteristics of the material that is being welded.

(c) Welding Speed: It varies depending on the depth of the weld and the breadth of the beads. The maximum amount of weld penetration is reached at a certain welding

speed, and it decreases when the speed of the welding process is changed. When the speed is slowed down, the amount of heat input increases per unit of length, which causes the weld width to expand, and vice versa. Bead form may also be affected by changes in travel speed while operating at a constant voltage and current. When the pace of the welding process is slowed down, the heat input per unit length of the joint goes up, while the penetration and bead width both go up. When the travel speeds are too high, the result is a crowned bard, in addition to an increased propensity to undercut and porosity.

(d) The Material's Thickness: The thickness of the material is an important factor to consider when choosing a process and configuring its settings. The needed amount of heat input is determined by the material thickness, which also controls the pace of cooling. When the thickness is greater, the cooling rate is also greater, which leads to an increase in the HAZ as well as the hardness of the weld metal.

(e) Welding Current: The welding current is one of the most important characteristics, as it has a direct influence on the speed of the welding process, which in turn impacts the degree of penetration and fusion achieved. During the process of producing a weld, the welding circuit is currently being supplied with welding current. If the current is extremely high throughout the welding process, then the depth of fusion or penetration will also be quite high. This is true regardless of the welding speed. If the plates are thinner, then they tend to melt through the metal being connected. It also causes an excessive amount of filler wire to melt, which results in an excessive amount of reinforcement. Therefore, adding more heat to the plates that are being welded causes an increase in the weld-induced distortions, and if the welding current is too low, it may result in a lack of fusion or insufficient penetration.

(f) Volts (V): The term "welding voltage" refers to the difference in electrical potential that exists between the surface of the molten weld pool and the end of the welding wire being used. It is responsible for determining the form of the fusion zone as well as the weld reinforcement. When the arc voltage is optimized, the highest

depth of penetration is achieved, and this has a direct impact on the bead width. Additionally, it has an impact on the cellular structure as well as the achievement or failure of the operation. The welding voltage, much like the welding current, affects the form of the bead and the composition of the weld deposit. A longer arc length and a bead that is proportionally larger, flatter, and with less penetration are the outcomes of an increase in the arc voltage, which leads to a longer arc length. When welding in grooves, even a little increase in the arc voltage causes the weld to bridge gaps between the grooves. An excessively high voltage produces a weld that is concave and has the form of a hat. This kind of weld has poor resistance to cracking and has a propensity to undercut. When the voltage is lowered, the arc length is shortened, which results in increased penetration. An abnormally low voltage will cause the arc to be unstable, which will lead to the formation of a crowned bead, which will have an irregular shape where it hits the plate.

1.7.5 Plasma Arc Welding (PAW)

Plasma arc welding is an arc welding process that is similar to TIG welding but with several key advantages, including higher productivity, deeper penetration, and the ability to weld a wider range of materials. It uses two separate gas fluxes: a plasma gas and a shielding gas. The plasma gas is forced through a narrow orifice in the welding torch, which constricts the arc and increases its temperature. (Sahoo and Tripathy, 2019).

i. Welding using microplasma with a current range of 0.1A to 20A.

ii. Welding using a plasma current that is medium in strength and ranges from 20A to 100A.

iii. Keyhole welding, which is performed over 100A and involves the plasma discharge penetrating the wall thickness.

It employs a high-velocity stream of ionized gas (plasma) to dissolve and join metal components. By passing a gas such as argon or nitrogen through a small orifice and then applying a high voltage between the orifice and the workpiece, plasma is generated. The resulting arc ionizes the gas, producing a highly concentrated plasma discharge that can

reach temperatures of up to 30,000 degrees Celsius. The plasma liquefies the metal components, which are then joined as they cool.

It has several advantages over other welding techniques, including high welding velocities, limited HAZs, and welds of superior quality with minimal distortion. It can also weld a variety of materials, such as SS, aluminum, titanium, and nickel alloys. This is distinguished by its ability to precisely control the size and configuration of the plasma discharge. This allows for precise control over the quantity of heat input into the weld, which is essential when welding thin or fragile parts. By increasing the diameter of the plasma arc, PAW can also be used to weld thicker sections (Wu *et al.*, 2014).

This weld technique also generates very little dust and vapors, making it a safer and more environmentally favorable welding technique. Plasma arc welding does, however, require specialized apparatus and knowledge to install and operate. Its capability to produce high-quality joints makes it an excellent option for a variety of industrial applications (Liu *et al.*, 2016).

1.7.6 Laser Beam Welding (LBW)

It is a welding technique that employs a high-energy laser beam to dissolve and join two or more metal segments. Concentrating the laser beam on the workpiece creates a compact, deep weld pool. As the laser proceeds along the joint, it dissolves the metal and solidifies it behind the beam, producing a weld of exceptional strength and quality. Laser beam welding makes use of several different kinds of lasers, the most common of which are CO_2 lasers, Nd: YAG lasers, and fiber lasers. Depending on the specific use, each kind comes with both benefits and drawbacks that are unique to itself. Either a fixed optic or a moving optic may be used to direct the laser beam onto the workpiece to complete the process (Khan *et al.*, 2012). Welds that need a high level of precision are often performed using fixed lenses, whereas bigger welds are typically performed using moving optics. Adjustments may be made to the laser power, the welding speed, and the beam diameter, to get the best possible results in terms of weld quality and speed. The following is a list of some of the benefits of LBW (Boumerzoug, 2021):

- High levels of precision and accuracy

- Heat input that is kept to a minimum, hence minimizing distortion and HAZs
- High rate of welding, which enables manufacturing in large quantities
- The capability to weld a broad variety of materials, especially dissimilar metals
- Required post-weld finishing is kept to a minimum.

Because of its capacity to generate welds that are superior in both quality and accuracy, LBW has found widespread use across a variety of business sectors. The following is a list of some of the characteristics of LBW as well as its applicability in various industries:

- In the automobile sector, LBW is a technique that is often used for body panels, doors, and roofs.
- It is used in the aerospace sector for the purpose of welding complicated components such as turbine blades and fuel nozzles.
- Welding small, complicated components, such as those found in medical devices and implants, requires the usage of LBW, which is why this process is used in the medical business. Because it offers such exact control and just a small amount of heat input, LBW is well-suited for welding fragile materials like titanium and SS.
- Welding of small components, such as cables and connections, requires the usage of LBW, which is why this technique is used in the electronics sector. The low-base-weight welder is suitable for welding fragile electronic components without causing damage to them due to its great accuracy and small heat input.
- It is also utilized in the manufacturing of jewelry and is perfect for welding tiny, complicated items because of its fine control and little heat input, which makes it possible to avoid harming the pieces being welded (Behm *et al.*, 2014).

1.7.7 Electron Beam Welding (EBW)

Electron beam welding is a kind of welding that involves melting and fusing together two or more pieces of metal by using a beam of electrons that is very energetic. The workpiece is employed as a focal point for the electron beam, which results in the formation of a shallow yet deep weld pool. The metal is melted as the beam travels along the joint, and it then cools and solidifies behind the beam, resulting in a weld that is robust and of excellent

quality (Yunlian *et al.*, 2000). The electron cannon is the device that generates the electron beam, which is made possible by heating a tungsten filament and directing electrons in the direction of the workpiece by use of an electric field. Magnetic lenses may be used to concentrate the beam of electrons, and their settings can be altered to regulate both the beam's width and its intensity. The welding chamber is a vacuum chamber that prevents electrons from clashing with air molecules, which may scatter the beam. This keeps the beam from being scattered and allows for more precise welding.

Some measure applications of EBW include welding reactor components, such as fuel rods and reactor vessels, which need high-quality welds to assure safety and dependability in the nuclear sector. The welding of high-strength steel components, such as chassis frames and suspension systems, is one of the applications for EBW, which is employed in the automobile sector. EBW is a process that is suited for the mass manufacture of vehicles (Węglowski *et al.*, 2016).

1.7.8 Flux-Cored Arc Welding (FCAW)

This method employs the use of a tubular wire electrode that has a flux-filled core. The wire feeder is in charge of delivering the electrode to the workpiece at a predetermined rate, while the welding machine is in charge of supplying the necessary amount of electrical current to generate an arc between the electrode and the workpiece (Alipooramirabad *et al.*, 2017). In addition to supplying extra deoxidizers and other materials that help enhance the quality of the weld, the flux acts as a shielding gas that protects the weld from the contamination that may be caused by the atmosphere. Welding several joint configurations, including butt joints, lap joints, and T-joints, may be accomplished via the use of FCAW. In most cases, cleaning the surfaces that are going to be welded and aligning the workpieces are included in the joint preparation.

Construction, shipbuilding, and the oil and gas sectors are examples of heavy industries that often use FCAW. Due to the fact that the shielding gas is created by the flux itself, rather than requiring the use of an external gas source, it is especially well-suited for welding thick materials as well as for welding in open-air environments. Additionally,

FCAW may be used for welding in confined areas where it may be difficult to operate a conventional gas cylinder, such as in engine compartments (Kannan and Murugan, 2006). Because of its rapid deposition rates and its capacity to weld thick materials, FCAW is often utilized in heavy sectors like construction, shipbuilding, and others.

The following is a list of some of the primary benefits of FCAW:

- A significant amount of precipitation.
- Strong ability to penetrate and fuse.
- It is possible to use it on thick materials.
- Shielding gas produced by the flux itself removes the need for an external gas source.

Having said that, the FCAW does have a few drawbacks, including the following:

- Greater amounts of spatter than those produced by other types of welding procedures.
- Can cause slag buildup that has to be cleaned off after welding.
- The ability to fuse thin materials is only partially available.

1.8 Need of the Study

The necessity for the current study is a direct result of the growing demand for materials that are both cost-effective and resistant to corrosion across several different sectors. The escalating costs of ASSs, which include a substantial amount of nickel, have prompted a major movement toward the discovery and development of alternative materials within the domain of SS alloys. This change has led to tremendous advancements in the field of SS. As an alternative to the typical high-nickel ASSs that have experienced extensive employment across a variety of applications, there has been a growing emphasis placed on the development of low-nickel ASSs and super FSSs. These two types of SSs are intended to be used in place of the usual high-nickel ASSs. This change in emphasis is mostly attributable to economic factors as well as the need to lessen dependence on expensive nickel supplies. Super FSSs have arisen as a compelling alternative, garnering recognition for their distinctive qualities and appropriateness in particular engineering situations. High-

nickel ASSs have traditionally had a prominent position in a variety of industrial applications; nevertheless, super FSSs have evolved as a viable alternative. This increased variety of SS alternatives not only solves concerns about costs but also opens up new possibilities for customized material selection based on particular performance needs, hence boosting the adaptability and sustainability of SS alloys in a variety of sectors. SS is used in a wide range of applications.

There has been very little investigation on the welding and corrosion behavior of low-nickel austenitic and super FSSs, especially when they are welded together. This lack of knowledge of their behavior in welding and corrosive conditions may lead to early failure of the welded structures, which can result in major economic losses and safety problems. Moreover, these failures can occur at a much earlier stage than they otherwise would.

As a result, the purpose of this research is to explore the welding and corrosion behavior of low nickel austenitic and super FSSs, both separately and when they are welded together. SS is often regarded as the most corrosion-resistant metal available. However, the microstructure and material composition of the weld joint might get altered by the welding process, which subsequently impacts its resistance to corrosion. Weld joints' ability to withstand corrosion in a variety of conditions may be evaluated and quality assurance can be achieved by observing their corrosion behavior. The weld joints of low nickel austenitic stainless steel and ferritic stainless steel should be fabricated under the guidelines provided in various international/national standard welding procedure specification like American Welding Society (AWS) standard B2.1-8-009 and B2.1-8-023, those are mainly applicable for welding thin sheets (Aguilar *et al.*, 2013) (Arifin, 2020).

This research will shed light on the microstructural changes that take place during welding, as well as the influence that varying welding conditions have on the material's ability to resist corrosion.

1.9 Organization of the Thesis

The present thesis work is compiled in total five chapters as described below:

Chapter 1 introduces SS and appropriate arc welding processes that are mainly used for joining various grades of SS. A detailed discussion comprises the key mechanical properties of SS, its application areas, a broad categorization of SS, and weldability aspects associated with these categories of SS has been incorporated. The introductory section describing the foundational content is included as well. To conclude this chapter provides a concise explanation of the goals of the current study.

Chapter 2 covers the literature review mainly including the processing of SS as well as the various investigations conducted in recent years related to the conventional welding processes focusing on the effect on microstructure, mechanical properties, weld morphology optimization, and corrosion behavior. This chapter provides a supportive foundation for the selected objectives of the present work.

Chapter 3 outlines the framework and procedures (research methods) that are used to conduct the current research work aiming to provide clarity with the help of a systematic and structured workflow. These research methods are aligned with the research objectives so that they can produce meaningful results.

Chapter 4 exhibits the experimental work that mainly evolves around the development of weld joints of selected material i.e., J204 Cu and AISI 444 with GTAW welding. Topics covered include base material detail, specimen preparation, and experimental investigations. This chapter details the full procedure for experimenting.

Chapter 5 presents an in-depth exploration of the experimental investigation surrounding the welding and corrosion characteristics of low nickel ASS and super FSS is presented, accompanied by an extensive analysis of the findings. The central aim of this research endeavor was to gain a comprehensive understanding of the weldability and corrosion resistance exhibited by these distinct SS grades, while also pinpointing the influential environmental factors affecting their performance. The outcomes of this investigation are meticulously portrayed through several key aspects, including a detailed examination of the microstructural properties within the weld zone, and a thorough scrutiny for any potential defects or imperfections. Furthermore, the impact of various process parameters on the overall weld quality is scrutinized in this chapter, shedding light on the critical

variables that play a pivotal role in achieving optimal welding results. In addition to this, an insightful analysis of the corrosion behavior exhibited by these two SS grades when subjected to a variety of corrosive environments, thereby offering a comprehensive perspective on their durability and suitability in real-world applications. The samples are exposed to various solutions, including acidic, alkaline, and chloride-containing environments. Utilizing techniques such as weight loss analysis, potentiodynamic polarization, and double loop electrochemical potentiokinetic reactivation (DLEPR) test corrosion rates are measured.

Chapter 6 exhibits a summary of the entire study, highlighting the most important findings, contributions to the field, limitations, and prospective future research areas. It provides a concise summary of the experimental methods and the outcomes of the numerous tests and analyses. The emphasis is on highlighting the key findings of the welding and corrosion studies conducted on both varieties of SS. The chapter describes how the study's findings contribute to the existing body of knowledge and fill in knowledge voids regarding the performance of these SS varieties in welding and corrosive environments.

CHAPTER 2

LITERATURE REVIEW

This chapter covers the review of literature which pacts the vital aims of outcomes of contributions of researchers towards TIG for Low Nickel Austenitic and Superferritic Stainless Steels. The published articles, book chapters, conference papers and reports are the main source of review. The unpublished work, magazine, books etc. are excluded for the expediting the review of literature. The prime results from the review helped to define the research gaps.

2.1 Austenitic Stainless Steels

With the use of a hot hardness tester, Kutty et al. (1992) investigated the high-temperature mechanical characteristics of SS 316 end-plug welds of nuclear fuel pins. The hardness of the BM, the weld pool, and the HAZ were all measured as a function of temperature, ranging from the ambient temperature to 1273 K. To determine the activation energy for creep, it was necessary to measure the hardness as a function of the dwell duration from 873 to 1173 degrees Celsius. It was discovered that the activation energy of the weld pool is much greater than that of the BM. The indentation method is well suited for determining the creep qualities of extremely tiny components because of its precise nature (Kutty and Ganguly, 1992).

TIG welding was performed on ASS and nickel-based alloys by Banovic et al. (2001), who then evaluated the influence of various process parameters and the characteristics of the fusion zone material. The authors were able to verify that an increase in filler metal feed rate and arc power leads to an increase in the amount of dilution in the weld metal (WM) (Banovic *et al.*, 2001).

Nassour et al. (2001) investigated the creep performance of two ASS welds AISI 316 L and AISI 347. The SAW was used to develop the weld joints successfully. Creep tests were carried out on welded joints under sustained loads, encompassing stress levels spanning

from 100 to 400 MPa and temperatures within the range of 600 to 700 °C. Norton's law was applied to establish the correlation between stress and the minimum secondary creep rate at a constant temperature. The findings indicated that AISI 347 WM exhibited superior resistance to creep, characterized by lower minimum strain rates and extended rupture lifespans. This enhanced performance is ascribed to the heightened alloy composition of AISI 347 SS, comprising elements such as chromium, nickel, and molybdenum. These alloy constituents facilitate the formation of stable carbides, effectively inhibiting grain boundary sliding and dislocation creep, which are the predominant mechanisms responsible for creep deformation. On the other hand, the ductility value of this weld was much lower than that of the AISI 316L weld. A survey of the microstructure of the WM was carried out both before and after the creep testing, and the results showed that the quantity of delta ferrite available differed (Nassour *et al.*, 2001).

The experimental investigation was conducted to study the effect of adding elements like manganese (Mn) and molybdenum (Mo) on the pitting corrosion resistance of AISI 304 and 316 in chloride-containing environments. The favorable impact of Mo additions was attributed to the creation of Mo insoluble mixtures in the hostile pit environment, which facilitated pit passivation, and the presence of Mo^{6+} inside the passive film, which made it more resistant to breakdown brought on by the assault of aggressive Cl ions. The addition of Mn had the opposite effect, and this was mostly owing to the existence of MnS additions, which served as pitting motivators. The charge of calcium ions (Cl^-) is aggressive enough to attack steel and start the pitting process (Ameer *et al.*, 2004).

Researchers investigated the causes of failure in dissimilar weld joints between two different types of steel: 2.25 Cr-1 Mo FSS and AISI 316. The weld joints were either buttered on the FSS side with Inconel 82, a nickel-based alloy, or not buttered. Using the X-ray diffraction (XRD) method, it became possible to figure out the residual stress profiles that were present throughout these welded connections. According to the findings of this research, the buttering layer made of Inconel-82 that is used in dissimilar weld joints helps lower the residual stresses in the HAZ of FSS. As a result, using the buttering will be

beneficial to prevent or limit failures of dissimilar weld joints that are connected to residual stress (Joseph *et al.*, 2005).

Nage et al. (2006) examined the effects of nitrogen on the microstructure and mechanical characteristics of ASS welds, as well as the function nitrogen plays in avoiding intergranular corrosion. The authors discovered that using nitrogen in welded joints may increase both the mechanical qualities and the resistance to corrosion of the joints (Nage *et al.*, 2006).

The effects of simultaneous wear and corrosion on the tribological behavior, X-ray peak widening, and microstructural alterations of carbon steel (CS) AISI 1045 and AISI 304 samples were explored in research that was carried out by Bateni and colleagues (2006). In the presence of a corrosive environment, the results of the wear test indicated that samples made of CS and SS displayed lower weight losses and lower friction coefficients than samples made of other steel grades. This was the case for both types of steel. This was attributed to the ability of CS and SS to withstand more corrosion. X-ray diffraction examination exposed that increasing the applied load resulted in a constant strain on the worn surfaces of CS samples, which was the onset of fracture and wear. This suggests that the corrosive environment helped to reduce the stress required for wear to initiate. The authors proposed that the synergistic effects of wear and corrosion in CS and SS samples were because of the development of a protective oxide layer on the worn surfaces. This oxide layer acted as a barrier to further wear and corrosion by reducing the contact area between the sliding surfaces and the corrosive environment. The findings of this study suggest that CS and SS are suitable materials for applications where wear and corrosion are likely to occur simultaneously. However, it is important to note that the optimal material selection will depend on the specific conditions of the application (Bateni *et al.*, 2006).

In their study, Dadfar et al. (2007) examined the corrosion characteristics of weldments made from 316L SS through the application of the GTAW technique. The findings demonstrated that the corrosion behavior of the Weld Zone exhibited superior performance compared to that of the BM. The surrounding regions of the WM exhibit diminished

resistance to corrosion and are more susceptible to attack when the steel is subjected to corrosive surroundings (Dadfar *et al.*, 2007).

Ruckert et al. (2007) inspected the impact of silica coating on weld penetration in the GTAW process of AISI 304. The researchers developed and utilized two distinct types of silica coating for this purpose. The study's discoveries illuminate that the diminished tensile strength of the joint may be ascribed to the presence of silica particles in the flux. The utilization of silica in welding processes leads to an increased density of inclusions in the weld metal, resulting in a drop in the tensile strength. Nevertheless, the decrease in penetrations during welding is relatively insignificant when evaluating the comprehensive analysis of the overall process (Rückert *et al.*, 2007).

Minak et al. (2008) studied and found that ASS exhibits exceptional tensile strength and demonstrates remarkable resistance to corrosion in various environments. The composition of this substance typically includes a Cr content ranging from 16 to 18%, which aids the formation of a protective film and enhances its resistance against corrosion. The material exhibits exceptional tensile strength and demonstrates superior resistance to corrosion in a wide range of environments. While SS is known for its corrosion resistance, it is also susceptible to issues such as cracking, decay, and pitting (Ceschini and Minak, 2008).

The experimental results to study the intricacies of weldment microstructure and their response to high-temperature oxidation made of 316L SS using either GTAW welding shows that the microstructure around the fusion border displays directionality, while the interior of the weld shows no such directionality. Over the WM zone of the 316L GTAW weldment, a scale that is much thicker than the one that has developed on the BM can be seen. Doping with cerium led to an increase in the metal's resistance to oxidation, which enabled it to be used more effectively (Samanta *et al.*, 2008).

Ramazan et al. (2009) examined the impact that various process parameters had on the characteristics of ASS of the AISI304 grade that had been spot welded and cold-deformed. This research effort intended to assess and comprehend the influences of weld duration and different welding atmospheres on the resistance spot weldability of AISI304 SS, which had undergone tensile deformation at levels of 5%, 10%, or 20%. The findings of the research

demonstrated that the annealing effects of welding may greatly cut down on the efficiency of cold deformation, which was shown by the findings of the study. As a result, structural designs that use spot welding need to take into consideration the strength losses that occur in cold-deformed SS. Additionally, the grain development that occurred in the HAZ next to the weld nugget was recognized as the foremost origin of the weakening of the weldment. Some of the welded samples that had been bent in tension by between 10% and 20% previous to the welding were found to have cleavage in the shape of a button (Karci *et al.*, 2009).

Shanping Lu and colleagues (2009) examined weld penetration in 304 SS. Helium's greater ionization potential than argon makes it harder to strike an arc in pure helium. Oxygen in the shielding gas also changed weld form. Pure He shielding made the weld bead large and shallow. However, adding a little oxygen narrowed and deepened the weld bead. This was due to Marangoni convection shifting from outward to inside. Marangoni convection is surface tension-driven weld pool flow. The inward Marangoni convection concentrates the heat and improves weld penetration. Weld penetration improved with oxygen in the shielding gas. Under He–50%Ar shielding, the weld depth/width ratio rose from 1:1 to 2:1. This was due to increased heat input and Marangoni convection inward. (Lu *et al.*, 2009).

Kang et al. (2009) devised a novel technique for delivering the shielding gas in the weld zone of 304 ASS weldments in an alternative manner. According to the findings, the degree of welding distortion that was created by the alternative approach (using pure argon and pure helium) was much lower than that which was produced by the standard way (using pure argon and a combination of argon and 67% helium). In addition, the alternative technique maintained the same rate of welding using a gas combination consisting of 33% argon and 67% helium without significantly affecting the depth of penetration in the welds (Kang *et al.*, 2009).

Goyal and his peers (2009) explored the low cycle fatigue behavior of welds made of 316 SS and subsequent results of thermal aging. They found that the changes in microstructure that take place in welds when they are subjected to high temperatures have an effect on the mechanical properties and need to be investigated by aging the welds at high temperatures.

This can only be done by subjecting the welds to high temperatures. A larger stress response was seen by the aged samples in comparison to the samples that had not been aged. The fatigue life of aged samples was lower than that of fresh samples regardless of the temperature or strain amplitude being applied. (Goyal *et al.*, 2009).

In research that Ibrahim and his colleagues (2009) carried out, they looked at the ability to withstand corrosion of a variety of ASS when they were exposed to chloride conditions. According to their results, increasing the proportion of molybdenum or chromium in the alloy composition of SSs led to an increase in the material's resistance against corrosion (Ibrahim *et al.*, 2009).

Kumar et al. (2011) conducted research to determine how the mechanical properties of WM and austenitic steels were affected by the application of a variety of heat sources. They discovered that raising the arc energy led to a drop in the hardness of the WM and the HAZ, while also increasing the breadth of the HAZ. This was in contrast to the fact that increasing the arc energy led to an increase in the width of the HAZ. This was the case regardless of the amount of heat that was introduced. Because of the coarsening of the grain structure, both the WM and the HAZ experience a reduction in their respective hardness. Because of the increased heat input, the weld pool stays at high temperatures for a longer period, which enables the grains to expand to a bigger size. In general, a lesser degree of hardness is related to larger grains. The slower rate of cooling may be related to the increase in the breadth of the HAZ that was observed. When there is a greater amount of heat introduced, it takes the weld pool and the HAZ more time to cool down. This makes it possible for carbon and other alloying elements to diffuse across a broader region, which ultimately results in a HAZ that is more expansive. When welding austenitic steels, one of the most significant factors to take into account is how the heat input will affect the mechanical characteristics of the WM and the HAZ. For instance, if a weld that has a high hardness is desired, a welding method that has a moderate heat input should be used. On the other hand, if a weld that has high ductility is desired, a welding method that has a high heat input may be used. (Kumar and Shahi, 2011).

Mathew and his colleagues (2011) investigated the creep behavior of ASS welds, and their findings led them to the conclusion that the failure of ASS weldments occurred in the weld metal. Both the duplex microstructure of the WM and the transformation of ferrite into brittle intermetallic phases, such as that which occurs during high-temperature aging, have a significant influence on the creep behavior of the weld metal. The aging of the WM is responsible for both of these processes, which take place simultaneously. Even minute changes in the chemical composition and quantity of ferrite present in one sort of electrode compared to another may be able to have a substantial influence on the behavior of the transformation. The composition of the electrode coating that is employed and the welding procedure that is carried out may both be potential contributors to variations in creep strength and ductility. This is true for whatever electrode that you choose to use. It is essential to have an in-depth understanding of the creep response of weldments to guarantee the safe design of high-temperature components and to conduct a life assessment that is based on reality. (Sakthivel *et al.*, 2011).

Dissimilar weldments formed by GTAW between sheets of low-CS and sheets of AISI 201 SS were investigated by the researchers. They discovered that the ER309L and ER316L fillers were appropriate candidates for increasing the pitting corrosion resistance of weld metals and that their performance was equivalent to that of the AISI 201 BM. In addition, they found that the performance of these fillers was comparable to that of the AISI 201 BM. This is because the ER309L filler has a high Cr concentration (24.791 wt%), while the ER316L filler has a mix of Cr (21.347 wt%) and Mo (2 wt%). Both of these factors contribute to the phenomenon. To put it another way, the ER309L and ER316L fillers may be used to generate weldments with pitting corrosion resistance equivalent to that of the AISI 201 BM. This is significant because dissimilar weldments between SS and low-CS are often employed in applications where corrosion resistance is a vital need. For example, the chemical processing industry and the oil and gas sector are two examples of these types of industries. Engineers can design and construct weldments that are up to the task of meeting the rigorous corrosion resistance criteria of these applications by making use of the ER309L or ER316L filler (Chuaiphan and Srijaroenpramong,2012).

In their study, Somrerk et al. (2012) investigated the effect of adding nitrogen to argon shielding gas on the microstructure and corrosion resistance of plasma arc welded joints between AISI 304 and AISI 201 SSs. They found that adding up to 12% (v/v) nitrogen to the shielding gas reduced the amount of delta ferrite in the austenite matrix from 20% to 16% (v/v). This is because nitrogen is a ferrite stabilizer, meaning that it promotes the formation of ferrite. However, at higher nitrogen concentrations, the austenite stabilizing effect of nitrogen becomes more dominant, which leads to a reduction in the amount of delta ferrite. The reduction in the amount of delta ferrite is beneficial for corrosion resistance, as delta ferrite is more susceptible to corrosion than austenite. In addition, the addition of nitrogen to the shielding gas increased the pitting corrosion potential of the WM from 401 to 472 mV (vs. Ag/AgCl). This is because nitrogen forms nitrides with alloying elements such as chromium and molybdenum, which improves the corrosion resistance of the WM (Chandra-ambhorn *et al.*, 2012).

Since Cl^- ions are so much smaller than other ions, they can pass through the passive oxide layer when an electric field is applied. It is possible to avoid repassivation by increasing the migration of Cl^- ions into pits. This helps preserve electrical neutrality and promotes hydrolysis of the corrosion products that are already present in pits, which leads to acidity. The increasing acidity inside pits acts as a catalyst, causing the dissolving rate to speed up, making the process an autocatalytic one (Lot, 2013).

In the GTAW process, the use of argon as a shielding gas can improve the mechanical properties of the welded joint by reducing porosity and improving weld penetration (Anand *et al.*, 2013).

The effect that the precipitation of secondary phases has on the behavior of corrosion of ASSs was studied. The authors examined the microstructural changes that occurred during the development of secondary phases as well as the effects those changes had on the materials' resistance to corrosion. They discussed the procedures of manufacturing, heat treatment, and welding, as well as extended exposure to high temperatures, and how these phases may be generated during such activities. The result supports the spinodal breakdown

that occurs at lower temperatures (350-550 °C) and the sigma phase precipitation that occurs at higher temperatures (700-900 °C) (Chan and Tjong, 2014).

Vasudevan et al. (2017) established that it is possible to create weld joints of high quality by performing autogenous GTAW welding in a single pass with full-depth penetration (DOP) on materials up to 10 mm thick for ASS such as 304L and 316L. In addition, the ideal values for the welding parameters such as speed, current, arc gap, and shielding gas must be used to produce the appropriate depth of penetration (Vasudevan, 2017).

Suman Saha et al. (2018) investigated how using activated flux affected TIG welding of ASS 316L alloy with a thickness of 6 millimeters. According to the findings, the use of TiO2 flux had a dual benefit: it enhanced the level of depth of penetration to its full potential and decreased the bead width by tightening the arc. It was determined that CrO3 flux was the least effective since it did not enhance the depth of penetration nor did it diminish the width of the weld bead (Saha and Das, 2018).

M. Thomas et al. (2018) discussed the categorization of ASS and stated that ASS (ASS) is primarily subdivided into the 300-series and 200-series. The 300 series (primarily 304L and 316L SS) is the most commonly employed ASS variety. Compared to 304L ASS, 316L ASS has greater corrosion resistance and resilience. The austenitic structure is produced by the 300-series alloy by using alloying elements such as nickel (Ni), nitrogen (N), copper (Cu), manganese (Mn), and carbon (C), in addition to the iron-Cr (Fe-Cr) alloy. Nickel (Ni), nitrogen (N), copper (Cu), manganese (Mn), and carbon (C) are examples of these alloying elements. Nickel is an essential ingredient in the process of stabilizing the austenitic structure, which makes metals more ductile, harder, and able to endure corrosive conditions more effectively. Nickel is also an essential ingredient in the production of nickel alloys. When gently heated or cooled, the ASS series will begin to precipitate Cr carbide ($Cr_{23}C_6$) between the temperatures of 450^0 and 900^0 C (Thomas *et al.*, 2018).

Laser welding can produce high-quality welds with minimal distortion and good mechanical properties while maintaining the corrosion resistance of the base material (Wu *et al.*, 2015). An investigation carried out related to the use of FSW for joining 304L ASS showed that FSW can produce high-quality welds with minimal distortion and good

mechanical properties while avoiding the problems associated with conventional fusion welding methods (Wang *et al.*, 2019).

Padmanaban et al. (2019) experimentally investigated a dissimilar joint between 316L ASS and C-22 alloy using GTAW. The results showed that the use of a nickel-based filler metal can improve the mechanical properties of the welded joint (Advaith *et al.*, 2019).

The effects of the presence of copper (Cu) on the microstructure and corrosion resistance of type 204 metastable ASSs with 15% cold-rolling reduction were examined by L. Liu and colleagues (2020). According to the findings of the research, the presence of copper inhibits the martensite transition. In addition, the incorporation of Cu into cold-rolled SSs improves both the material's ability to passivate and its resistance to pitting corrosion (Liu, Liu, *et al.*, 2020).

The microstructure, micro texture, and deformation mechanism of the 316L hybrid laser MIG weld joint were shown in research work carried out by Zhu et al. (2020), and the authors demonstrated that an increase in the amount of δ-ferrite in the material affected the tensile fracture in the fusion zone (Zhu *et al.*, 2020).

Pankaj Biswas et al. (2022) investigated the viability of developing a dissimilar weld joint of Inconel 718 and AISI 204Cu using the friction stir welding (FSW) approach. The effects of varying traverse speeds on the microstructure and mechanical properties of the weldments were explored. Small particles of carbide together with equiaxed grains of recrystallized austenite and ferrite were found to have formed in the nugget zone as a consequence of the experiment's findings, which led to an enhancement in the material's mechanical properties (Raj and Biswas, 2022).

In research that investigated the influence of pulsed GTAW parameters on joints made of 304 ASS, it was discovered that using a high-frequency pulsed current and a low heat input had a positive impact on the quality of the weld. Specifically, this approach reduced the likelihood of sensitization and concurrently enhanced the properties of the welded joints (Raj and Biswas, 2022).

Anoop et al. (2022) experimentally investigated GTAW welded AISI 304L. They used two different filler metals: a nickel-based filler metal and a standard ASS filler metal. The

results showed that the use of a nickel-based filler metal resulted in a welded joint with improved mechanical properties. Nickel-based filler metals are less likely to produce porosity than ASS filler and typically have a higher penetration depth. This is because nickel has a higher thermal conductivity than iron, which allows the heat from the welding arc to penetrate deeper into the BM. Nickel-based filler metals typically produce a finer grain structure. In addition to the improved mechanical properties, the nickel-based filler metal also produced a welded joint with a more uniform microstructure. This is because nickel-based filler metals are less likely to form ferrite in the weld metal. Ferrite is a phase that can be detrimental to corrosion resistance (Kumar *et al.,* 2022).

The influence of copper (Cu) on hot-rolled 301 ASS was investigated by looking at the microstructures and evaluating the electrochemical corrosion resistance aspects of the material. According to the findings, the number of chromium (Cr) carbides steadily reduced as the copper concentration increased. This suggests that the solid solution of copper in stainless steel supports the solid solution of chromium and carbon, which is favorable to the production of passivation films that are rich in chromium. As a direct consequence of this, the 301 stainless steel's corrosion resistance is enhanced (Li *et al.*, 2023).

2.2 Ferritic Stainless Steels

Ramirez-Baltazar et al. (2007) investigated the effect of preheating temperature and filler metal type on the microstructure, fracture toughness, and fatigue crack growth of SS welded joints. It has come to attention that the heterogeneity in mechanical properties of the HAZ and the presence of defects produce dispersion in the crack growth results, causing insufficient correlation. Because the HAZ of the welds made with austenitic filler metal and 12% Cr steel has a dissimilar filler metal, it goes through a thermal cycle in which the cooling rate is accelerated because preheating is not necessary. The pace at which the material is cooling causes the transition process from delta ferrite to austenite and then to martensite to be disrupted, which results in the development of delta ferrite in the HAZ. The delta ferrite that forms in the HAZ is a phase that has poor resistance to the propagation

of fatigue cracks. Despite the material's great hardness, the fracture traveled swiftly across it, which leads one to believe that it is vulnerable to hydrogen's effect of making it more brittle. This conclusion is drawn from the findings of this investigation. The welded joint made of 12% CS with dissimilar filler metal has excellent mechanical properties. In spite of this, it is necessary to exercise control over the quantity of delta ferrite present in the HAZ, as well as the amount of hydrogen present in the consumable and the environment outside (Sánchez-Cabrera *et al.*, 2007).

The microstructure of nearly every type of FSS is composed of a combination of ferrite and carbides. When this microstructure is heated to a high temperature in the HAZ near the fusion zone, an array of metallurgical processes have the potential to take place. In the course of the heating cycle, all deposits, including carbides, are dissolved. During the reheating process, if there is martensite present, it will melt and transform into either ferrite (which will result in the creation of carbide) or austenite. It is common for martensite to form in WM and HAZ in SSs with low and medium Cr content, especially in FSS (Du Toit *et al.*, 2007).

Sathiya et al. (2007) investigated that FSS welds are nearly flawless and fully penetrated. These welds can offer satisfactory performance with reasonable cost savings, based on both technical and economic considerations (Sathiya et al., 2007).

Silva et al. (2008) observed that the HAZ of FSS exhibits substantial grain growth relative to the BM in the partially melted zone. Regardless of the welding energy used, the presence of fine needle-like precipitates is observed known as the Laves phase. Fine-dispersed precipitation is another effect of the weld heat cycle in the HAZ. At the ferrite grain boundaries, chi and sigma phase precipitation have also been found in some locations (Silva *et al.*, 2008).

The effects of aging at temperatures ranging from 560^0C-800^0C on the microstructure, as well as the mechanical and magnetic characteristics, were studied. Before being exposed for 100h, the material did not have the potential to create a sigma phase. At temperatures between 560^0C-800^0C, the material was shown to soften gradually before undergoing a little degree of annealing. At these temperatures, the formation of Mo-rich phases such as

Fe_2Mo and FeMoSi may be seen. The decline in hardness may be traced back to an increase in the average particle size that occurs when the temperature is raised over 650^0C. The accumulation of the Mo-rich phases increases coercive power (Tavares *et al.*, 2008).

Hongyun et al. (2009) used Thermo-calc software, scanning electron microscopy (SEM), and transmission electron microscopy (TEM) to evaluate the influence of isothermal aging on the behavior of precipitation and the mechanical characteristics of Nb-modified FSS. They found that the aging process had an effect. TiN, NbC, and Fe_2Nb were found to have developed in the steel that was under investigation, and the findings of the studies on the coarsening of NbC and Fe2Nb precipitates in Nb-bearing steel during isothermal aging at 800 °C were found to be in excellent agreement with the results calculated using the Thermo-Calc software program. These results were observed in Nb-bearing steel during isothermal aging at 800 °C. The pace at which Fe2Nb coarsens is much quicker than that of NbC. This is because Fe2Nb is a precipitate that is less stable than NbC. In addition, the anticipated values for the average diameters of NbC and Fe2Nb in the aged specimen were in excellent agreement with the findings from the experiments. This was determined by comparing the calculated sizes to the actual sizes of the aged specimen. In addition, the tensile strength of the FSS rose with increasing aging time from 24 hours to 48 hours. The microhardness of the material also increased (Yan *et al.*, 2009a).

Yan et al. (2009) investigated the microstructure, texture, and grain boundary character distribution of Nb+Ti stabilized FSS. In FSS, the creation of TiN, NbC, and Fe_2Nb may occur as a result of the incorporation of alloying elements like as titanium and niobium into the structure. The fiber predominated in the samples' textures after they had been cold rolled, but the fiber was quite prominent in the samples' textures when they were annealed. The features of the grain boundaries are intimately connected to the morphological changes that take place (Yan *et al.*, 2009b).

The consequences of autogenous arc welding techniques on the tensile and impact characteristics of FSS that conformed to the AISI 409M grade were studied by Lakshminarayanan et al. (2009). As the base material, rolled plates with a thickness of 4 millimeters have been used for the preparation of single-pass butt welded connections.

Evaluation and comparison of the tensile and impact characteristics, microhardness, microstructure, and fracture surface morphology of joints produced by continuous current GTAW (CCGTAW), pulsed current GTAW (PCGTAW), and PAW were carried out. When compared to CCG-TAW and PCGTAW joints, it has been shown that PAW joints of FSS exhibit improved tensile and impact capabilities. There are further important factors that contribute to this phenomenon, with the primary one being the decrease in heat input during the welding process. The reduction in heat input is a crucial factor in determining the attributes of the resultant weld. Moreover, an additional pivotal aspect pertains to the reduced particle size seen inside the fusion zone, hence augmenting the overall excellence of the weld. Furthermore, the increased hardness seen in the fusion zone is an additional noteworthy element that has a substantial impact on the result of the welding procedure. When taking into account these components in combination, they jointly contribute to the enhanced quality of the weld (Lakshminarayanan *et al.*, 2009).

Cr deposition occurs at grain boundaries during the welding process, leading to intergranular corrosion in SS. Various methods can be employed to manage intergranular corrosion in SS. These methods include: (1) regulating interstitial elements, (2) controlling the ferritic factor, (3) utilizing stabilization techniques, and (4) managing weld heat input and cooling rate. The welding process has the potential to significantly lower FSS's resistance to corrosion. In addition to intergranular corrosion (IGC), crevice corrosion, and pitting corrosion, these steels are vulnerable to a wide variety of other forms of corrosion as well. These materials are often resistant to SCC since nickel is not present in them; as a result, they offer a viable alternative to ASSs in environments that include chloride. IGC is very sensitive to the welding procedure and the state of the weld after it has been completed, however, crevice and pitting corrosion can often be prevented by selecting the appropriate alloy (Amuda and Mridha, 2011).

FSS is commonly utilized due to its favorable corrosion resistance and lower cost. FSSs possess favorable properties and reduced nickel content, rendering them a viable substitute for Fe-Cr SS in various industrial sectors (Lakshminarayanan and Balasubramanian, 2012) (Lakshminarayanan *et al.*, 2012).

Constant load testing and metallographic inspection were used to estimate the impact of the WM chemistry on the susceptibility of AISI 444 weldment to SCC in hot chloride. This was done to determine how susceptible the weldment is to SCC. To establish fusion zones with distinct chemical compositions, two distinct kinds of filler metal made of ASS (E316L and E309L) were used. The findings of the SCC test indicated that the area most prone to SCC was the interface that separated the fusion zone (FZ) from the HAZ. In addition, the results demonstrated that the weldment made of AISI 444 SS with E309L weld metal (WM) offered the highest level of SSC resistance. It was determined via microstructural investigations that the fractures began in the WM and then spread to the HAZ of the AISI 444. This is where the fracture took place, and it was noted that a significant number of precipitates were present. Additionally, the enhanced resistance to SCC that is found in the weldment of AISI 444, particularly when using E309L WM, may be largely attributed to the presence of a non-continuous delta-ferrite network within its microstructure. Analyses using fractography revealed that the transgranular quasi-cleavage fracture mode was prevalent in the AISI 444 weldment made with E316L weld metal, while the mixed fracture mode was predominant in the AISI 444 weldment made with E309L weld metal. Both modes were found to be present in the AISI 444 weldment (Antunes *et al.*, 2013).

Bitondo et al. (2014) investigated the behavior of corrosion of annealed and unannealed AISI 444 FSS in tap water with and without the addition of specified amounts of chloride ions. In order to analyze the pitting and crevice corrosion susceptibility of annealed and unannealed AISI 444, cyclic potentiodynamic macro and micro polarization measurements (CPP), a salt spray test, SEM, and energy dispersive spectroscopy (EDS) studies were used. According to the findings that were gathered, annealing did not result in an improvement in the resistance to pitting and crevice corrosion. In addition, the micro CPP test reveals a local vulnerability to pitting on materials that have been annealed as well as materials that have not been annealed, but the macro polarization test did not reveal this susceptibility (Bitondo *et al.*, 2014).

In order to prevent hydrogen-induced cracking and embrittlement caused by martensitic microstructures, the welding of 12% Cr steel with comparable filler metal needs a

combination of preheating and post-weld heat treatment (PWHT) operations. This is necessary to keep the welding process from failure. The lack of ductility in the HAZ is the most significant disadvantage associated with FSS welding. This issue is brought on by the development of coarse grain in the HAZ of fusion welds. This area achieves a temperature that is considered to be critical, which is 955 degrees Celsius, which leads to the fast formation of ferrite grains. In addition, despite FSS's low carbon content, rapid cooling may lead to the formation of martensite at grain boundaries and/or low Cr concentration regions along HAZ's grain boundaries. Both of these phenomena can occur in conjunction with one another. Even in modest amounts, the production of martensite in the HAZ brings about a reduction in ductility as well as toughness. Carbide precipitation may expose the steel to intergranular corrosion (Sarkari Khorrami *et al.*, 2014).

The absence of Cr in the weld matrix close to the HAZ is the root cause of intergranular corrosion, which is a challenge for FSS welds. Because of a widespread issue that affects all applications, certain engineering applications could have difficulties that are unrelated to cost considerations, corrosion resistance, corrosion and acid resistance, and the quality of their FSS. These difficulties are brought about by a common issue. The term "sensitization" is often used to refer to this sensitivity. It is generally believed that sensitization is the cause of SCC in particular FSSs, which might ultimately result in failure (Vashishtha *et al.*, 2014).

The combination of nitrogen into a shielding gas that is based on argon during GTAW allows for the development of equiaxed grains, which raise the microhardness as the nitrogen dissolves into the weld pool. The hardness of the WM also greatly rises as a result of microstructure refinement (Devakumar and Jabaraj, 2014).

While welding FSS with welding processes that involve shielding gas, adding nitrogen gas to an argon-based shielding gas may result in a narrow HAZ, an increase in microhardness, and grain refinement with extra equiaxed crystals. This can be accomplished by providing a second layer of shielding. The microstructure of the welded FSS joint may be improved to a great extent, which leads to an improvement in the toughness of the welded joint. It

has also been noticed that the zone of ductile fracture generally occurred quite close to the surface of the weld (Keskitalo *et al.*, 2015).

The development of this non-continuous network of delta-ferrite is a crucial structural characteristic. The aforementioned barrier serves as a severe obstacle, substantially hindering the development of fractures. When SCC takes place, fractures often originate at the fusion zone and endeavor to spread into the material. Nevertheless, the existence of these delta-ferrite islands or fragmented networks serves as an inhibitory factor, impeding the propagation of fractures. As a consequence, the weldment exhibits a notable enhancement in its resistance to SCC, making it a favored option in scenarios where the prevention of corrosion holds utmost importance (Donahue *et al.*, 2017).

Zhang et al. (2018) performed experiments and found that to ensure better fatigue life of the weld joints intermittent welds should be preferred over welds with long continuous weld runs. The selection of a class of weld is very crucial as it directly affects the allowable stress range for fatigue (Zhang *et al.*, 2018).

Being an effective method for joining FSS sheets, laser beam welding (LBW) may also be used to make weld joints that are similar or dissimilar. When the welding speed is increased, the HAZ shrinks, and at the same time, the material's hardness increases to a greater extent. The change in welding speed does result in a larger amount of elongation when the speed is increased (Fu *et al.*, 2019).

The location of the heat sources has an impact on the weld's integrity in terms of its geometry, microstructure, micro-segregation, and mechanical qualities. When the heat source is placed away from the contact, the weld microstructure's homogeneity is reduced, which causes noticeable hardness differences. The production of martensitic structures is caused by the heat source driving the cooling rate at the WM contact (Kang and Luo, 2020).

The sound dissimilar weld joint was formed of the SS grades AISI 316L and 430 with no defects using GTAW. The microstructure reveals an equiaxed and columnar structure. It was discovered that the weld included martensite as well as chromium carbide precipitates. The tensile strength and impact toughness of an ER 316L weld are discovered to be

significantly greater when contrasted with those of an autogenous weld and an ER309L weld (Tembhurkar *et al.*, 2021).

The weld joints of SS grade AISI 430 prepared using GMAW that have been subjected to a greater amount of heat have wider HAZ zones, although this does not have a significant impact on the material's hardness or tensile properties. Nevertheless, the root bend specimen that was subjected to a greater heat input fractured while being tested for bending (Şenol and Çam, 2023).

The whole literature review has been consolidated in Table 2.1 to present a clear and succinct summary of the current research that is pertinent to the chosen subject, establish the backdrop for the thesis, and emphasize the results of each examination. This summary is vital for illustrating the importance of the study, explaining how it adds to the body of information that already exists, and justifying the relevance of the research that was conducted. In addition to this, it will help to pick out the most important ideas, approaches, and methodologies available in the proposed research area.

Table 2.1: Summarized Literature Review

S. No	Year	Author Detail	Material	Domain/ Criteria	Findings	Limitations
1	2004	Ameer et al.	AISI 304 and 316	Corrosion Behavior	Mo addition was attributed to the creation of Mo insoluble mixtures in the hostile pit environment, which facilitated pit passivation, and the presence of Mo^{6+} inside the passive film. The addition of Mn had the opposite effect, and this was mostly owing to the existence of MnS additions, which served as pitting motivators.	This research work didn't cover the effect of other alloying elements on the corrosion behavior of selected stainless-steel grades. In addition, a few other corrosion tests may contribute to better recommendations.
3	2006	Nage et al.	AISI 317L	Welding Aspects	The availability of nitrogen in welded joints may increase both the mechanical properties and the resistance to corrosion.	This study did not comprise the effect of adding availability of nitrogen on hardness and impact behavior of material which may support its advantages.

4	2006	Bateni et al.	AISI 1045 and AISI 304	Corrosion Behavior	In the presence of a corrosive environment, the results of the wear test indicated that samples made of CS and SS displayed lower weight losses and lower friction coefficients than samples made of other steel grades.	The research did not address various corrosion tests like immersion test, PDP test, DLEPR test, etc. that would have resulted in some other critical findings.
5	2007	Dadfar et al.	AISI 316 L-GTAW	Corrosion Behavior	The corrosion behavior of the weld zone exhibited superior performance compared to that of the BM.	The coring phenomenon with an optic microscope has been mentioned in the result section, but its relation with the corrosion behavior is not properly discussed.
6	2007	Ruckert et al.	AISI 304-GTAW	Welding Aspects	The utilization of silica coating in welding processes leads to an increased density of inclusions in the weld metal, resulting in a drop in the tensile strength.	This study lacks a comparative study to explore the effect of silica coating on other mechanical properties.
7	2008	Samanta et al.	AISI 316L-GTAW	Welding Aspects	(1) The microstructure around the fusion line displays directionality, while the interior of the weld shows no such directionality. (2) Doping with cerium led to an increase in the metal's resistance to oxidation.	This study was limited to AISI316L material only and also corrosion testing was not covered.
8	2008	Silva et al.	AISI 444	Welding Aspects	The HAZ of FSS exhibits substantial grain growth relative to the BM in the partially melted zone. Regardless of the welding energy used, the presence of fine needle-like precipitates is observed known as the Laves phase.	This study did not discuss the corrosion aspects of the material.
9	2009	Kang et al.	AISI 304	Welding Aspects	The degree of welding distortion that was created by the alternative approach (using pure argon and pure helium) was much lower than that which was produced by the standard way i.e. a combination of argon and 67% helium.	This research work lacks the study of corrosion behavior.

10	2009	Ibrahim et al.	AISI304 L, 304H, 316H, 304H	Corrosion Behavior	Increasing the proportion of molybdenum or chromium in the alloy composition of SSs led to an increase in the material's resistance against corrosion.	This study lacks the implications of other alloy compositions.
11	2009	Gyeong -Cheol Lee et. al.	AISI 444 and AISI 429L, GMAW	Welding Aspects	The tensile strength of 444 is higher than that of 429L and the test result showed 429L indicating higher tensile strength once it is butt welded with 444.	This study did not include comparative analysis of the joint properties welded with other weld processes.
12	2011	Satya Prakash	AISI 304 & AISI 4140- GTAW	Welding Aspects	The tensile strength of the joint produced by EBW is much higher as compared to the joints formed by GTAW and friction stir welding. The ductility of EBW and GTAW weldments exhibited greater values in comparison to the friction weldment.	This research work lacks the study of corrosion behavior.
13	2012	Chuaip han and Srijaroe npramo ng	Low CS and AISI 201- GTAW	Corrosion Behavior	The ER309L and ER316L fillers were appropriate candidates for increasing the weld strength to endure the pitting corrosion.	This research deficits analyzing the electrochemical corrosion behavior.
14	2012	J.H. Potgiet er et.al.	AISI 444	Corrosion Behavior	444 has better corrosion resistance in chloride environments.	This study did not include the analysis of the corrosion behavior of selected stainless-steel grades in an aggressive corrosion environment.

15	2012	Chandraambhorn et al.	AISI 304 and AISI 201-PAW	Corrosion Behavior	Adding up to 12% nitrogen to the shielding gas reduced the volume of delta ferrite in the austenite matrix. The reduction in the amount of delta ferrite is beneficial for corrosion resistance, as delta ferrite is more susceptible to corrosion than austenite. In addition to this, adding nitrogen to the shielding gas increased the pitting corrosion potential of the WM. This is because nitrogen forms nitrides with alloying elements such as chromium and molybdenum, which improves the corrosion resistance of the WM.	This study did not comprise the effect of adding nitrogen on the mechanical properties of the material
16	2013	Anand et al.	AISI 304 L	Welding Aspects	In the GTAW process, the use of argon as a shielding gas can improve the mechanical properties of the welded joint by reducing porosity and improving weld penetration.	This research work lacks the study of corrosion behavior.
17	2013	Antunes et al.	AISI 444	Welding Aspects	The SCC test results showed that the interface between the fusion zone and the HAZ was the most susceptible region.	This research work lacks an in-depth analysis of the mechanical properties of selected material.
18	2013	Villaret et al.	AISI 444	Welding Aspects	Filler wire with higher Ti content improved the penetration of the weld pool and promoted the columnar to equiaxed grain transition (CET) in the fusion zone.	This study did not explore the effect of alloying elements of filler wire on corrosion behavior.

19	2013	L.K. Singhal	Cr- Mn Stainless Steels (e.g. J204 Cu)	Mechanical properties and corrosion resistance	Cr-Mn stainless steels demonstrate a desirable amalgamation of mechanical properties, including strength, ductility, toughness, formability, weldability, as well as resistance to wear and corrosion. The yield strength of general-purpose Cr-Mn alloy is observed to be 30-40% more compared to that of counterparts in the 300 and 400 series. The ductility of the material under consideration exhibits a level of comparability to that of the 300 series grades, while significantly surpassing the ductility seen in the 400 series grades. Grade J204 has a high degree of similarity to Grade 304 across a diverse range of media.	This study did not focus on weldability aspects.
20	2014	Devakumar and Jabaraj	GTAW- An overview	Welding Aspects	The combination of nitrogen into an argon-based shielding gas during the welding of FSS GTAW allows the development of equiaxed grains, which raise the microhardness as the nitrogen dissolves into the weld pool. The hardness of the WM also greatly rises as a result of microstructure refinement.	This review study only covers certain aspects considering the GTAW process, not others.
21	2014	Bitondo et al.	AISI 444	Corrosion Behavior	Annealing did not result in an improvement in the resistance to pitting and crevice corrosion.	This investigation did not include the effect of annealing on weldability aspects.
22	2014	Anoj kumar et.al.	J204 Cu	Pipe material in the sugar industry	J204Cu is an appropriate material to be used for pipes in sugar industries when consideration, such as cost, is taken into account.	This research did not cover the weldability and corrosion behavior of J204 Cu.
23	2015	Wu et al.	FSS with Cr-21-LW	Welding Aspects	Laser welding can produce high-quality welds with minimal distortion and good mechanical properties while maintaining the corrosion resistance of the base material.	The study skipped over comparing the corrosion resistance of WM and HAZ.

24	2017	Vasudevan et al.	304L and 316L-GTAW	Welding Aspects	It is possible to create weld joints of high quality by performing autogenous GTAW welding in a single pass with full-depth penetration (DOP) on materials up to 10 mm thick for ASS.	This research did not cover analyzing the corrosion behavior.
25	2018	M. Thomas et al.	316L	Welding Aspects	Welds produced with the MP-TIG (multi-pass- TIG) method exhibited the highest resistance, followed by A-TIG welds. Interestingly, for a given stress intensity factor range, A-TIG welds show slower crack growth compared to both the BM and the HAZ. Notably, MP-TIG welds significantly reduced crack growth in the HAZ compared to the BM. Based on these results, the MP-TIG process stands out as a promising method for enhancing a material's resistance to fatigue crack growth.	This study did not include the comparison of selected weld processes on the corrosion behavior of metals.
26	2019	Wang et al.	AISI 304L-FSW	Welding Aspects	FSW can produce high-quality welds with minimal distortion and good mechanical properties while avoiding the problems associated with conventional fusion welding methods.	This research did not cover analyzing the corrosion behavior.
27	2019	Advaith et al.	AISI 316L-GTAW	Welding Aspects	The results showed that the use of a nickel-based filler metal can improve the mechanical properties of the welded joint.	This research did not cover the corrosion behavior.
28	2020	Liu, Liu, et al.	AISI 204 Cu	Corrosion Behavior	The presence of copper inhibits the martensite transition and improves both the material's ability to passivate and its resistance to pitting corrosion.	This study did not investigate the effect of copper on the weldability of selected material.

29	2021	C. Tembhurkar et al.	AISI 316L and 430-GTAW	Welding Aspects	The sound, defect-free dissimilar weld connection was produced from the appropriate grades. The generated microstructure displayed characteristics of an equiaxed and columnar structure. Both martensite and chromium carbide precipitates were seen in the weld. When compared to ER309L and autogenous weld, the tensile strength and impact toughness of an ER 316L weld are found to be much stronger.	This study was limited to the GTAW process.
30	2022	Pankaj Biswas et al.	Inconel 718 and AISI 204Cu-FSW	Welding Aspects	Small particles of carbide together with equiaxed grains of recrystallized austenite and ferrite were found to have formed in the nugget zone.	This research did not cover analyzing the corrosion behavior.
31	2022	Raj and Biswas	AISI 304-GTAW	Welding Aspects	Using a high-frequency pulsed current and a low heat input had a positive impact on the quality of the weld.	This research did not cover analyzing the corrosion behavior.
32	2022	Kumar et al.	AISI 304-GTAW	Welding Aspects	The use of a nickel-based filler metal resulted in a welded joint with improved mechanical properties.	This study did not address corrosion behavior analysis.
33	2022	Yuanyuan et al.	Alloys of low carbon SS with different Cu content	Effect of Cu as an alloying element	Cu-rich clusters first formed with alloying elements such as Ferrum (Fe) and nickel (Ni), and subsequently developed to become precipitates as a result of the rejection of the alloying elements and strengthen tensile strength.	This study did not focus on weldability aspects.
34	2023	Senol et al.	AISI 430-GMAW	Welding Aspects	Joints with increased heat input have broader HAZ regions, but it does not produce any substantial effect on hardness and tensile properties. However, the root bend specimen with higher heat input cracked during the bending test.	This research work did not cover the effect of increased heat input on the corrosion behavior of selected material.

35	2023	Li et al.	AISI 301	Effect of Cu as an alloying element	The solid solution of copper in stainless steel supports the solid solution of chromium and carbon, which promotes chromium-rich passivation coatings. This improves stainless steel's corrosion resistance.	This study did not focus on weldability aspects.

2.3 Comparative Analysis on Low Nickel Copper-Based ASS and FSS

Low Ni, Cu-based ASS J204Cu:

- ✓ Cu addition improves corrosion resistance and stress corrosion cracking resistance.
- ✓ Nitrogen increases strength and pitting resistance.
- ✓ Manganese as austenite former replaces a part of nickel and has a beneficial effect on weldability.
- ✓ Has a higher annealed strength, similar corrosion resistance in a variety of mild corrosive media, and similar formability & weldability in comparison with 304.
- ✓ Applications are in Architecture Building and construction, Transport (Automotive), Consumer durables, Catering and food process, Industry etc.

Superferritic SS 444:

- ✓ A low carbon, dual stabilized, molybdenum-containing FSS with good ductility, toughness, and resistance to sensitization.
- ✓ Reduced interstitial elements such as carbon and nitrogen with the addition of stabilizing elements like molybdenum, titanium, and niobium.
- ✓ Lower cost, higher thermal conductivity, smaller linear expansion, higher corrosion resistance (pitting and crevice), and better resistance to chloride stress-corrosion cracking.
- ✓ It has a pitting resistance equivalent (PRE) to Grade 316, allowing it to be used in more corrosive outdoor environments
- ✓ Due to enhanced corrosion resistance, it is used in hot water tanks, solar water heaters, exhaust system parts, electric kettles, microwave oven elements, as well as automotive trips.

2.4 Research Gap

In response to the growing need for materials that are cost-effective and environment-friendly, low-nickel SSs have attracted a lot of attention due to the beneficial features they possess. Based on a preliminary literature review it appears that there is a significant research gap in the investigation of weldability aspect and corrosion behavior of low nickel SSs. These low nickel SSs have enough potential to replace traditional ASSs since they provide superior mechanical strength, resistance to corrosion, and the capacity to be welded. Among the available grades of low nickel SSs, AISI 444 (FSS grade) is a popular grade and has received much attention in the past few years from researchers. Few studies have directly examined the welding and corrosion behavior of this FSS. An ASS grade J204 Cu is another low nickel SS that must be considered as a replacement for available conventional SSs considering its better mechanical properties. Therefore, it becomes a need in the current situation to study the weldability aspects as well as the long-term endurance of welded joints in corrosive environments of material J204 Cu and to establish a comparative analysis of the behavior of welding and corrosion between these two varieties of low nickel SSs.

The following significant areas, among others, may provide light on this research gap if they were investigated:

Optimization of the welding process: Very little study has been done on the ideal welding process and corresponding welding parameters for joining the above SS grades. To produce welds of high quality, it is necessary to identify the appropriate welding techniques, such as GTAW, GMAW, or LBW, and to determine the ideal welding parameters, such as welding current, welding speed, heat input, and shielding gases. In order to better understand the effect of welding process parameters on the microstructure and mechanical characteristics of welded joints, this gap has to be addressed.

Microstructural characterization: It is necessary to conduct a complete analysis of the microstructural changes that take place in low nickel ASS and super FSS while the welding process is being carried out. It will be easier to estimate the mechanical performance and

susceptibility to corrosion if one understands the formation of different phases, grain boundaries, and intermetallic compounds in the weld zone and HAZ.

Corrosion behavior in challenging environments: Although low nickel ASS and super FSS are well-known for their resistance to corrosion, the behavior of these SSs in challenging environments, such as seawater, acidic solutions, and high-temperature applications, is still relatively unexplored. The process of choosing the materials that are best suited for a given application may be simplified by first gaining an understanding of the corrosion performance of various materials and then locating the key parameters that are most influential on corrosion resistance.

2.5 Objectives of the Research

1. To obtain sound weld joints of low Nickel austenitic and super FSS.
2. To investigate the microstructural and mechanical properties of the weldments.
3. To assess the intergranular and pitting corrosion behavior of the weldments.
4. To study the texture behavior of the weldments and its co-relation with the mechanical properties and corrosion resistance.

2.6 Description of Objectives

- ✓ The first objective involves the preparation of defect-free similar/dissimilar weld joints of low Nickel ASS (ASS) and super FSS. One of the most versatile welding processes i.e., GTAW has been selected to produce the weld joints.
- ✓ The second objective of the proposal will lead the investigation of microstructural behavior and various mechanical properties of the weldment.
- ✓ The third objective mainly emphasizes evaluating the corrosion behavior of the two low Ni SS grades.
- ✓ Further, the texture behavior of the weldments and their correlation with the mechanical properties and corrosion resistance will also be studied.

CHAPTER 3

RESEARCH METHODOLOGY

The proposed research will use a thorough experimental strategy to accomplish the defined objectives and will offer useful insights into the welding and corrosion behavior of low nickel ASS and super FSS. The approach of this research (research methodology) outlined in this work will allow for a systematic and thorough inquiry, eventually contributing to the growth of knowledge in the area of materials science and engineering. This chapter acts as a road map that directs through the whole of the research process, describing how the research questions and objectives are met. The research methodology adopted for the current research work has been subdivided into four different phases as shown in Figure 3.1.

Phase 1 covers the material selection and its further preparation before conducting the welding. With an emphasis on research objectives, appropriate grades of low nickel ASS and super FSS will be chosen based on their chemical composition and mechanical properties. The subsequent experimental results must have a greater chance of being applicable in the real world and hence the materials selected should be such that they may also provide an additional and relevant option for the relevant industrial sectors. The accessibility of the materials and the practicability of the experiments both need to be taken into account. The progression of this research work will be aided significantly by selecting readily available materials that can be handled without facing considerable obstacles. This will also make it simpler to generalize your findings to real-world situations. Once, the appropriate materials i.e. low nickel austenitic and super FSS are selected, the next important step is to perform solution annealing. It is a well-known fact that during the manufacturing of SS, it undergoes processes such as rolling, bending, or machining and, is often subjected to cold working. This may cause the material to have residual stresses, which can then lead to the material distorting or splitting as it is being welded. It is possible to alleviate these residual stresses by the process of solution annealing, which in turn makes

the material more stable and less likely to distort as a result of welding. In this phase, the various aspects related to solution annealing and the related process parameters will also be included. Following the necessary standards and procedures, specimens will be prepared for testing in both the welding and corrosion categories.

Phase 2 deliberates the identification of an appropriate welding process to join the selected SS grades and the development of sound weld joints. Welding is one of the joining techniques that have been invented and used in the past. There are several welding processes available to join SS. It is still a challenging task for researchers to choose an appropriate welding process and its optimal weld parameter. The current study fills this research vacuum by analyzing all conceivable welding processes for ASS and ranking them using the grey relational analysis (GRA) methodology based on the stated criteria. The GRA approach uses the opinions and/or experience of personnel mainly involved in the welding industry as specialists, working in prestigious welding laboratories, and academicians with a strong research background in materials and joining processes to rate the currently available welding techniques. Based on the collective responses received in a significant number, the welding techniques are ranked and then further utilized. After selecting the welding process, separate weld joints will be developed for both materials (similar joints) and then these two materials will be welded together to investigate the sustainability of their weld in terms of mechanical properties and corrosion behavior.

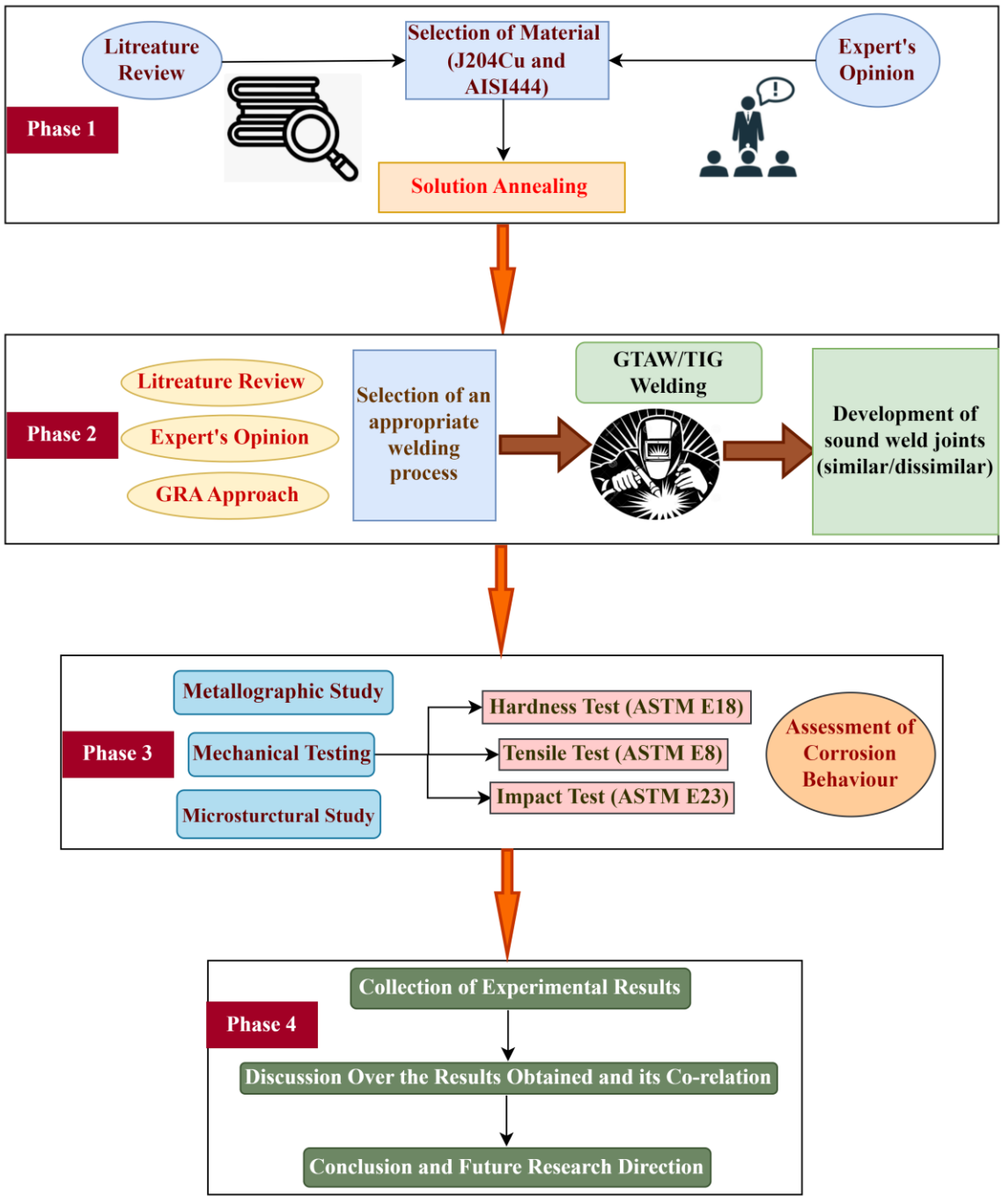

Figure 3.1: Research Methodology

Phase 3 offers a comprehensive metallographic examination, mechanical tests, and an investigation of the microstructural behavior of these two distinctive SS alloys. The purpose of the metallographic research is to get an understanding of the basic characteristics of low nickel ASS and super FSS by understanding the grain structures, crystallography, and phases that are present. To determine their structural integrity and whether or not they are suitable for a variety of applications, the welded joints of these steels will undergo mechanical testing that evaluates their tensile strength, hardness, and other mechanical properties. In addition, an extensive examination of the microstructural behavior will be carried out to get an understanding of how welding affects the characteristics of the material, with a particular emphasis on the changes in grain boundaries and probable flaws. This phase also includes the study to investigate the corrosion behavior of both alloys to get a knowledge of how susceptible they are to different corrosive conditions.

Phase 4 contemplates the experimental findings of systematically identified tests following the international standards succeeded by the results and discussion portion of this research work. These findings will focus on the microstructural analysis, mechanical characteristics, and the corrosion performance of the materials in a variety of corrosive situations, offering insights into their long-term durability and whether or not they are suitable for certain applications. The consequences of the results obtained and significant insights into the selected research work have been represented in the conclusion with suggestions for future research work in the area of emerging SS grades.

CHAPTER 4

EXPERIMENTAL WORK

To begin with, the experimental work of two distinct low nickel SS grades i.e., an ASS grade J204 Cu and a super ferritic stainless steel AISI 444 were procured in the form of flat plates with a thickness of 3 mm. The samples of needed dimensions for further tests were wire-cut using electric discharge machining (EDM). After the plates had been cleaned, the solution annealing procedure was carried out. Following the solution annealing process, the chemical compositions of both the BM were studied, as well as the microstructure. After that, the samples were joined together using a single pass of GTAW with the assistance of filler ER308L. Electric discharge machining was again used to cut the samples for examining microstructure and evaluating mechanical properties such as hardness, tensile strength, and impact testing. The weight loss test was carried out so that we could examine the behavior of weldments of both materials when exposed to general corrosion. To determine the degree of sensitization (DOS), a test known as the double loop electrochemical potentiokinetic reactivation test (DLEPR) was carried out. In the last step of the process, the welded test samples were put through a potentiodynamic polarization (PDP) test to check for pitting corrosion.

4.1 Selection of Materials

Among the available low nickel SS, J204 Cu and FSS 444 grades have been selected for the proposed research work. These selected grades contain very low Nickel and have better mechanical properties and corrosion resistance as compared to 300 series ASS grades. These materials are collected in the form of sheets of 300 (length) x 300 (width) x 3 (thickness) [mm].

SS J204 Cu is a Cr-magnesium ASS to which 2-4% copper and 0.05-0.25% nitrogen have been added. The addition of copper improves the formability of the alloy. Copper also increases corrosion and SCC resistance in certain media. J204Cu bridges the cost-

performance disparity between the stainless 200 and 300 series. Nitrogen increases SS's resilience and resistance to pitting. As an austenite former, manganese replaces a portion of nickel and improves weldability. J204Cu has a higher annealed strength, comparable corrosion resistance in a variety of mildly corrosive media, and comparable formability. It can be substituted for the type 300 series in a variety of applications where higher strength, greater formability, and lower cost are required. After cold working, alloy 204Cu is mildly brittle, but this can be minimized.

AISI 444 is an FSS commonly used in applications requiring excellent corrosion resistance and high-temperature strength. It contains high concentrations of Cr (approximately 18%) and molybdenum (approximately 1.5-2%) that provide excellent corrosion resistance in a variety of environments, including chloride-rich environments like seawater. It is highly resistant to pitting and crevice corrosion caused by chloride, making it appropriate for marine and coastal applications. Additionally, it is corrosion-resistant in many corrosive and alkaline environments.

Common applications for AISI 444 include marine and coastal environments, effluent treatment facilities, and chemical processing facilities. It is also utilized in applications requiring excellent weldability, formability, and SCC resistance. Common AISI 444 applications include automobile exhaust systems, hot water containers, laundry machines, and kitchen sinks. The chemical compositions of both steels have been identified through spectroscopy i.e. based on automated spectrometer and given in Table 4.1 and Table 4.2.

Table 4.1: Chemical Composition of J204Cu

Element	C	Mn	S	P	Si	Ni	Cr	Cu	N	Fe
Weight %	0.1	8.5	0.01	0.06	0.75	1.5	17	3.5	0.1	Balance

Table 4.2: Chemical Composition of FSS 444

Element	C	Si	Mn	P	S	Mo	Cr	Ni	Ti	Fe
Weight %	0.025	1	1	0.04	0.03	2	18.5	1	0.2	Balance

4.2 Solution Annealing

As received milled metals possess residual stress and some amount of precipitates due to the thermo-mechanical process can be removed by the solution annealing process which also helps to homogenize the microstructure. The process of solution annealing is a kind of heat treatment that consists of heating a metal or alloy to a high temperature for an adequate period of time in order to dissolve any carbides or other precipitates into the solid solution. After that, the metal or alloy undergoes a quick quenching process to freeze the carbides in the solid solution. Depending on the kind of steel being worked with, the solution annealing process is normally carried out at temperatures ranging from 900 to 1100 degrees Celsius (1652 to 2012 degrees Fahrenheit). The length of time spent at the temperature of solution annealing is determined not only by the kind of steel being used but also by the thickness of the material.

The steel may be improved in many ways by undergoing solution annealing, including the following:

a) The quantity of carbon in the steel that is bound up in carbides may be reduced by solution annealing, which results in improved formability. Because of this, the steel becomes more ductile and is simpler to shape.
b) Solution annealing is a process that may increase the resistance of steel to corrosion when exposed to certain acids, such as sulfuric acid and nitric acid. This is because Cr carbides, which are more prone to corrosion than austenite, are dissolved during the solution annealing process. (Šmíd *et al.*, 2021) (Kashiwar *et al.*, 2012).

Here, both the materials, J204 Cu and FSS 444 were heated to a temperature of 1050˚C and 850˚C in a furnace as shown in Figure 4.1, for a time duration of 1 hour and 2 hours and then allowed to be cooled at room temperature to get homogenized structures (Badji *et al.*, 2008) (Gholami *et al.*, 2015) (Tan *et al.*, 2009) (Kim *et al.*, 2023). The specimens needed to perform solution annealing were cut from the plates by an EDM.

Figure 4.1: Furnace used for Solution Annealing

4.3 Selection of Welding Process

Due to SS's exceptional resistance to corrosion, durability, and aesthetic appeal, welding is an essential activity in a variety of sectors, from manufacturing to construction. SS is used in a wide range of applications. When working with a material that is as adaptable as SS, choosing the appropriate welding procedure is of the utmost significance if one wants to achieve a weld that is robust, clean, and accurate. The choice of welding method is determined by several criteria, including the grade of SS being welded, the design of the joint being welded, the location of the weld, and the required mechanical properties of the finished weld (Balasubramanian *et al.*, 2009) (Omar and Soltan, 2020). The decision of which welding technique to use ultimately has to be determined by striking a healthy balance between the quality of the weld that is sought, the level of efficiency that is required, and the requirements that are unique to the application. The procedure that is used should produce a weld that is not only structurally sound but also visually perfect and one that is up to the high requirements that are established by the excellent qualities of SS.

Among the two selected grades of SS, AISI 444 has already been the subject of the most research, incorporating welding and its other characteristics. Due to the adaptability of AISI 444 to be welded with a variety of fusion welding processes, such as GMAW, GTAW, SMAW, etc., it is simple to choose an appropriate welding process. However, the grade J204 Cu has a negligible amount of research on its welding and potential welding processes/techniques. Therefore, there is an immediate need to identify a viable welding

technique for developing J204 Cu weld joints, and then validate and investigate the possibility of using the same welding technique for AISI 444. As J204 Cu is an ASS, the next proposed stage in this experimental study was to examine and choose the most suitable welding technique for ASS.

Fusion welding stands as the predominant method for joining austenitic SSs on an industrial scale. Nevertheless, it presents several challenges, including issues like porosity, microsegregation, solidification cracking, and the precipitation of secondary phases. These challenges often emerge due to disparities in the chemical, thermal, and physical properties between the BM and filler metal. Among these concerns, solidification cracking is a foremost issue due to its potential to substantially affect weldment properties. Solidification cracking arises during the cooling and solidification of molten metal, leading to crack formation. To mitigate solidification cracking, it is essential to carefully select the appropriate welding process and associated parameters (Coniglio and Cross, 2013). Processes characterized by low heat input and a slow cooling rate, such as GTAW and LBW, are less prone to solidification cracking (Hochanadel *et al.*, 2011). Furthermore, employing a filler metal with minimal ferrite content can reduce the risk of this type of defect. The identification and utilization of suitable welding processes and parameters that yield an optimal ferrite concentration in the WM represent effective strategies for averting welding defects (Vashishtha *et al.*, 2017).

There are several fusion welding processes in existence SMAW, SAW, FCAW, GMAW, or MIG, GTAW, electron beam welding (EBW), and laser welding (LW), etc. to ensure better joint strength (Liu, Jin, *et al.*, 2020) (Attah *et al.*, 2023). Out of these, the majority of welding techniques have been used to develop sound weld joints of SS material with specific mechanical and thermal properties (Hossein Nedjad *et al.*, 2023). However, there is still an untouched area that simplifies the selection of an appropriate welding process that can ensure the success of welded joints for a considerable period. To overcome this research gap and to identify the appropriate welding technique for selected SS there was a requirement to utilize a suitable decision-making approach.

In the present scenario and real-world situation, the emphasis is more often on collecting and analyzing data/information that is not trustworthy, very unrealistic, and ambiguous. Currently, many decision-making approaches are in existence including TOPSIS (Singh *et al.*, 2022), AHP (Analytic Hierarchy Process) (Singh and Rathi, 2022), VIKOR (Rathi *et al.*, 2017), PROMETHEE (Preference Ranking Organization Method for Enrichment Evaluation) (Yadav *et al.*, 2018), etc. Attributing the success rate of various approaches available for decision-making, the Grey Relational Approach (GRA) has been selected for the present study.

4.3.1 Grey Relational Analysis (GRA)

It is a multi-criteria decision-making approach that exposes the most critical factors based on the grey relational degree and the contribution in the system or the influence degree between the system. The prime benefit of the GRA approach is that it can effectively handle multiple input factors and output responses simultaneously, which is useful in optimizing complex manufacturing processes. GRA can also handle uncertainties and variations in the data, making it a robust method for process optimization (Liu *et al.*, 2013).

Considering the effective decision-making ability of GRA, it has been utilized here for selecting an appropriate welding technique that involves certain execution phases as shown in Figure 4.2.

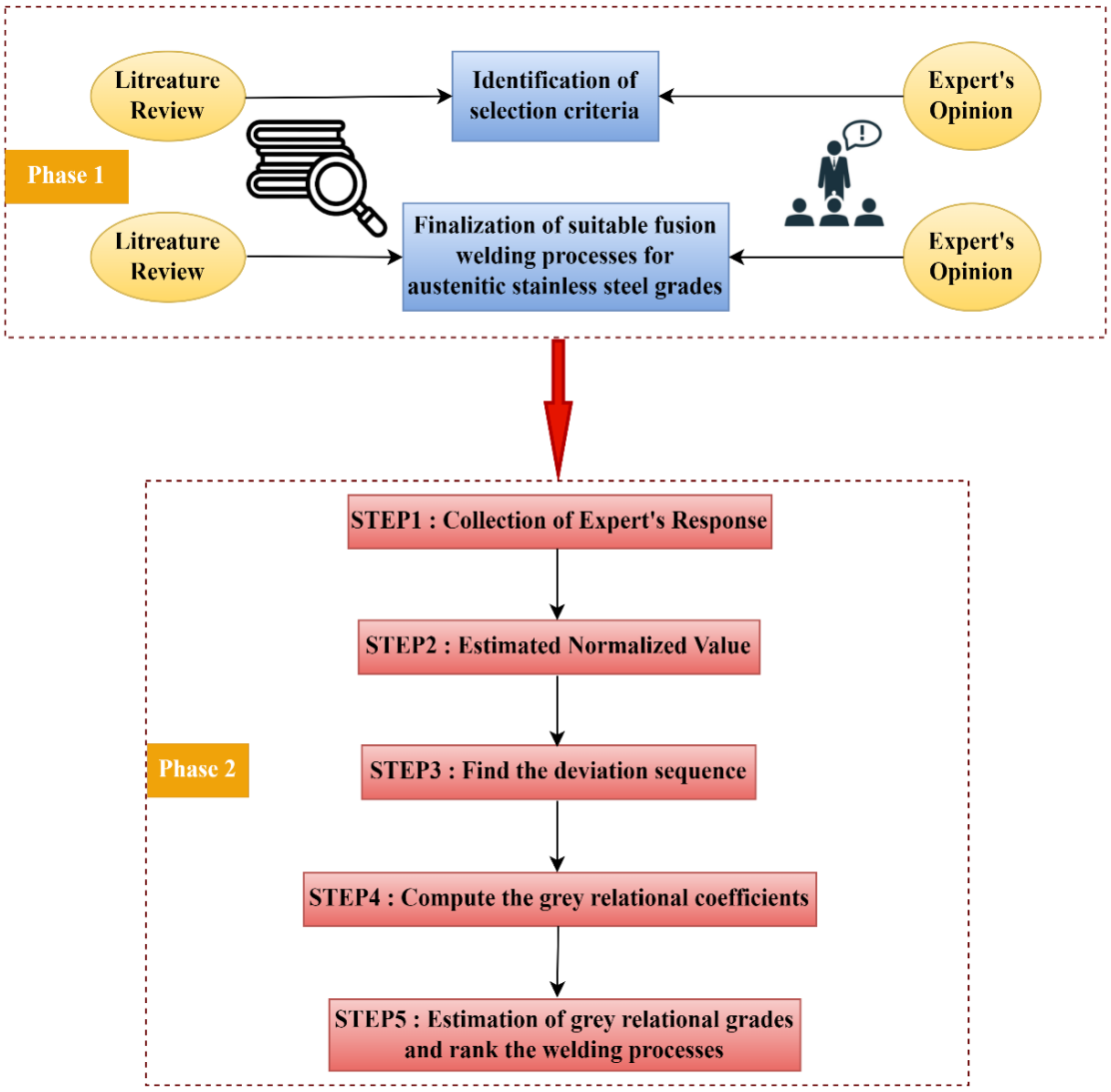

Figure 4.2: Steps involved in Grey Relational Analysis

Phase 1: The selection of the appropriate fusion welding technique to join ASS mainly requires recognizing the parameters (selection criteria) that significantly affect the performance of welded joints over a while. These critical parameters are derived from the literature and further from the opinions of industry experts, technical experts, and academicians. The acknowledged parameters are then designated with certain codes as represented in Table 4.3.

Table 4.3: Selection Criteria for Welding Techniques

S.No.	Parameters (Selection Criteria)	Code
1	Sound Weld	C1
2	HAZ	C2
3	Weld Suitability in Various Positions	C3
4	Joint Configuration	C4
5	Equipment Portability	C5
6	Weld Penetration	C6
7	Capital Cost	C7

To achieve a pertinent result of the objective, primarily the focus has been given to collecting more appropriate and justified responses/opinions from relevant resources. GRA and its attributes were further found to be very useful in establishing a significant approach to recognizing a suitable welding technique.

The selection of an appropriate fusion welding process in the joining of ASS is always an intricate task. It requires high expertise to decide on a particular fusion welding process out of all available alternatives that can guarantee better performance in terms of post-weld mechanical and metallurgical properties. To assist the decision-making, a hierarchical structure has been established as shown in Figure 4.3. This stipulates our goal of the appropriate fusion welding process from existing processes (alternatives) under the consideration of our selection criteria. The alternatives that are taken here include SMAW, FCAW, GMAW, or MIG, SAW, EBW, GTAW, and LBW.

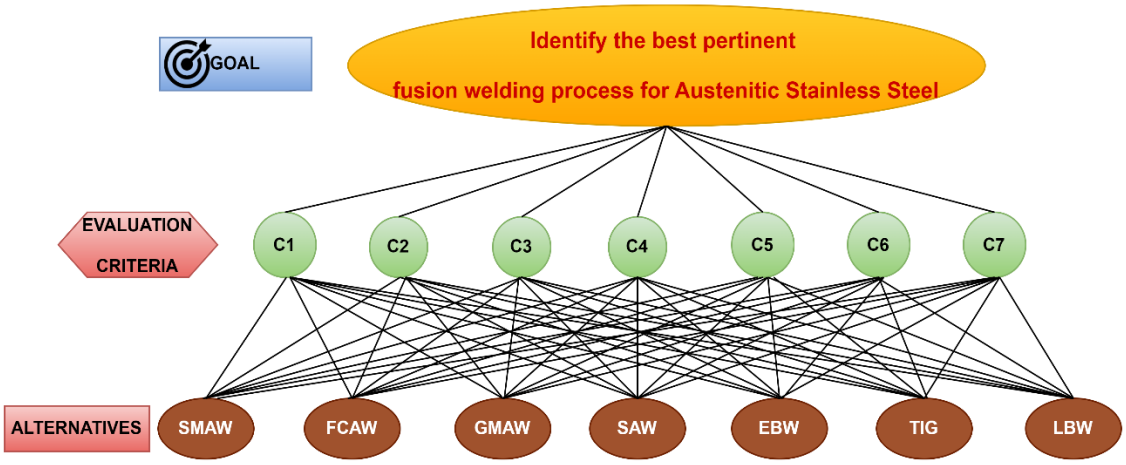

Figure 4.3: Hierarchical Structure Presenting the Evaluation Criteria and Alternatives

The alternatives under consideration for a given decision are completely dependent on the selection parameters that are chosen. This demonstrates the difficulty of the decision-making process. Once the selection parameters have been identified, the next step is to prioritize them, based on which one has the greatest impact on the known alternatives. This means that the different alternatives that are being considered for a decision cannot be evaluated independently of the selection parameters. The selection parameters will define the criteria by which the alternatives will be evaluated. For example, if the selection parameters are cost, performance, and reliability, then the alternatives will be evaluated based on their cost, performance, and reliability. The difficulty of the decision-making process is because the different selection parameters may be conflicting. For example, if the goal is to select the alternative with the lowest cost and the highest performance, then there may be a trade-off between these two criteria. In this case, it is important to prioritize the selection parameters and decide which one is more important. Once the selection parameters have been identified and prioritized, the next step is to evaluate the different alternatives based on these criteria.

This is also to be noted here that certain parameters have a negative impact, which means the higher value of these parameters leads to the elimination of the corresponding

alternative. For the existing circumstances, the HAZ and the capital cost hurt the selection of the desired alternative i.e., fusion welding process.

The experts that had been requested for their responses/views are professionals with good experience in the area of welding, industry experts, professionals working in welding labs of high repute, and academicians with an excellent research background in materials and their joining techniques. A questionnaire was framed stating the alternatives available and the selection criteria like parameters on which the response was expected to rank the welding process. The questionnaire was sent to almost 250 people out of that 143 people accepted the request to give their responses and finally, 95 experts submitted their responses. The demographic detail of these experts is provided in Table 4.4.

Table 4.4: Detail of Experts

S. No.	Designation	Average Experience (Years)	Background	No. of Experts
1	Professor	21	Academia	13
2	Quality Engineer	8	Industry	18
3	Manager	23	Industry	15
4	Welding Section Head	12	Industry	22
5	Associate Professor	10	Academia	16
6	Plant Head	22	Industry	11

Through a questionnaire survey, the collective response received from various experts has been screened and documented in Table 4.5.

Phase 2: Grey relational analysis (GRA) is a powerful tool for evaluating and judging the performance of complex projects with limited information. GRA is a multi-criteria decision-making (MCDM) method that can be used to compare different alternatives based on multiple criteria, even if the criteria are not quantitative or if the information is incomplete.

Table 4.5: Collective Responses of Experts for Alternatives v/s Criteria

Alternatives	Selection Criteria						
	Sound Weld	**HAZ**	**Weld Suitability in Various Positions**	**Joint Configuration**	**Equipment Portability**	**Weld Penetration**	**Capital Cost**
SMAW	216	313	298	311	321	197	191
FCAW	196	224	227	187	163	217	315
GMAW	221	231	211	294	352	256	192
SAW	287	239	104	143	116	111	278
EBW	191	113	101	217	116	289	310
PAW	183	189	169	233	119	287	311
TIG	303	211	323	329	339	277	301
LBW	310	101	154	119	126	323	319
min	183	101	101	119	116	111	191
max	310	313	323	329	352	323	319

However, to use GRA, the data must first be preprocessed into quantitative indices. This is done by normalizing the raw data to a scale of 0 to 1. This is necessary because GRA compares the different alternatives based on their relative performance, and it is important to ensure that the data is on the same scale. The steps of GRA used to conduct the prioritization of welding techniques are explained as follows:

Step 1: The first step of the GRA method is normalized or data processing. The responses were collected from experts from academia and industry backgrounds against each alternative (welding techniques) concerning selection criteria. x_i^0, represents the response of alternative "i" to particular expert group "o" The normalized values have been obtained using equation (1). Here, x_i^{o*} represents the normalized value of the critical success factor "i" to the particular expert group "o".

$$x_i^{o*} = \frac{x_i^0 - \min x_i^0}{max\ x_i^0 - min\ x_i^0} \quad (1)$$

Further, the normalized values of the collected responses are computed through Equation 1 and recorded in Table 4.6. Normalization introduces the downsizing of the informational index to such an extent that the standardized information falls the reach somewhere in the

range of 0 and 1. Such standardization methods assist with looking at relating standardized values from at least two distinct informational collections in a manner that takes out the impacts of the variety in the size of the informational collections i.e., an informational index with enormous qualities can be effortlessly contrasted.

Table 4.6: Normalized Values

Alternatives	Selection Criteria						
	Sound Weld	**HAZ**	**Weld Suitability in Various Positions**	**Joint Configuration**	**Equipment Portability**	**Weld Penetration**	**Capital Cost**
SMAW	0.2598	0.0000	0.8874	0.9143	0.8686	0.4057	1.0000
FCAW	0.1024	0.4198	0.5676	0.3238	0.1992	0.5000	0.0313
GMAW	0.2992	0.3868	0.4955	0.8333	1.0000	0.6840	0.9922
SAW	0.8189	0.3491	0.0135	0.1143	0.0000	0.0000	0.3203
EBW	0.0630	0.9434	0.0000	0.4667	0.0000	0.8396	0.0703
PAW	0.0000	0.5849	0.3063	0.5429	0.0127	0.8302	0.0625
TIG	0.9449	0.4811	1.0000	1.0000	0.9449	0.7830	0.1406
LBW	1.0000	1.0000	0.2387	0.0000	0.0424	1.0000	0.0000
Min	0.0000	0.0000	0.0000	0.0000	0.0000	0.0000	0.0000
Max	1.0000	1.0000	1.0000	1.0000	1.0000	1.0000	1.0000

Step 2: For the second step of the GRA, the deviation sequence ($\triangle_{oi}$) has been calculated using equation (2).

$$\triangle_{io}=\|max\ x_i^{o*} - x_i^{o*}\| \qquad (2)$$

The obtained normalized values are further converted into deviation sequences using equation 2 and recorded in Table 4.7.

Table 4.7: Deviation Sequence

Alternatives	Selection Criteria						
	Sound Weld	**HAZ**	**Weld Suitability in Various Positions**	**Joint Configuration**	**Equipment Portability**	**Weld Penetration**	**Capital Cost**
SMAW	0.7402	1.0000	0.1126	0.0857	0.1314	0.5943	0.0000
FCAW	0.8976	0.5802	0.4324	0.6762	0.8008	0.5000	0.9688
GMAW	0.7008	0.6132	0.5045	0.1667	0.0000	0.3160	0.0078
SAW	0.1811	0.6509	0.9865	0.8857	1.0000	1.0000	0.6797
EBW	0.9370	0.0566	1.0000	0.5333	1.0000	0.1604	0.9297
PAW	1.0000	0.4151	0.6937	0.4571	0.9873	0.1698	0.9375
TIG	0.0551	0.5189	0.0000	0.0000	0.0551	0.2170	0.8594
LBW	0.0000	0.0000	0.7613	1.0000	0.9576	0.0000	1.0000
min	0.0000	0.0000	0.0000	0.0000	0.0000	0.0000	0.0000
max	1.0000	1.0000	1.0000	1.0000	1.0000	1.0000	1.0000

Step 3: In this step, the grey relational coefficients (ξ_{io}) have estimated using equation (3). Here, $\triangle_{min}$ represents the minimum value of the deviation sequence and $\triangle_{max}$ designates the maximum value of the deviation sequence. ξvalue considered here is 0.5.

$$\xi_{io} = \frac{\triangle_{min} + \xi.\triangle_{max}}{\triangle_{oi} + \xi.\triangle_{max}} \qquad (3)$$

Moreover, the grey relational coefficient (GRC) is computed for the individual output quality characteristics using equation 3 and the output is noted in Table 4.8.

Table 4.8: Computation of Grey Relational Coefficients

Alternatives	Selection Criteria						
	Sound Weld	**HAZ**	**Weld Suitability in Various Positions**	**Joint Configuration**	**Equipment Portability**	**Weld Penetration**	**Capital Cost**
SMAW	0.4032	0.3333	0.8162	0.8537	0.7919	0.4569	1.0000
FCAW	0.3577	0.4629	0.5362	0.4251	0.3844	0.5000	0.3404
GMAW	0.4164	0.4492	0.4978	0.7500	1.0000	0.6127	0.9846
SAW	0.7341	0.4344	0.3364	0.3608	0.3333	0.3333	0.4238
EBW	0.3479	0.8983	0.3333	0.4839	0.3333	0.7571	0.3497
PAW	0.3333	0.5464	0.4189	0.5224	0.3362	0.7465	0.3478
TIG	0.9007	0.4907	1.0000	1.0000	0.9008	0.6974	0.3678
LBW	1.0000	1.0000	0.3964	0.3333	0.3430	1.0000	0.3333

Step 4: In this step, the grey relational grades (γ_{i0}) have estimated using equation (4). Here "n" is the number of the expert group in the case industry

$$\gamma_{i0}=\frac{1}{n}\sum_{i=1}^{n}\xi_{io} \quad (4)$$

In the last step of the GRA approach, the grey relational grades (GRG) are estimated (Table 4.9) using Equation 4 from the obtained output in terms of GRC.

Table 4.9: Ranking of Welding Techniques as Per GRG Values

Grey Relational Grade	Alternatives	Rank
0.665026543	SMAW	3
0.429536004	FCAW	7
0.672947997	GMAW	2
0.422318054	SAW	8
0.500522508	EBW	5
0.464495481	PAW	6
0.765342547	TIG	1
0.629445499	LBW	4

Based on the grey relational grades ranks of the welding techniques have been estimated. In the last phase of the adopted methodology, the ranks of the welding techniques were validated using expert input.

With the help of GRA, it has been identified and hence proposed that the appropriate fusion welding technique for joining ASS is Tungsten Inert Gas (TIG) welding also called GTAW (Pandey *et al.*, 2023). GTAW yields high-quality welds with minimal spatter and a seamless bead aspect. GTAW is ideally suited for welding thin materials because it allows for greater heat input control and reduces the likelihood of burn-through and deformation (Sarolkar and Kolhe, 2017) (Kutelu *et al.*, 2018) (P. Chauhan and P. Panchal, 2016).

GTAW permits precise heat input regulation during welding which is an essential and integral part and provides a barrier for excessive heat formation that may cause sensitization and the formation of Cr carbides reducing the material's corrosion resistance. It produces relatively minimal heat input compared to other welding procedures, which reduces the risk of distortion and HAZ problems (Li *et al.*, 2022). This is especially

advantageous for the preservation of the mechanical and corrosion-resistant properties of SS grades such as AISI 444.

Keeping the result obtained from the GRA approach in view and analyzing the suitability, advantages, and associated limitations, GTAW has been selected as a welding technique to develop weld joints that further be investigated for mechanical properties and corrosion behavior. For the current research work, GTAW has been used with filler metal as American Welding Society (AWS) A5.9 ER 308L, and the chemical composition of the selected filler metal is given in Table 4.10.

Table 4.10: Chemical Composition of AWS A5.9 ER 308L (wt%)

C	Mn	Mo	S	Si	Cr	Ni	Fe
0.024	1.65	0.02	0.002	0.42	20.1	10.3	Balance

To develop the weld joints using the proposed welding technique with AWS standard, the welding machine used TIG500P-AC/DC-E312 is a product of *JASIC* technologies as shown in figure 4.4. This machine can develop a peak current of around 500 A and hence is very capable of welding ferrous and nonferrous metals with a greater scope of high thicknesses. Some important technical information about this welding machine has been summarized below in Table 4.11.

Table 4.11: Important technical information about Welding Machine

Weld Parameter	Range
Initial current (A)	DC: 10-510 AC: 20-250
Peak current (A)	DC: 10-510 AC: 20-510
Background current (A)	DC: 10-510 AC: 20-510
Crater current (A)	DC: 10-510 AC: 20-250
DC pulse frequency (Hz)	0.5-200
DC pulse duty ratio (%)	10-90
AC frequency (Hz)	20-70
+/- half wave duty ratio (%)	10-60
AC pulse frequency (Hz)	0.5-5.0
AC pulse duty cycle (%)	10-90

Up/Down-slope (S)	0-60
Pre-flow time (S)	0-15.0
Post-flow time (S)	2-20.0
Spot welding time (S)	0.0-8.9

Figure 4.4: Welding Machine Set-up and Welding Process

Direct current electrode negative (DCEN) polarity was used for the welding process. The optimization of parameters was achieved by the development of pilot weld joints, followed by the characterization of weld joints. The primary consideration was always to minimize the heat input. The pilot weld joints were first made using a modest heat input of 100A and 24V. Subsequently, additional welding parameters were used, and an analysis of the weld bead shape was conducted. The challenges encountered throughout this experimental study i.e. during the development of pilot weld joints as shown in Figure 4.5 mainly include:

1. Incomplete Penetration: This refers to a situation where the weld does not fully penetrate the base material, resulting in a weak joint.
2. Excessive Reinforcement: This occurs when there is an excessive amount of weld material deposited, leading to an uneven surface and potential structural weaknesses.
3. Excessive Penetration: This occurs when the weld penetrates too deeply into the base material, potentially compromising the integrity of the joint.

4. Arc Spatter: The term "arc spatter" pertains to the occurrence seen in arc welding procedures, whereby minute molten droplets of the welding material are released from the weld pool and have the potential to fall on adjacent surfaces. These little liquid particles are often known as "spatter."

In addition to these deficiencies, it has also been observed that the root gap (1.2 mm) chosen for the first few weld connections reduces progressively as the welding process advances, owing to the thermal expansion of the plates at the root face. Consequently, the narrowing of the distance between the plates restricts the filler wire's ability to penetrate, resulting in inadequate melting at the root of the joint. During process parameter optimization it has been observed that low weld current and/or high welding speed results in incomplete penetration, while if the current is on the higher side it results in excessive penetration or disproportionate melting of BM.

Figure 4.5: Improper Weld Bead Profiles of Pilot Weld Samples

After several trials with pilot weld joints, the optimum process parameters were selected as depicted in Table 4.12. As the thickness of each plate was 3 mm, complete penetration was obtained in a single pass for all weldments.

Table 4.12: Selected Process Parameters for GTAW

Material	Current	Voltage	Travel Speed	Shielding Gas flow rate (l/min)
J204 Cu	110 A	22 V	10 cm/min	15
AISI 444	110 A	24 V	12 cm/min	15
J204 Cu + AISI 444	110 A	25 V	13 cm/min	15

Before final welding, the plates were meticulously cleansed with ethanol to eliminate contaminants in addition alignment, set-up, and weld joint measurements were all confirmed to prevent welding defects.

During welding, root penetration, interpass temperature, weld bead cleanliness, and conformity with the appropriate process (i.e. voltage, amperage, heat input, and travel speed) were all monitored (Moteshakker and Danaee, 2016) (Vinoth Jebaraj *et al.*, 2018). To ensure that the developed weld joint is defect-free, non-destructive tests were done to ensure the soundness of the generated welds. Before and after welding, visual tests/inspections (VT) were performed. The appearance of final welds was evaluated and assessed following welding to discover typical surface discontinuities such as porosity, partial fusion, incomplete joint penetration, and fractures. A liquid penetrant (PT) was used on the weld joints to identify any weld surface discontinuities, particularly fractures. Finally, ultrasonic testing was performed and some flaws were found at the start and end of the weld bead. To obtain better test results the weld material from these locations was removed in the transverse direction of the weld. Figure 4.6 shows the final weld joints of both materials taking the similar material sheets and a dissimilar weld joint once these materials are welded together.

Figure 4.6: Final Weld Joints

4.4 Sample Preparation

To facilitate the testing process, specimens from welded plates were obtained by cutting with a wire-cut EDM into standard dimensions. The used EDM is shown in Figure 4.7. Figure 4.8 displays the welded specimen used for conducting various tests, including

microstructural analysis, tensile testing, impact testing, hardness testing, and corrosion tests including DLEPR and PDP tests.

Figure 4.7: Wire Cut Electron Discharge Machining Set-Up

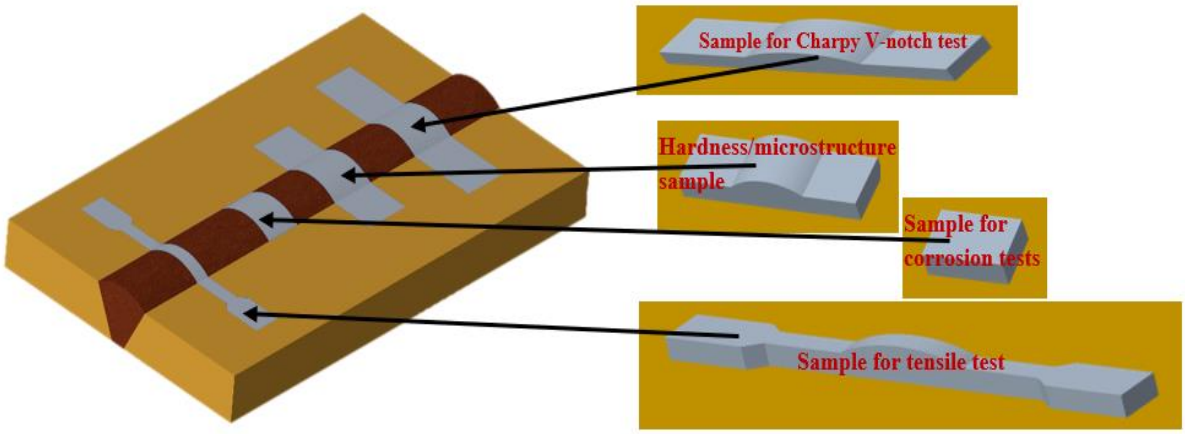

Figure 4.8: Schematic Diagram for Test Samples for Mechanical and Corrosion Testing

Table 4.13 offers information on the sizes of various samples used for evaluating the mechanical properties of materials (such as strength, hardness, etc.) and the corrosion resistance of such materials. Testing a material's resistance to degradation when exposed to corrosive conditions is evaluated by corrosion testing, while evaluating a material's

response to varying loads, or stresses is evaluated by mechanical testing. The information that is given would probably be included with the primary emphasis being on the kind of test and the sample size.

Table 4.13: Specimen Size for Different Samples for Testing

Sr.No.	Name of the test	Dimension of samples
1	Microstructural Analysis	30 x 10 x 3 mm^3
2	Microhardness test	30 x 10 x 3 mm^3
3	Tensile test	As per ASTM E8
4	Impact test	55 x 10 x 3 mm^3 with notch angle 45^0
5	Corrosion test	10 x 05 x 3 mm^3

4.5 Metallographic and Microstructural Studies

In metallographic studies, the structure of metals and metal alloys was examined with a metallurgical microscope. Metallographic samples were prepared (taking a transverse section of the welded region) as per ASTM E3-95 standards and then by polishing using a metallographic disc polisher as shown in figure 4.9 (a), on successively fine emery papers followed by polishing using an appropriate etchant. The final polishing has been done with diamond paste to achieve a mirror finish. Microstructures of different zones like WM and HAZ have been observed using optical microscopy which is shown in Figure 4.9 (b). To study the fracture behavior of tensile tested specimens, SEM has been used, and that has also been shown in Figure 4.9 (c). EBSD (Electron backscatter diffraction) has been carried out to know the texture behavior.

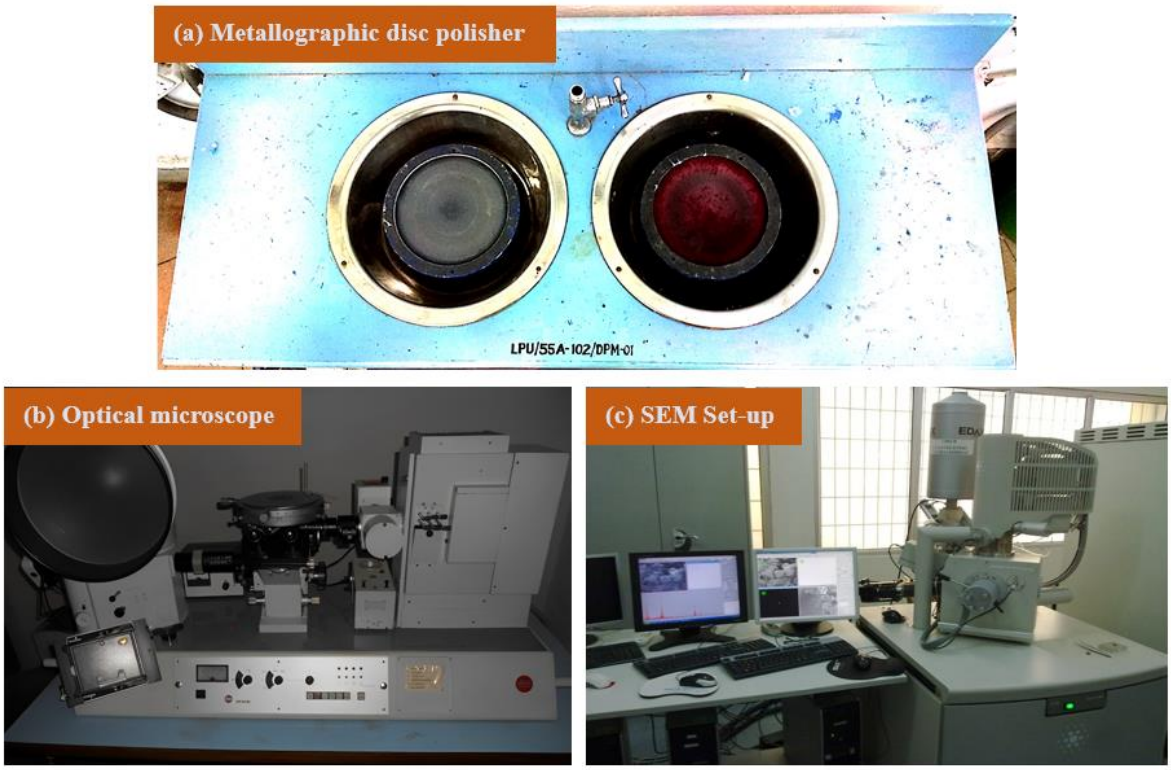

Figure 4.9: Set Up for Metallurgical and Microscopic Studies: (a) Metallographic disc polisher (Courtesy: Lovely Professional University, Punjab); (b) Optical microscope and (c) SEM Set-up (Courtesy: IIT, Roorkee)

4.6 Mechanical Testing

Various mechanical tests have been done to evaluate the different mechanical properties of WM as well as the BM. These tests include impact test (ASTM E-23), hardness test (ASTM E-18), and tensile test (ASTM E-8M). The test samples of required dimensions were cut from the welded joint using a wire-cut EDM process in an endeavor to ensure less stress, heat, and deformation to the sample, hence reducing the possibility that the weld structure will be altered. To identify the impact strength of the weld samples Charpy V notch impact test was performed and the hardness test was executed using Vicker's hardness testing machine. A hydraulically operated dynamic universal testing machine (UTM) was used to conduct the tensile test and to ensure more accurate results associated with this test and data reproducibility, a set of three samples was taken for each state.

4.6.1 Hardness Test

For the hardness test, the same specimen was used which was prepared for the microstructure study. The hardness test of the weld, HAZ, and BM of the weld joint was carried out by the Vickers microhardness test method as evidenced in Figure 4.10, while the indentations were taken at a load of 100 gms. The hardness was taken at different closest locations to ensure the best results. The data obtained from the hardness test is used to study the hardness behavior in different regions along the weld joint.

Figure 4.10: Vickers Microhardness Test Set-Up for Hardness Test (Courtesy: IIT, Roorkee)

4.6.2 Tensile Test

The tensile test was done on a hydraulically operated dynamic universal testing machine as shown in Figure 4.11 (a) using standard ASTM E8 M-04. The ultimate tensile load, elongation, and failure mode characteristics were recorded for each specimen. SEM was then used to analyze the fractured faces of the tensile-tested specimens. Considering the thickness (small) of the plate used for the current study sub-sized tensile specimens were prepared. The dimension of the specimen is confirmed in Figure 4.11 (b), while actual specimens are shown in Figure 4.11 (c).

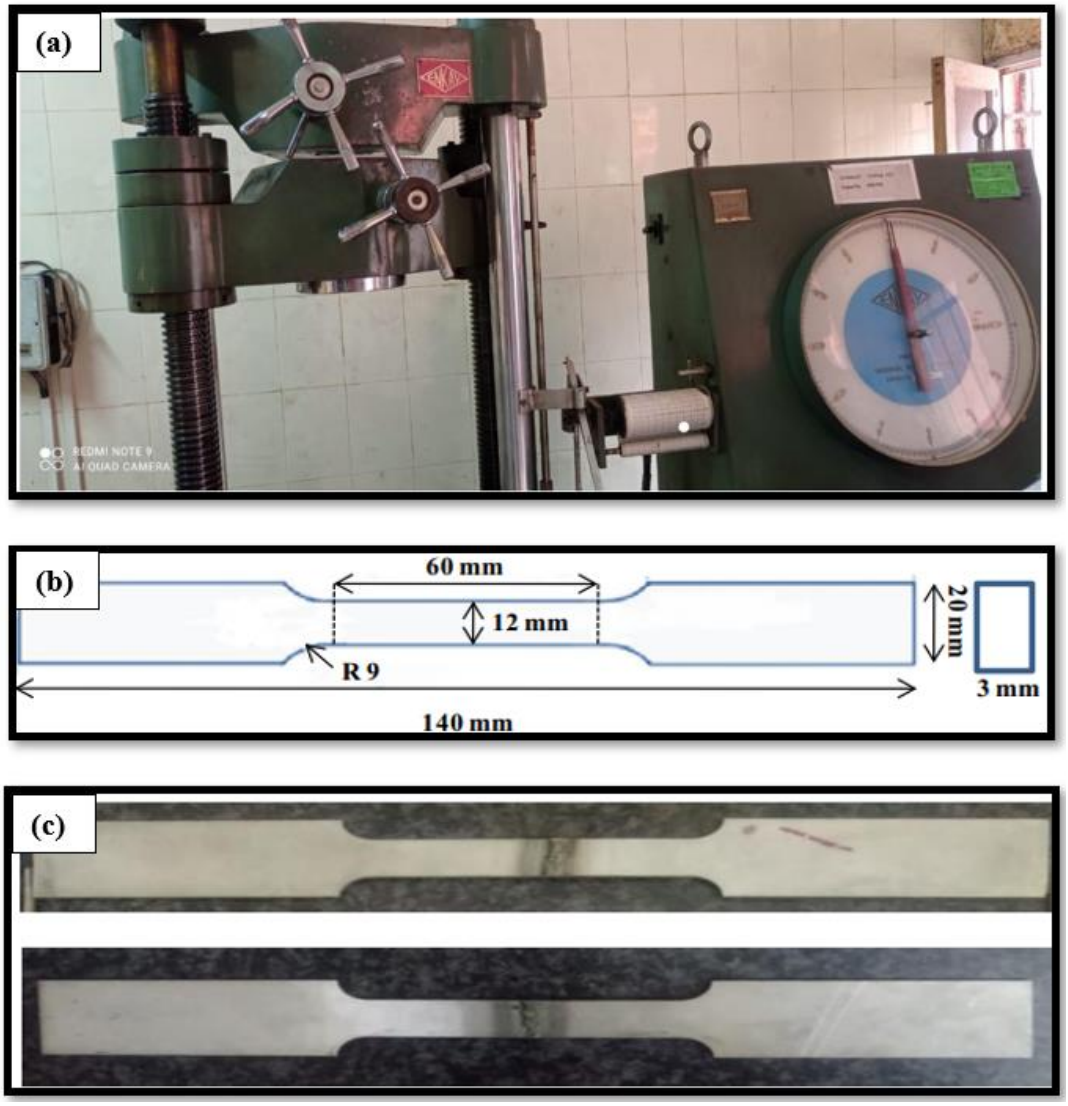

Figure 4.11: (a) Universal Testing Machine Used to Conduct Tensile Test (b) Schematic Diagram of The Tensile Test Specimen as Per ASTM E8 Standard (c) Actual Specimens

4.6.3 Impact Test

A Charpy impact test was conducted using a 300 J machine. The loaded notched specimen is subjected to plastic deformation at the notch region. The Charpy impact test calculates the amount of energy expended when a notched sample is hammered by a swinging impactor while merely resting on both ends. When the specimen can no longer absorb energy, normal stress begins to develop at the base of the notch, and fracture occurs. The

difference between the sample's drop height before and after the fracture serves as a measure of the impact energy that the sample has absorbed. Through ultrasonic cleaning, the fractographic inspection is carried out. To investigate the impact toughness of WM transverse test samples were created as per the American Society for Testing and Materials (ASTM) - E23 standards as shown in Figure 4.12 below.

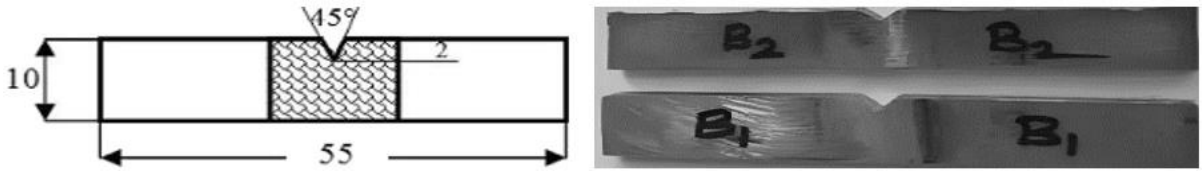

Figure 4.12: Standard Dimensions of Impact Test Samples and Actual Samples

4.7 Assessment of Corrosion Behavior

Due to the vital role that SS plays in a broad variety of sectors, including construction, manufacturing, transportation, and healthcare, conducting research on the corrosion behavior of SS weld joints is of the utmost significance. SS is famous for its outstanding corrosion resistance, however, when SS is welded, its corrosion resistance might be compromised owing to several variables that are intrinsic to the welding process. Both the weld joint's microstructure and its susceptibility to corrosion may be affected by factors such as the amount of heat input, the method used to weld, and the composition of the shielding gas. As a result, researching the corrosion behavior of SS weld joints is very necessary to guarantee the dependability, safety, and durability of components and structures used in a variety of sectors.

4.7.1 Weight Loss Test

The specimens for weight loss assessments were prepared in accordance with the procedures indicated in ASTM G 1. Rectangular samples having a cross-sectional area of 1 cm^2 were cut for weight loss testing. To suspend the sample in the tank and connect the string, two holes were drilled at the ends of the sample. Before stringing the sample, it was polished with emery paper up to a 1200 grade, then rinsed in distilled water to get rid of

any dirt or oils that had built up on the surface. Polished and pre-weighed samples were subjected to 0.1 M hydrochloric acid, 0.1 M sulphuric acid (H_2SO_4), and sulphuric acid containing 3.5 % NaCl solution (Potgieter *et al.*, 2012). Hydrochloric acid and sulfuric acid are powerful acids that can deteriorate metals, particularly stainless steel. In weight loss tests, these are frequently employed to imitate antagonistic and acidic environments, such as those found in industrial processes or chemical exposures. Exposing stainless steel to these acids can cause the protective passive coating on its surface to dissolve, resulting in corrosion. Further addition of sodium chloride (NaCl) to sulfuric acid simulates corrosive chloride environments, such as those found in marine or salty atmospheres. Chlorides are known to make stainless steel more susceptible to corrosion, particularly pitting corrosion. At room temperature, all of the experiments were run. At three-day intervals, weight loss measurements were taken throughout the 60-day experiment on weight loss.

4.7.2 Potentiodynamic Polarization Test

The potentiodynamic polarization test is one of the most common methods utilized to evaluate the effectiveness of coatings, inhibitors, and other compounds designed to prevent corrosion. In addition to this, it may be utilized to evaluate the corrosive behavior of materials in a variety of situations. The potentiodynamic polarization test being an electrochemical method is utilized to analyze how a material reacts to corrosion. During this particular test, the component is first submerged in a solution, then a potential is given to it, and finally, the current that is carried by the component is observed. After that, the potential is changed at a predetermined pace, and the current that results from that change is recorded. The information that was gathered as a consequence may be utilized to ascertain the rate of corrosion, the potential for corrosion, and the kind of corrosion process (Esmailzadeh *et al.*, 2018) (Bellezze *et al.*, 2018).

Potentiodynamic polarization experiments were conducted utilizing a potentiostat (BIO Logic VMP-300) with a conventional cell configuration in a 3.5% NaCl solution, as seen in Figure 4.13. The open circuit potential (OCP) was measured for 1 hour, during which the potential reached a stable state as part of the PDP test. The experiments were conducted

within the voltage range of -0.7 V (against saturated calomel electrode, SCE) to 1.2 V (SCE), with a scan rate of 0.5 mV/sec (Verma and Taiwade, 2016). Three samples were collected to assess the repeatability of the results. The experiment was performed under ambient conditions, using a surface area of 0.50 cm^2, which exclusively included the weld region. The data that was acquired was analyzed via EC-lab software. The corrosion potential (Ecorr), corrosion current density (Icorr), and pitting potential (Epit) were assessed by the use of the PDP test (Thirumalaikumarasamy *et al.*, 2014).

During the test, the potential is raised linearly concerning time, beginning at a value that is lower than the corrosion potential and proceeding to a value that is higher than it after the procedure. This results in the production of a curve that plots current against potential and is known as a polarization curve. This curve may be utilized to identify the electrochemical behavior of the material.

In most cases, the polarization curve will have three distinct regions: the anodic area, the cathodic region, and the passive region. In the anodic area, the dissolving of the metal results in a rise in the current that is proportional to the potential. In the cathodic zone, there is a drop in the amount of dissolved oxygen or hydrogen ions, which causes the current to decrease in proportion to the potential. The production of a protective oxide layer on the surface of the material results in the existence of the passive area, which is characterized by an extremely low current density.

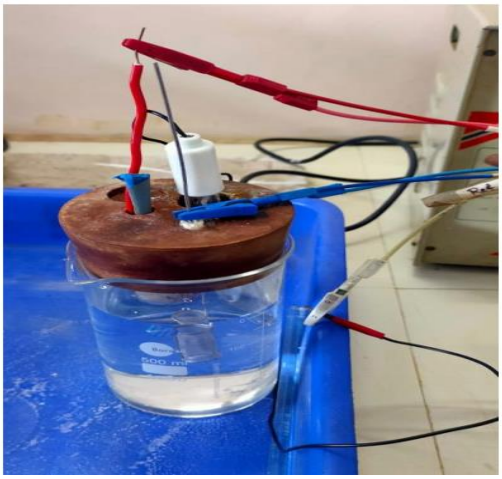

Figure 4.13: Sample for PDP test in BIO logic VMP-300

4.7.3 Double Loop Electrochemical Potentiokinetic Reactivation (DLEPR) Test

The DLEPR corrosion test is an electrochemical corrosion measurement technique used to determine the corrosion rate and corrosion resistance of metals and alloys in different environments. A modest AC is applied to the metal's surface while it is submerged in a corrosive solution. The AC oscillates the metal surface between anodic and cathodic phases, thereby generating a voltage signal. The amplitude of the voltage signal is proportional to the metal's corrosion rate, whereas the phase shift between the AC and voltage signal provides information about the corrosion mechanism (Taiwade *et al.*, 2013). It is a non-destructive, rapid, and accurate method for determining the corrosion resistance of metals and alloys, and it can be used both in the lab and in the field. It is particularly helpful for assessing the corrosion resistance of coatings, surface treatments, and other protective measures applied to metal surfaces.

The DLEPR test can determine some corrosion parameters, including:

i. Resistance to polarization (Rp): a measure of a metal's ability to resist corrosion.
ii. Corrosion rate (CR): the rate at which the test solution causes the metal to corrode.
iii. The Tafel slope measures the rate of the anodic and cathodic reactions.
iv. Corrosion potential (Ecorr): the potential at which the metal in the test solution begins to corrode.

The DLEPR test was performed in a potentiostat (Solartron-1285) at room temperature using modified electrolytes 0.5 M H_2SO_4 + 0.01 M NH_4SCN to determine intergranular corrosion and/or degree of sensitization (DOS). Sensitization in stainless steels occurs when chromium carbides precipitate at grain boundaries during welding or heat treatment, lowering the chromium content in those areas. The presence of ammonium thiocyanate (NH_4SCN) in the electrolyte is decisive in increasing the test's sensitivity. NH_4SCN in the electrolyte interacts with chromium carbides at the grain boundaries, generating soluble complexes. This facilitates the preferential dissolving of chromium-depleted regions during the electrochemical test. On the other hand, sulfuric acid (H_2SO_4) is often utilized in corrosion experiments due to its ability to create a hostile environment. The combination of sulfuric acid and ammonium thiocyanate provides conditions that favor an attack on

sensitized regions, which aids in determining the material's susceptibility to intergranular corrosion.

The first stage of this process is the elimination of the oxide layer present on the working electrode's surface. The aforementioned procedure involves the application of a potential of -0.7 V for 120 seconds inside the same solution used as the electrolyte. After the removal of the oxide layer, the stabilization of the working electrode surface is achieved by subjecting the electrode to open circuit potential (OCP) for 30 minutes. The open circuit potential (OCP) refers to the voltage differential that exists between the working electrode and the reference electrode in the absence of any external current flow. Once the working electrode has achieved a state of stability, the experimental procedure begins by initiating a potential scan on the working electrode. The potential scan is often implemented with a triangle waveform, whereby the potential undergoes a transition from a negative value to a positive value, followed by a return to the negative value. The scanning rate refers to the rate at which the voltage is altered, specifically at a value of 1.667 mV/s.

The potential range has been selected on the basis of literature that also include the DLEPR test to analyze the corrosion behavior of stainless steel and it spans from -0.7 V (SCE) to +0.7 V (SCE) (de Lima-Neto *et al.*, 2008) (Tembhurkar *et al.*, 2021). The acronym SCE denotes the saturated calomel electrode, which serves as a widely used reference electrode in many applications. The peak activation current density (Ia) and peak reactivation current density (Ir) are determined using the forward and backward scans. The ratio (Ir/Ia) x 100 is used to calculate the percent DOS. The samples mounted for testing DLEPR test are shown in Figure 4.14.

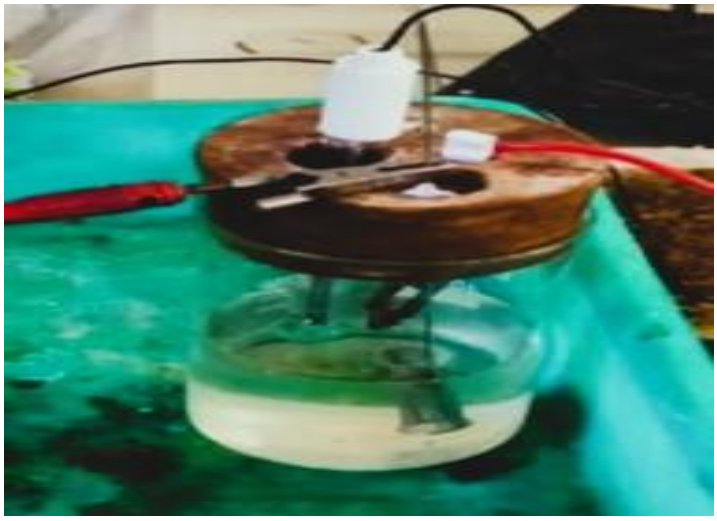

Figure 4.14: Sample for DLEPR test in Solatron-1285

CHAPTER 5

RESULTS AND DISCUSSION

This chapter is structured in such a way that it demonstrates the results, the analyses associated with the results, and then further discussion about them. To begin with, the effect of solution annealing on the microstructure of the selected materials has been discussed, followed by the microstructure of the welded joints of these materials. These microstructures are going to serve as a foundation for a discussion on the influence of different welding parameters. The results obtained of similar/dissimilar welding of J204 Cu ASS and 444 FSS are presented to show the effect of welding processes on microstructure, microhardness, tensile, impact, and corrosion tests by the GTAW process.

5.1 Microstructural Analysis

The microstructures of the weld metal, HAZ, and BM have been studied to find out the behavior of the grain growth and its structure at different locations along the weld joint. The optical micrograph of the J204 Cu weld illustrated in Figure 5.1 (b), confirms the formation of a fine dendritic structure in HAZ that enhances the tensile strength and hardness in that region. These fine dendritic structures create obstacles in the path of dislocation moment and hence significantly affect the material's behavior by increasing its resistance to deformation (Rezaei and Naffakh-Moosavy, 2018) (Kumar and Shahi, 2011) (Choubey and Jatti, 2014). The prime reasons for the development of these fine dendritic structures include rapid cooling rate due to high thermal gradient in HAZ, elemental segregation, the solidification behavior of weld pool, nucleation at the grain boundaries, etc. As shown in Figure 5.1 (c), the micrograph of WM (dissimilar weld of J204 Cu and AISI 444) yields columnar grains. The precipitation of carbide and other alloying elements has been observed at the grain boundary, while the dark spot shows the inclusion of foreign elements during welding. The microstructures at the fusion line in Figure 5.1 (c) clearly show the epitaxial solidification near the fusion boundary. At the fusion line, the columnar grains have been observed which further transform into dendrites due to the higher cooling

rate during solidification. Due to this higher cooling rate fine dendritic structure has been observed in the HAZ. The white regions in HAZ show the presence of ferrites. The microstructure of BM depicts the presence of predominate ferrite.

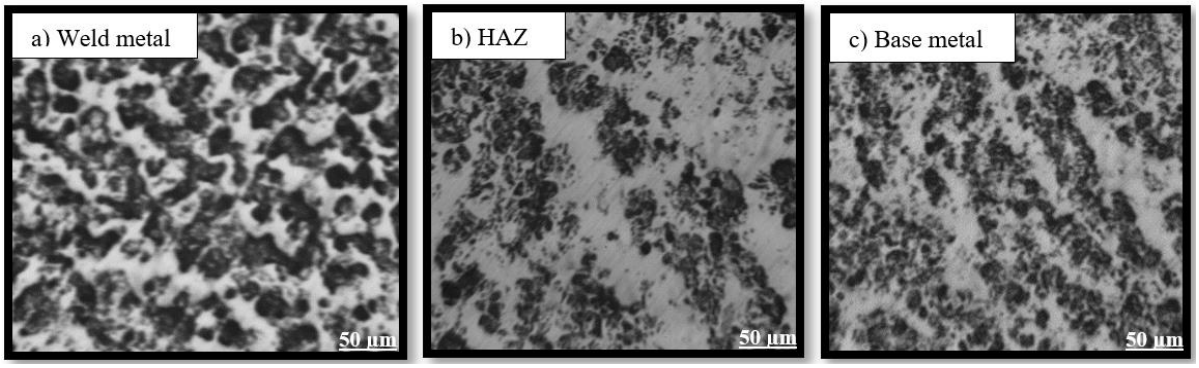

(a) Optical micrographs of AISI 444 weld

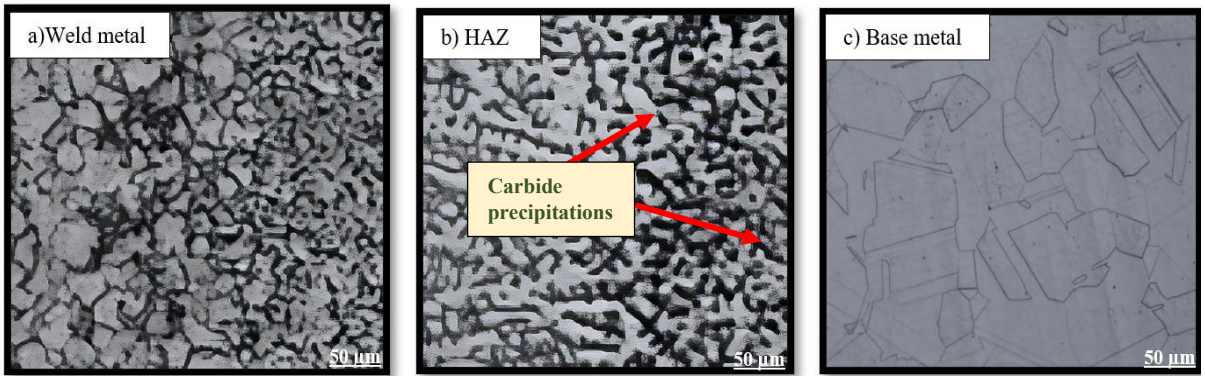

(b) Optical micrographs of J204 Cu weld

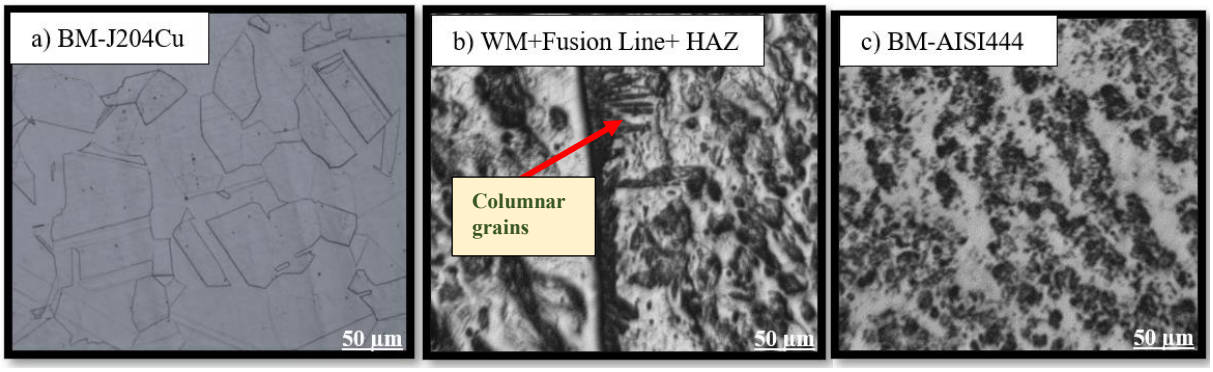

(c) Optical micrographs of dissimilar weld of J204 Cu & AISI 444

Figure 5.1: Optical Micrographs Showing The Microstructure of The Weld Zone

5.2 Tensile Testing

The prepared test samples (three samples for each weld joint as well as BMs) were tested to check their tensile strength using the universal testing machine (UTM). During the tensile test, it was found that all the test samples were broken from the BM closer to the weld not from weld joints. The results obtained are summarized in Table 5.1, representing the average values of tensile properties and indicating that J204 Cu exhibits better ultimate tensile strength and percentage elongation as compared to AISI 444. Literature reveals that commonly ultimate tensile strength value of ASS grades (200 series) found within the range of 500-600 MPa (Vashishtha *et al.*, 2017) . It can be seen in Figure 5.2 that the tensile strength of the BM increases with a small amount post welding and that may be due to the localized heating and swift cooling of the BM during welding creating small, refined grains in the HAZ next to the weld. Compared to the coarser grains of the parent metal, these smaller grains typically result in increased strength and durability. In addition, the inclusion of alloying filler metals in GTAW may interact with the BM, resulting in the development of new phases or strengthening mechanisms that increase tensile strength.

Table 5.1: Tensile Test Results

S.N.	J204 Cu (similar)		AISI444 (similar)		J204 Cu & AISI 444	
	UTS (Average)	% EL (Average)	UTS (Average)	% EL (Average)	UTS (Average)	% EL (Average)
1-BM	845.43 MPa	42.44	423.7 MPa	15.2	------	-------
2-Post Welding	863.6 MPa	42.83	467.26 MPa	16.73	410.43 MPa	15.72

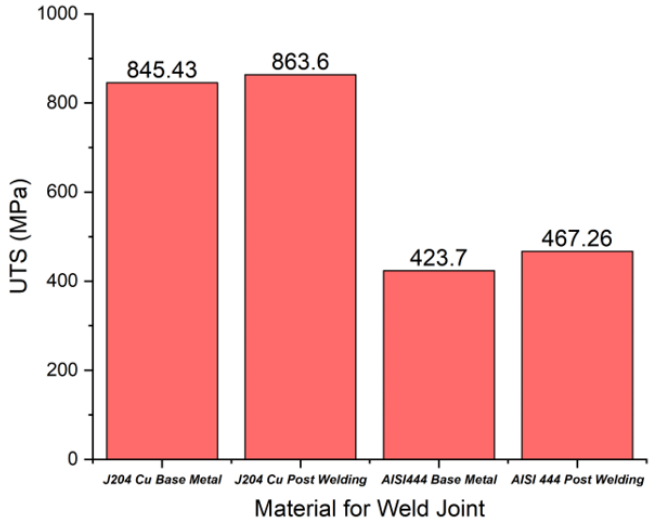

Figure 5.2: Ultimate Tensile Strengths of Weld Joints

5.3 Impact Test

Taking a sample size of 55 mm × 10 mm × 3 mm, notch angle of 45^0, and depth of 2 mm, the V notch Charpy impact test was performed at room temperature. To achieve better and more accurate results two samples were tested for each weld joint. The test samples were taken from the transverse section of the WM of dimensions as per the standard. To ensure the stress concentration and failure of the samples from the weld zone, the notch was created in the weld zone only. The distinct weld of J204 Cu and AISI 444 showed an average toughness value of ~53 J and ~ 31 J respectively, on the other side the dissimilar joint of J204 Cu and AISI 444 exhibited a toughness as ~46 J as summarized in Table 5.2. Literature exhibits the mechanical properties testing of FSS grade (AISI 409M) using GTAW and reveals that the impact toughness of selected material confirms to be in the range of 20 J and comparing that the material selected for the current study has better impact toughness (Lakshminarayanan *et al.*, 2009). It is believed that the addition of copper as an alloying element in J204 Cu promotes the formation of advantageous precipitates, such as copper-rich intermetallic phases, which contribute to the alloy's strengthening mechanisms. These reinforcing mechanisms can further increase the material's impact strength.

Table 5.2: Impact Test Results

Weld Material	Impact Toughness Value
J204 Cu	~53 J
AISI 444	~31 J
J204 Cu and AISI 444	~46 J

5.4 Hardness Test

The hardness test of the weld, HAZ, and BM of the weld joints was carried out by the Vickers microhardness test method. The hardness was taken at different closest locations to ensure the best results. The data obtained from the hardness test is used to study the hardness behavior in different regions along the weld joint. It is observed that the average hardness value in HAZ is more than WM and BM. The primary reason behind this is because of the different cooling rates that occur throughout the welding process. During the welding process, the BM in the HAZ is brought to a high temperature, either close to or over its melting point, and is then rapidly cooled by the surrounding BM, which is typically cooler and functions as a heat sink. Because of the rapid cooling, the metal in the HAZ solidifies very quickly, producing a microstructure that is both harder and brittle than the BM.

The hardness distribution across weld joints made of a similar material of J204 Cu has been shown in Figure 5.3. In ASSs like J204 Cu, the precipitation of Cr carbides is one of the key factors that contribute to the high hardness value in the HAZ. These carbides are difficult to fracture, and their presence in the HAZ may be responsible for the region's increased hardness. Apart from this, the WM in J204 Cu (ASS) normally has a more uniform and homogeneous microstructure comprised of austenite, which has a lower hardness value than the hard microstructures created in the HAZ.

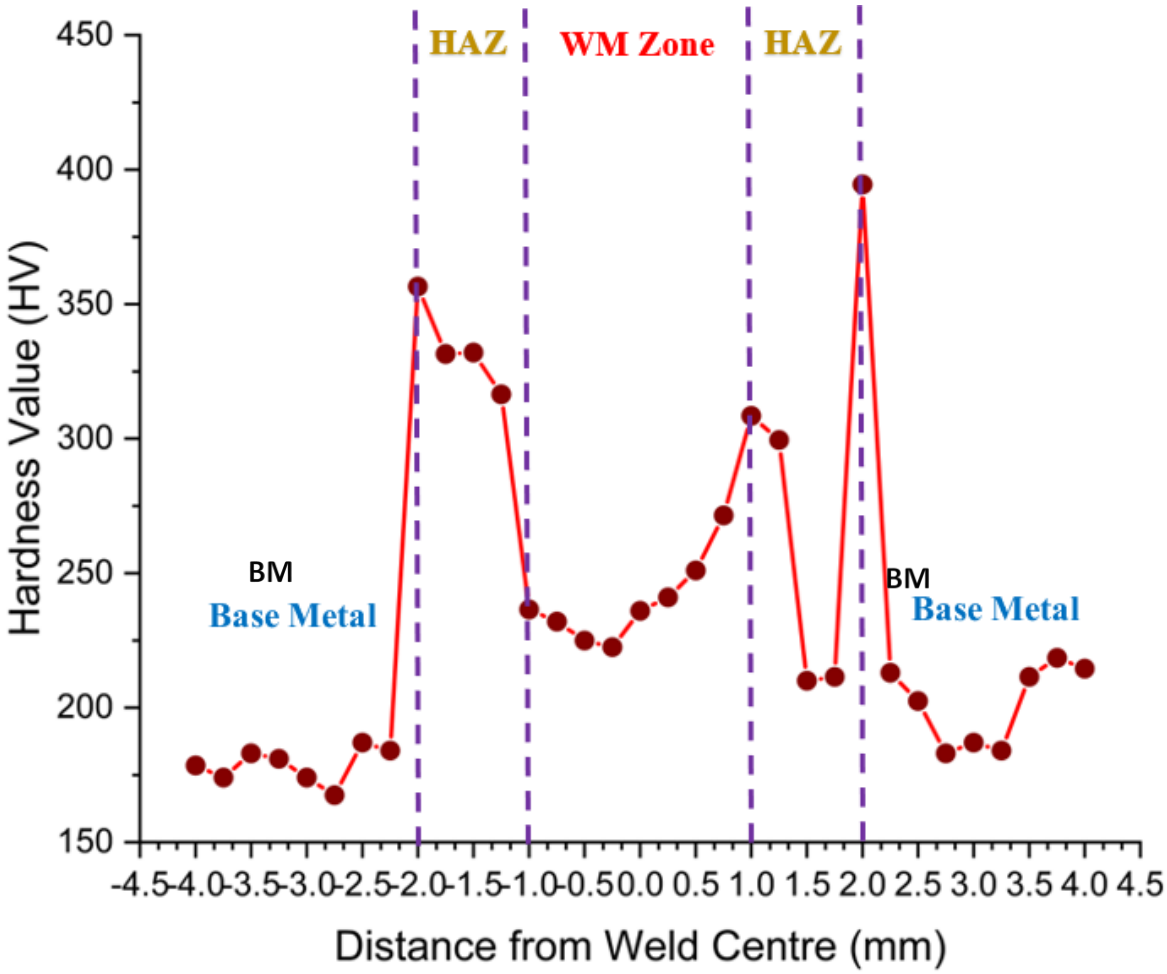

Figure 5.3: Hardness Distributions in Weld Joint (similar) of J204 Cu

The investigation done on hardness distribution along the weld joint of a similar joint made of AISI 444 reveals that the average value of hardness in HAZ of these weld joints is more and it can be seen in Figure 5.4. This is because super FSSs, such as AISI 444, contain higher concentrations of Cr, molybdenum, and nitrogen than conventional FSSs. During the welding of super FSSs, the HAZ undergoes a thermal cycle that results in microstructure transformation, which may impact hardness value. In these steels, the precipitation of secondary phases, such as the sigma phase and chi-phase, is primarily responsible for the high hardness value in the HAZ relative to the weld metal.

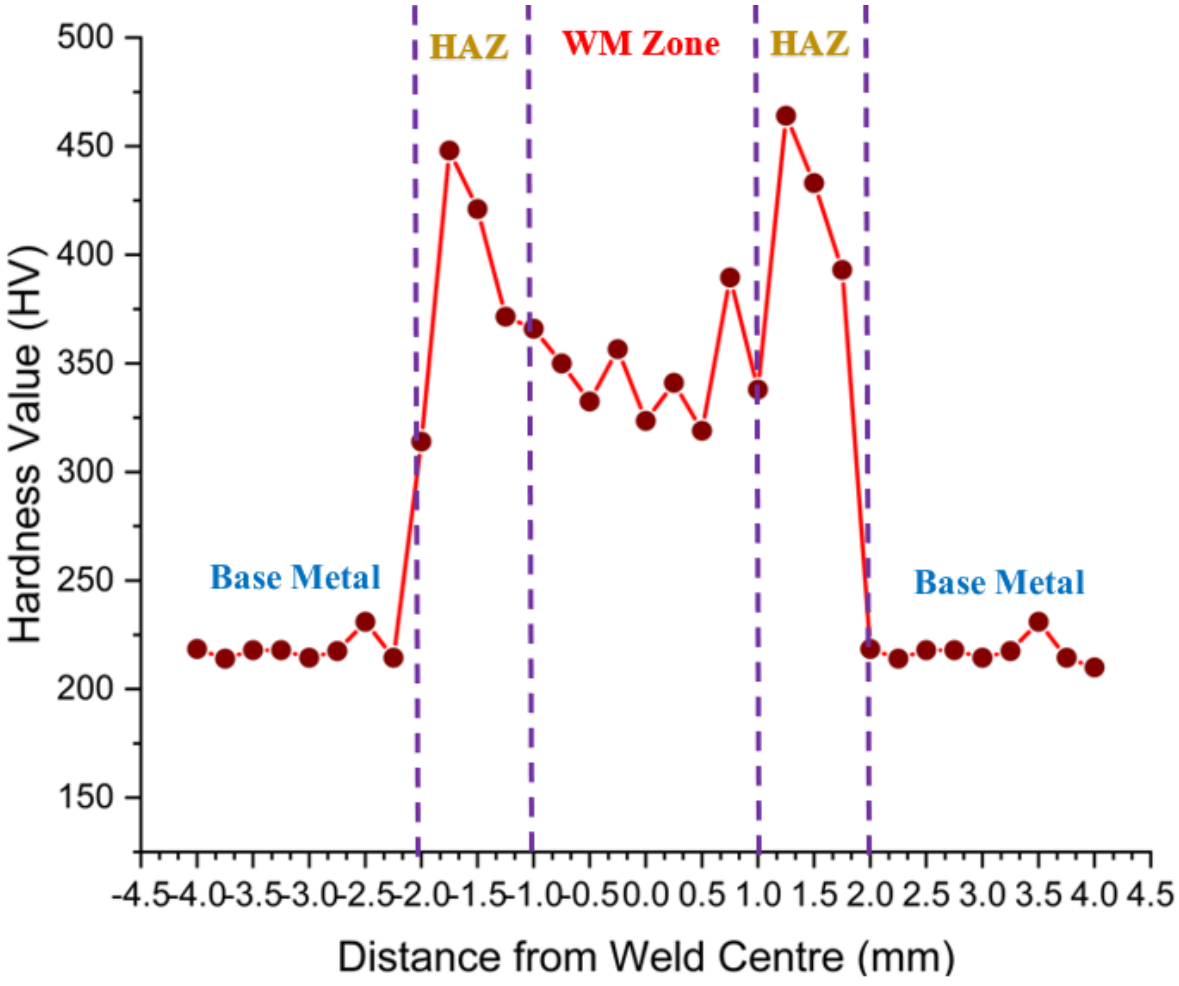

Figure 5.4: Hardness Distributions in Weld Joint (similar) of AISI 444

Figure 5.5 depicts a comparative analysis of hardness distribution along the weld joints prepared with similar materials of J204 Cu, AISI 444, and dissimilar joints once these materials are welded together. In the case of welding J204Cu and 444, the compositional and crystalline distinctions between the two BMs will likely result in the formation of a mixed or transitional zone. Due to the unique microstructure formed during welding, the mixed zone will likely have a distinct hardness value from the BMs.

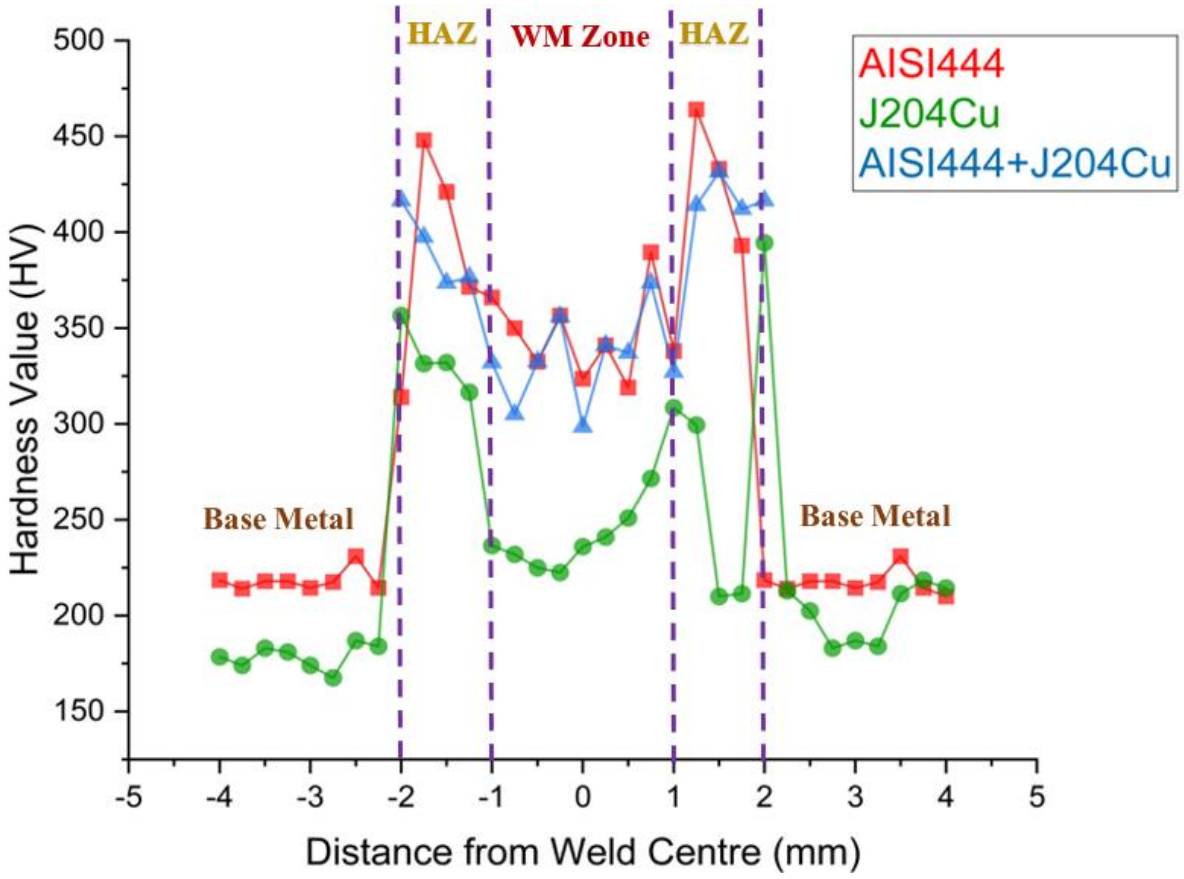

Figure 5.5: Hardness Distribution Near The Weld Center of All Welded Joints

5.5 Scanning Electron Microscopy

The results obtained from SEM of the fracture surface of different specimens of the tensile test show the BM is fractured in a ductile manner. Fractures began at the center of the specimens and then extended towards the outer surface by a shear separation. As the specimens were fractured from the BM, therefore analysis of any of the specimens was sufficient to characterize the morphology of BM fracture mode. The SEM micrograph (Figure 5.6) shows that the fracture surface is in the form of dimples which is evidence of the occurrence of ductile fracture in the BM, while the small holes/voids indicate the availability of more strain before fracture.

SS is a polycrystalline material, which means that it is composed of a large number of crystalline grains that are relatively small. The grains have the potential to elongate and distort when subjected to tensile stress, which gives the micrograph the appearance of

fibers. The appearance of elongated and linked structures that are visible on the surface of the material is normally what is meant when the term "fibrous network" is used. The direction and organization of these fibrous networks indicate that the material deforms predominantly via slip or twinning.

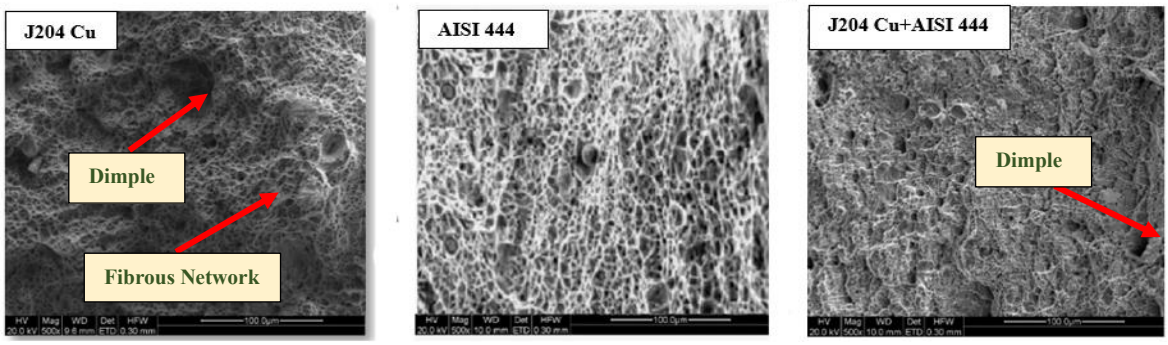

Figure 5.6: Scanning Electron Micrographs of The Fracture Surface of Base Metals

5.6 Corrosion Studies

5.6.1 Weight Loss Test

It was noted that the solutions changed their color when the alloys were submerged in the 0.1 M concentration of all the used solutions. When a specimen of SS is placed into a solution of 0.1 M hydrochloric acid or sulfuric acid, a chemical reaction normally takes place between the acid and the SS, which causes the solution to change color. The change in color acts as a visible indication of the interaction that takes place between the acid and the SS. This reaction might result in the creation of colored compounds or the dissolution of particular components from the SS into the solution, both of which would lead to a change in color. Iron is the primary component of SS, and when this material is exposed to strong acids like hydrochloric acid or sulfuric acid, it may undergo a reaction that results in the formation of iron compounds.

On the first cycle of the test, there was an evident increase in the alloy's weight/mass loss, but no further appreciable change was seen until the test was through. The test result also shows the greatest weight loss of these alloys in terms of corrosion rate in the HCL solution

than the sulphuric acid solution. Figure 5.7 shows the weight loss distribution for 60 days in various corrosive environments.

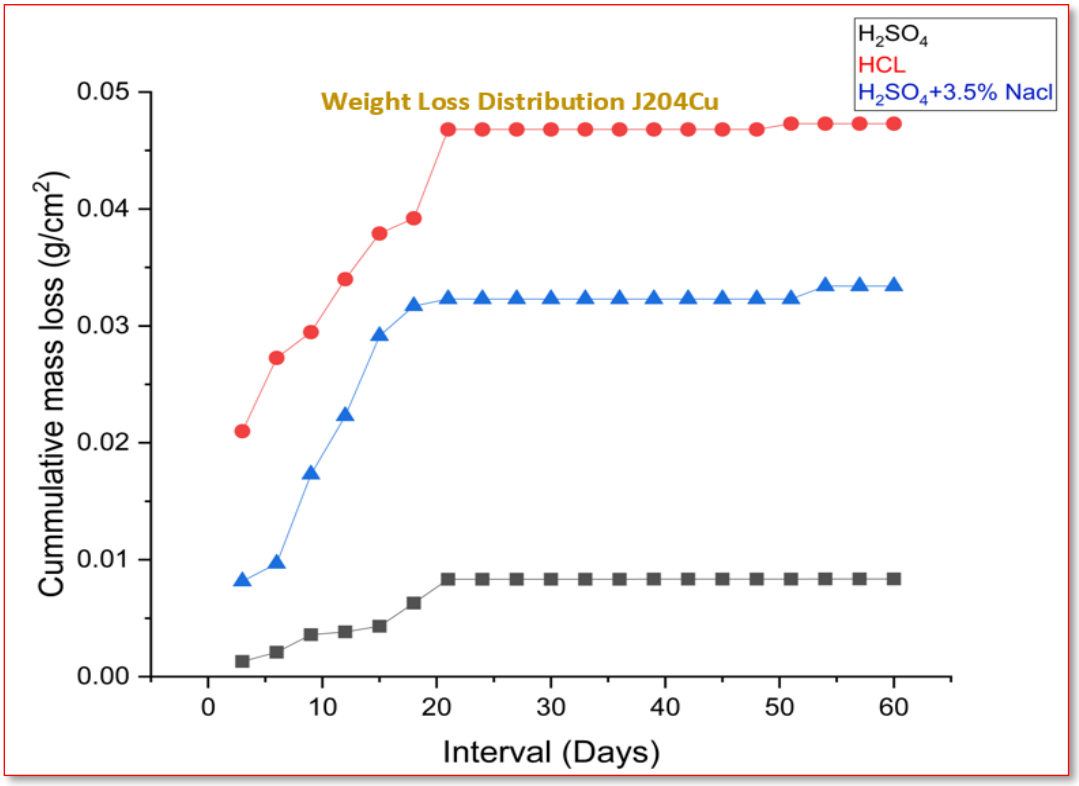

(a) Weight loss distribution of J204 Cu weld samples

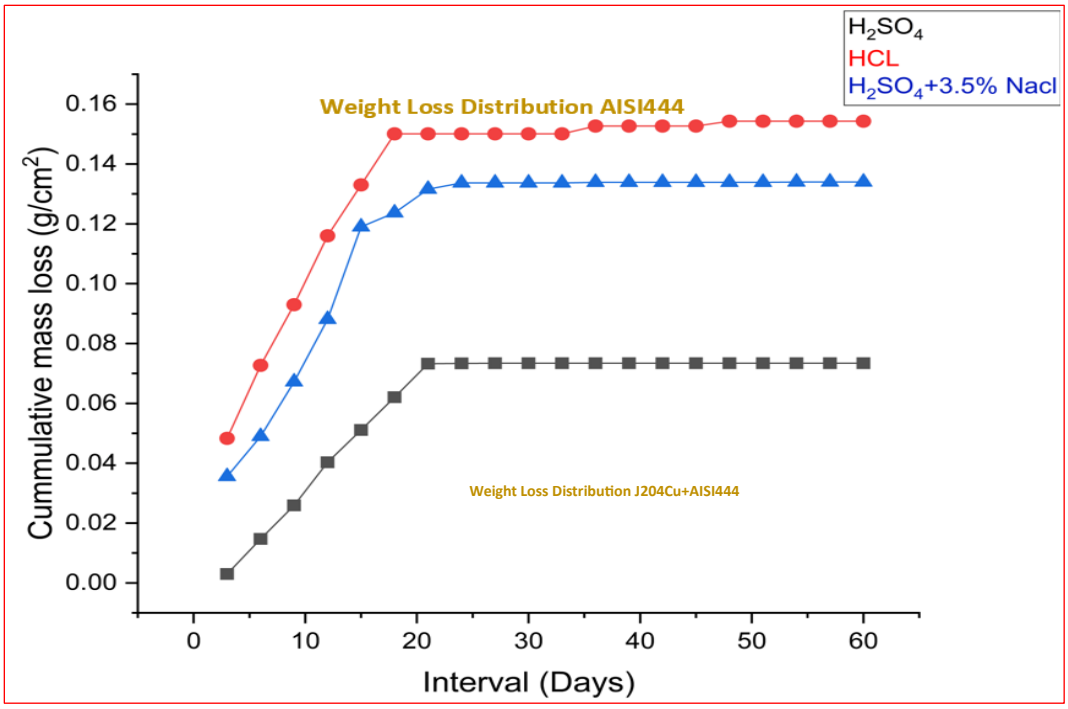

(b) Weight loss distribution of AISI 444 weld samples

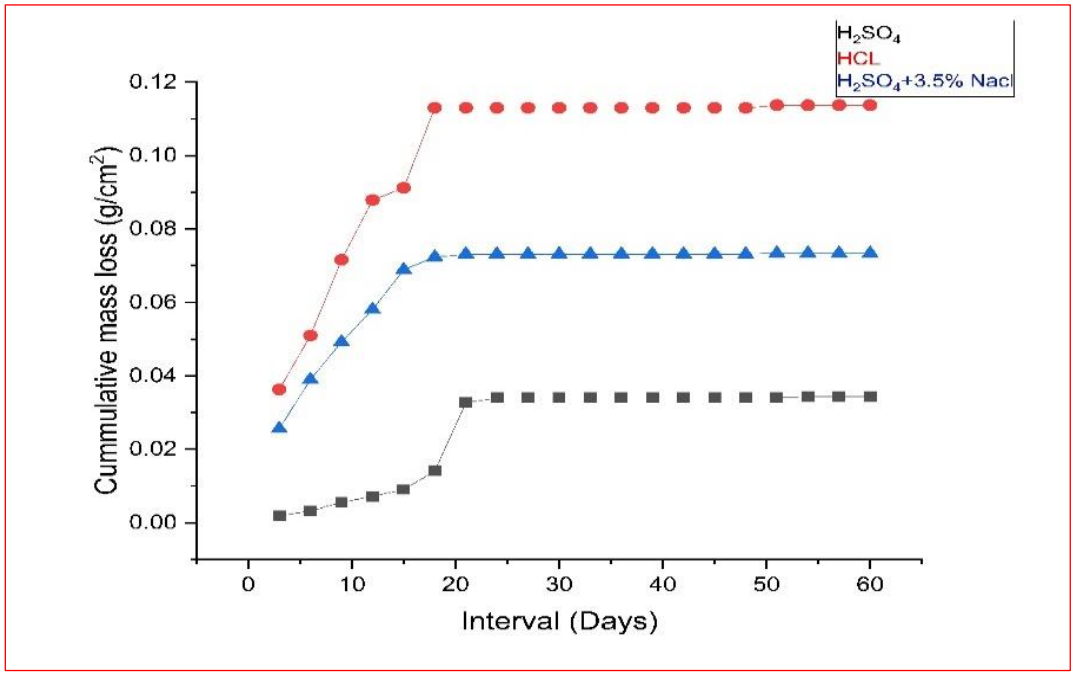

(c) Weight loss distribution of samples of dissimilar weld joints between J204 Cu and AISI 444

Figure 5.7: Weight Loss Distribution of Various Weld Samples in Different Corrosive Solutions

Several parameters, including acid concentration, temperature, and length of exposure time, would affect the rate at which J204 Cu would lose weight in hydrochloric acid (HCl) solution compared to the sulfuric acid solution. Sulfuric acid is less corrosive to copper and copper alloys than hydrochloric acid since copper surfaces can be protected from further corrosion by a passive coating formed by sulfuric acid, however, hydrochloric acid can dissolve this film and speed up the corrosion process. As a result, it is reasonable to anticipate that, all else being equal, the weight loss of J204 Cu in sulfuric acid solution will be less than that in hydrochloric acid solution. However, other variables, such as the presence of additional pollutants or impurities in the acid solution, can also affect the corrosion behavior of copper alloys.

The high Cr and molybdenum content of FSS AISI 444 makes it resistant to corrosion in many different conditions. During a weight loss test, AISI 444 loses significantly less mass in sulfuric acid solution than it does in hydrochloric acid solution. This is likely owing to the different chemical characteristics of the two acids. Strong sulfuric acid can react with the Cr in AISI 444 to generate an inert layer on the steel's surface. This passive layer may prevent additional corrosion of the steel, resulting in less weight loss during the experiment. Additionally, the passive film can aid in re-forming any damaged regions of the steel surface, which further improves its resistance to corrosion. Hydrochloric acid, on the other hand, is a more aggressive acid that can dissolve the passive coating created on the surface of the steel, resulting in a greater corrosion rate and more weight loss during the test. AISI 444's molybdenum might react with hydrochloric acid, decreasing the alloy's resistance to rust and corrosion.

5.6.2 Potentiodynamic Polarization (PDP)Test

This method was utilized to compare the electrochemical properties of welds. As depicted in Figure 5.8, the polarization curves of J204 Cu, AISI 444, and dissimilar J204 Cu and AISI 444 weldments were plotted. AISI444 had the highest pitting potential, followed by the dissimilar joint of J204 Cu-AISI444 weld, whereas J204 Cu had the lowest pitting potential. This is predominantly due to the difference in the formation and stability of their

passive films. This passive film serves as a barrier against aggressive environments, such as chloride ions, which are known to induce pitting corrosion. The pitting potential (Epit) is an important measure for evaluating materials' corrosion resistance, particularly in harsh situations where localized corrosion, such as pitting corrosion, may occur. it is the electrochemical potential at which pitting corrosion begins on the surface of a material. It is a vital parameter in electrochemical corrosion testing, notably in cyclic and potentiodynamic polarization tests. It is determined by constructing a potentiodynamic polarization curve. This test sweeps the applied potential throughout a range while measuring the current.

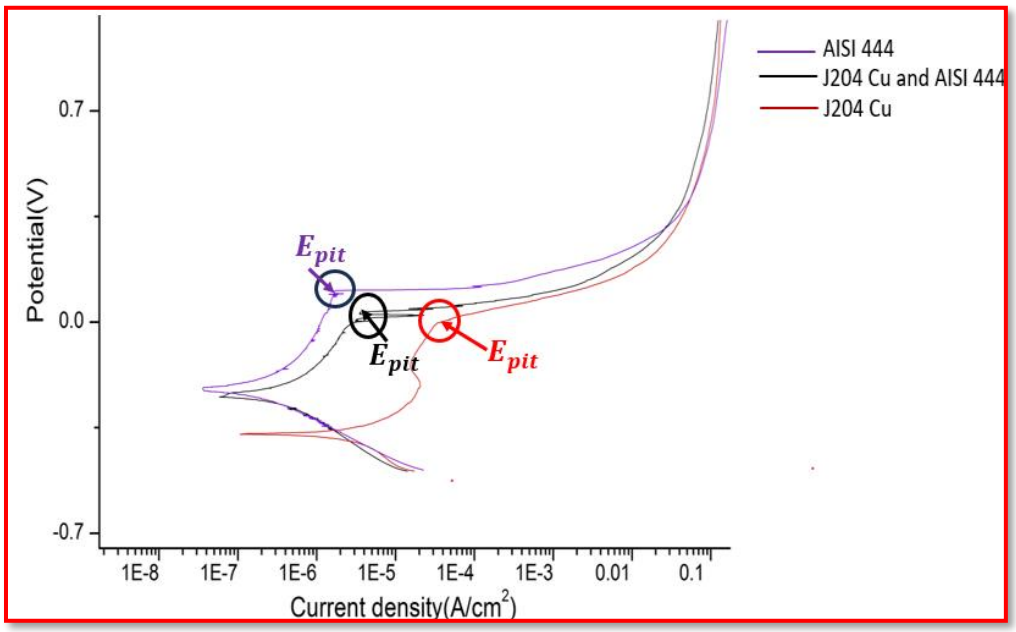

Figure 5.8: Anodic Polarization Curves of Welds

5.6.3 Double Loop Electrochemical Potentiokinetic Reactivation (DLEPR) Test

Welded joints, as a result of a variety of metallurgical changes, the establishment of a Cr-depleted zone, and larger potential differences between grain and grain boundary, are known to be more vulnerable to corrosion attack. As a consequence of this, it is of the

utmost importance to analyze the response of welded materials against corrosion to predict the amount of time that weldments will remain in service in aggressive environments.

The % DOS was calculated using the ratio Ir/Ia, where Ia represented the peak current density during the anodic scan and Ir represented the peak current density during the reversed scan. It is well known that welding conditions are more susceptible to corrosion due to metallurgical changes. The disparity in potential between grain boundaries and grains has accelerated corrosion because of the formation of precipitates, Cr-depleted regions, and strain between grains and grain boundaries. Figure 8 shows the DLEPR curves for similar welds of J204 Cu and AISI 444 as well as for the dissimilar welds of these two materials. The % DOS values calculated for these welds (Table 5.2) showed that among these welds, the J204 Cu weld has the highest DOS followed by dissimilar welds of J204 Cu and AISI 444 weld, while the FSS AISI 444 displays the lowest value of % DOS.

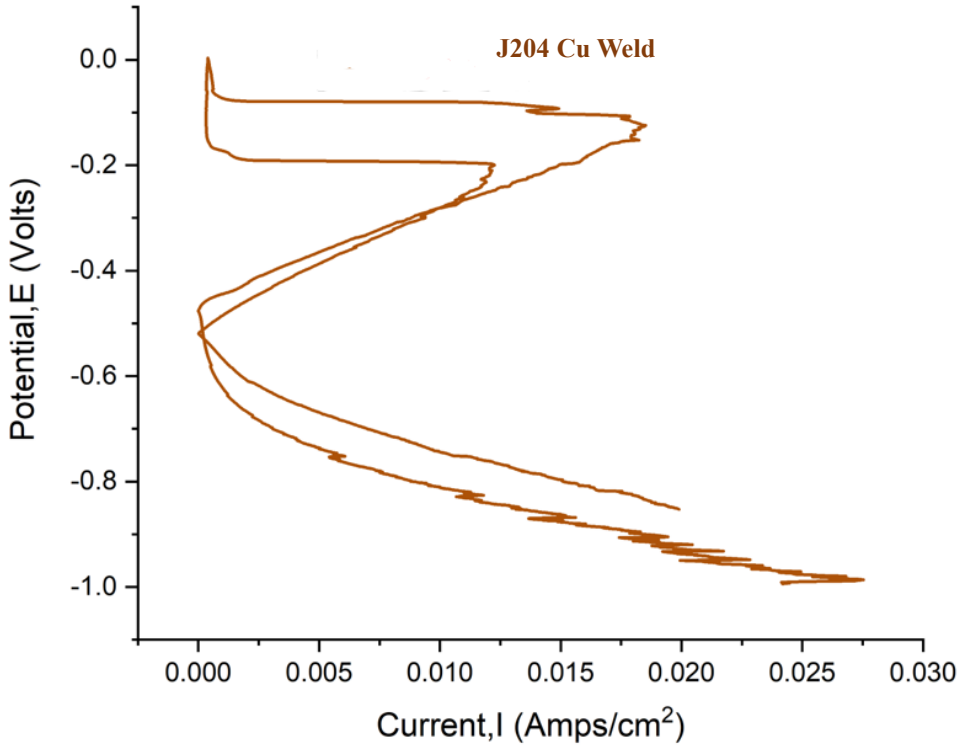

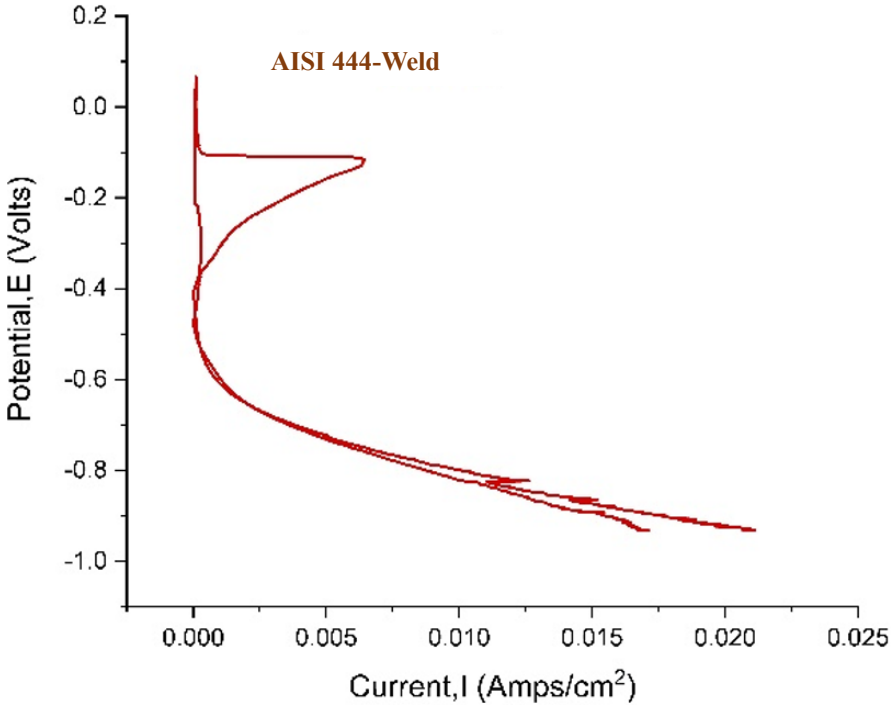

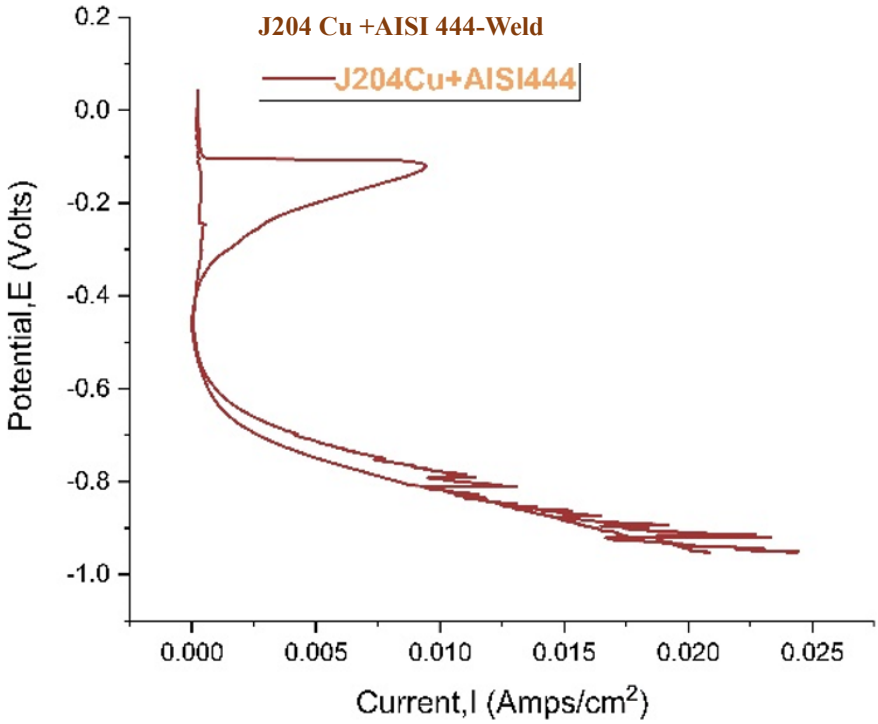

Figure 5.9: DLEPR Curves of Welds

Table 5.3: Weld Sensitivity (DOS)

Sample	Ir, A/cm^2	Ia, A/cm^2	Ir/Ia, % DOS
J204 Cu (similar weld)	0.01225	0.01859	65.89
AISI444 (similar weld)	0.0003	0.0064	4
J204Cu + AISI444 (dissimilar weld)	0.00051	0.00947	5

5.7 EBSD Analysis of the Weldments

Electron backscatter diffraction (EBSD) was used to study the evolution of the microstructure to know the structure of a material revealed by microscopy and micro-texture which is a set of crystallographic orientations with major emphasis on phase analysis of weldments and HAZ. EBSD maps were taken from the transverse direction of the samples perpendicular to the welding direction.

EBSD image maps of weld metals for similar joints of J204 Cu and AISI 444, as well as dissimilar joints of J204 Cu and AISI 444, were shown in Figure 5.10. The use of EBSD makes it possible to make a clearer distinction between the microstructure of the WM microconstituents and the microtexture of the material. The inverse pole figure, often known as the IPF, is a representation of the microstructure's texture and orientations plotted with crystal directions as the axes for the figure. Figure 5.10 illustrated the IPF of J204Cu ASS and AISI 444 FSS and dissimilar weld respectively, which indicated heterogeneous structure in the cases. J204 Cu weld showed face center cubic (FCC) austenite phase along with a small amount of body center cubic (BCC) ferrite. On the other hand, the AISI 444 WM sample exhibited different textural behavior; it showed a ferrite (BCC) matrix with intergranular martensite and showed banded morphology along the welding direction. Martensite is formed as a result of a highly rapid and diffusion-free transition, during which the carbon is kept in solution. In all the cases grain growth occurred which is directly related to the heat input, the higher the heat input larger the grain growth. The color indicated grain orientation in the phase map.

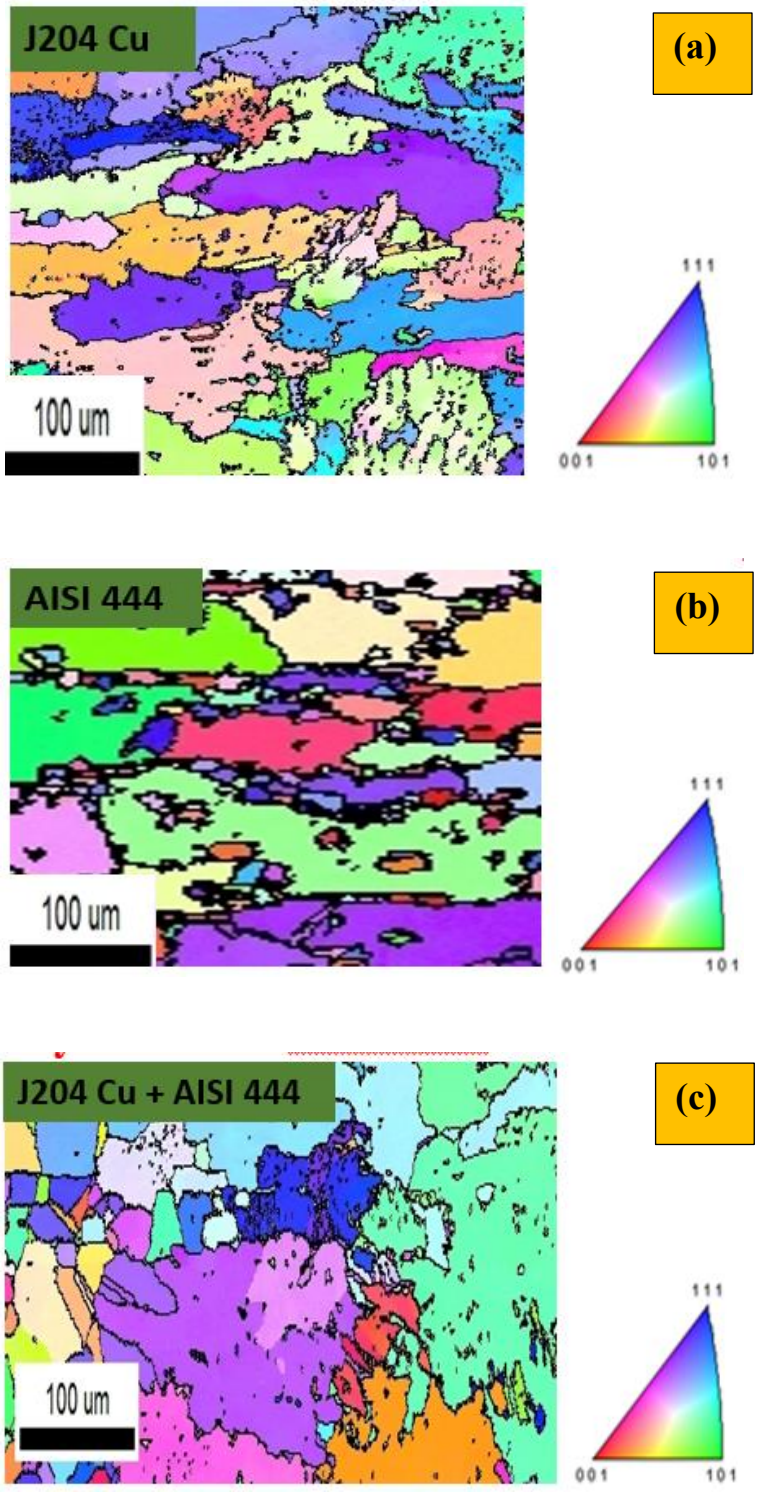

Figure 5.10: EBSD Image Pole Figures (a) J204 Cu WM, (b) AISI 444 WM, (c) J204 Cu + AISI 444 WM.

CHAPTER 6

CONCLUSION AND FUTURE PERSPECTIVES

6.1 Concluded Remarks

The nickel supply constraint and price fluctuations prompted researchers to develop SS alloys with less nickel. J204 Cu and AISI 444 are low nickel SSs with outstanding mechanical properties and corrosion resistance in acidic, alkaline, and chloride conditions which further establishes them to be used in chemical, marine, and food processing sectors where corrosion resistance is essential for long-term reliability. Given the appropriateness of AISI444 and J204 Cu for diverse industrial purposes, they may need to be joined, either to achieve a joint of similar materials or be of dissimilar characteristics. Welding is frequently regarded as the superior method for joining various grades of SS since it creates a metallurgical bond between the base materials, resulting in joints that are robust and durable.

The sound weld joints were obtained for selected SS grades J204 Cu and AISI444 for the various welding conditions using GTAW. The microstructure of WM shows that at the grain boundary, carbide and other alloying materials precipitate. The presence of dark spots in the micrographs supports the availability of foreign elements during welding, while the white spots predominantly in HAZ indicate the presence of ferrite. Owing to increased cooling rates, columnar grains near the fusion line solidify into dendrites. J204 Cu exhibits better ultimate tensile strength and percentage elongation as compared to AISI 444. The SEM images of fractured samples during the tensile test show the ductile fracture in the BM, while the impact toughness tests using Charpy V notched reduced-size samples reveal that ASS grade J204 Cu exhibits better impact toughness as compared to AISI 444. The average hardness value in HAZ is more than WM and BM. The primary reason behind this is because of the different cooling rates that occur throughout the welding process. The precipitation of Cr carbides and secondary phases, such as the sigma phase and chi-phase are the other possible reasons for the high hardness value in HAZ. In each solution, the

corrosion resistance for the welds varies during the weight loss test. The welds of both these steels showed better resistance to sulphuric acid solution than other chloride environments such as hydrochloric acid and sulphuric acid containing 3.5% NaCl. AISI444 has the highest pitting potential, followed by the dissimilar joint of J204 Cu-AISI444 weld, whereas J204 Cu had the lowest pitting potential as a result of the potentiodynamic polarization test and further supported by the DLEPR test.

The important conclusions that can be drawn from the current thesis work have been elaborated in the following points:

Concluded remarks on objective 1:

- As received milled metals like SS sheets possess residual stress and some amount of precipitates due to the thermo-mechanical processes and hence certain pre-weld heat treatment techniques such as solution annealing should be utilized that help in minimizing these undesirable deficits and contribute to homogenizing the microstructure.
- Among the two selected grades of SS for the current work, AISI 444 has already been the subject of the most research, incorporating welding and its other characteristics. However, being a newly developed considering the present industrial revolution and demand, the grade J204 Cu has almost a negligible amount of research on its welding and potential welding processes/techniques. Thus, a suitable welding procedure for J204 Cu weld joints, followed by its validation and investigation of applying the same welding technique for AISI 444 was needed immediately. To overcome this research gap and to identify the appropriate welding technique for SS (J204 Cu) there was a requirement to utilize a suitable decision-making approach and hence attributing the success rate of various approaches available for decision-making, Grey Relational Analysis (GRA) was selected and it has been identified and hence proposed that an appropriate fusion welding technique for joining J204 Cu will be Tungsten Inert Gas (TIG) welding also called GTAW. Considering the GRA approach's results and appropriateness, GTAW was chosen to generate weld joints of both specified SS grades and sound weld joints.

The optimal welding process parameters were 110 A welding current, 22-25 V voltage, 10-12 cm/min travel speed, and 15 liters/min shielding gas flow.

Concluded remarks on objective 2:

- The microstructures obtained using optical microscopy display the precipitation of carbide and other alloying elements at the grain boundaries and the inclusion of foreign elements as a result of welding. The micrograph of dissimilar weld joints developed taking both the steel grades i.e., J204 Cu and AISI 444 yields columnar grains. The microstructures at the fusion line clearly show the epitaxial solidification near the fusion boundary. Columnar grains along the fusion line become dendrites owing to the greater cooling rate during solidification.
- The J204 Cu weld displays better ultimate tensile strength and percentage elongation (~ 863 MPa, ~ 42 %) as compared to AISI 444 weld (~ 467 MPa, ~ 17 %), while the average UTS value of dissimilar weld of these two grades was investigated to be as around 410 MPa.
- The tensile strength of the BM increases with a small amount post-welding and that may be due to the localized heating and swift cooling of the BM during welding creating small, refined grains in the HAZ next to the weld. Compared to the coarser grains of the parent metal, these smaller grains typically result in increased strength and durability. In addition, the inclusion of alloying filler metals in GTAW may interact with the BM, resulting in the development of new phases or strengthening mechanisms that increase tensile strength.
- The specimens prepared out of each weld joint were fractured from the BM and hence supports that produced weld joints have better tensile strength as compared to the respective BM. The results obtained from SEM of the fracture surface indicate that the fracture surface is in the form of dimples which is evidence of the occurrence of ductile fracture of different specimens of the tensile test.
- The distinct weld of J204 Cu and AISI 444 showed an average toughness value of ~53 J and ~ 31 J respectively, on the other side the dissimilar joint of J204 Cu and AISI 444 exhibited a toughness as ~46 J. It is believed that the addition of copper

as an alloying element in J204 Cu promotes the formation of advantageous precipitates, such as copper-rich intermetallic phases, which contribute to the alloy's strengthening mechanisms. These reinforcing mechanisms can further increase the material's impact strength.

- The AISI 444 weld holds higher hardness as compared to the weld of J204 Cu and the dissimilar weld of these two grades. It is observed that the average hardness value in HAZ is more than WM and BM mainly due to the different cooling rates that occur throughout the welding process. In ASSs like J204 Cu, the precipitation of Cr carbides is one of the key factors that may contribute to the high hardness value in the HAZ. AISI 444, contains higher concentrations of Cr, molybdenum, and nitrogen than conventional FSSs. During the welding of these steels, the HAZ undergoes a thermal cycle that results in microstructure transformation, which may impact hardness value. In these steels, the precipitation of secondary phases, such as the sigma phase and chi-phase may also be responsible for the high hardness value in the HAZ relative to the weld metal.

Concluded remarks on objective 3:

- The weight loss test conducted to study the behavior of the weld joints against general corrosion displays that during the initial cycles of the test, there was an evident increase in the alloy's weight/mass loss, but no further appreciable change was seen until the test was through. The test result also shows the greatest weight loss of these alloys in terms of corrosion rate in the HCL solution than the sulphuric acid solution.
- AISI444 weld had the highest pitting potential, followed by the dissimilar joint of J204 Cu-AISI444 weld, whereas J204 Cu had the lowest pitting potential. This is predominantly due to the difference in the formation and stability of their passive films.
- In the DLEPR test, the J204 Cu weld has the highest DOS followed by dissimilar welds of J204 Cu and AISI 444 weld, while the FSS AISI 444 displays the lowest value of % DOS.

Concluded remarks on objective 4:

- Electron backscatter diffraction (EBSD) illustrated the IPF of J204Cu ASS and AISI 444 FSS and dissimilar weld respectively, which indicated heterogeneous structure in the cases. J204 Cu weld showed face center cubic (FCC) austenite phase along with a small amount of body center cubic (BCC) ferrite. On the other hand, the AISI 444 WM sample exhibited different textural behavior; it showed a ferrite (BCC) matrix with intergranular martensite and showed banded morphology along the welding direction.

The findings of this study have immediate consequences for industries that rely on corrosion-resistant stainless steels, such as the petrochemical, marine, and chemical processing sectors. The knowledge gained from this thesis not only increases academic understanding of these materials, but also gives practical solutions to problems encountered by experts in the field. The welding methods investigated in this study, together with thorough microstructural investigations, gave a more comprehensive knowledge of the metallurgical modifications. By shedding light on optimal welding ailments and processes, this study makes it easier to develop robust welds that fulfill industry requirements, improving the structural integrity and performance of stainless-steel components. Furthermore, corrosion resistance studies done under diverse environmental circumstances provide vital information for applications in corrosive industry.

6.2 Limitations and Future Scope

While this study strives to provide valuable insights into the welding and corrosion behavior of low-nickel austenitic and superferritic stainless steels, it possesses some limitations also. Firstly, the available materials and sample sizes might restrict the generalizability of the findings to a broader range of steels. Additionally, replicating real-world conditions perfectly in the lab can be challenging due to the extreme sensitivity of corrosion behavior to environmental factors. External conditions like temperature, humidity, and specific chemical exposures may influence the results to some extent. Furthermore, even within the same grade, inherent variations in steel characteristics can

impact the repeatability of observations. Despite meticulous planning and execution, human error is an ever-present possibility, potentially affecting the accuracy and reliability of the data. Recognizing these limitations allows for a more nuanced interpretation of the results and guides future research to address these areas for comprehensive understanding. The present research work is consisting the following future research scope for the researchers:

(a) Investigation of the effects of various welding parameters (such as heat input, welding speed, and shielding gas composition) as well as other weld processes on the microstructure and corrosion resistance of selected stainless steels.

(b) Further experimental investigation can be done using other suitable weld fillers for the GTAW process and a comparative study may be established.

(c) Mechanical tests like bending tests and cryogenic tests may be conducted to provide further insights into the toughness and resilience of the welded samples and their weld integrity.

(d) A fatigue test may be performed to explore the performance of the weld against dynamic loading conditions.

(e) The performed corrosion tests in the current study may again be repeated in another corrosive environment that may provide added acumens about welded joints.

REFERENCES

Advaith, V., Vaisikan, A., Thirumalini, S., Padmanaban, R., Arivarasu, M. and Ram Prabhu, T. (2019), "Comparative studies on pulsed GTAW and AGTAW on dissimilar alloy C-22 and AISI 316L weldments", *Materials Today: Proceedings*, Vol. 27, doi: 10.1016/j.matpr.2020.01.613.

Aguilar, S., Tabares, R. and Serna, C. (2013), "Microstructural Transformations of Dissimilar Austenite-Ferrite Stainless Steels Welded Joints", *Journal of Materials Physics and Chemistry*, doi: 10.12691/jmpc-1-4-2.

Akisanya, A.R., Obi, U. and Renton, N.C. (2012), "Effect of ageing on phase evolution and mechanical properties of a high tungsten super-duplex stainless steel", *Materials Science and Engineering: A*, doi: 10.1016/j.msea.2011.12.087.

Alipooramirabad, H., Paradowska, A., Ghomashchi, R. and Reid, M. (2017), "Investigating the effects of welding process on residual stresses, microstructure and mechanical properties in HSLA steel welds", *Journal of Manufacturing Processes*, Vol. 28, doi: 10.1016/j.jmapro.2017.04.030.

Ameer, M.A., Fekry, A.M. and Heakal, F.E.T. (2004), "Electrochemical behaviour of passive films on molybdenum-containing austenitic stainless steels in aqueous solutions", *Electrochimica Acta*, Vol. 50 No. 1, doi: 10.1016/j.electacta.2004.07.011.

Amuda, M.O.H. and Mridha, S. (2011), "An overview of sensitization dynamics in ferritic stainless steel welds", *International Journal of Corrosion*, Vol. 2011, doi: 10.1155/2011/305793.

Anand, N.R., Chavan, V.M. and Sawant, N.K. (2013), *THE EFFECT OF SHIELDING GASES ON MECHANICAL PROPERTIES AND MICROSTRUCTURE OF AUSTENITIC STAINLESS STEEL WELDMENTS*, *Int. J. Mech. Eng. & Rob. Res*.

Antunes, P.D., Correa, E.O., Barbosa, R.P., Silva, E.M., Padilha, A.F. and Guimaraes,

P.M. (2013), “Effect of weld metal chemistry on stress corrosion cracking behavior of AISI 444 ferritic stainless steel weldments in boiling chloride solution”, *Materials and Corrosion*, Vol. 64 No. 5, pp. 415–421, doi: 10.1002/maco.201106186.

Arifin, A. (2020), “Dissimilar metal welding using Shielded metal arc welding : A Review”, *Technology Report of Kansai University*.

Arora, H., Bajwa, M., Pandey, P.K. and Singh, V. (2015), “Finite element simulation of angular distortion in carbon steel butt welded joint”, *International Journal of Applied Engineering Research*, Vol. 10 No. 7.

Attah, B.I., Lawal, S.A., Bala, K.C., Ikumapayi, O.M., Adedipe, O., Mahto, R.P. and Akinlabi, E.T. (2023), “Optimization and numerical analysis of friction stir welding parameters of AA7075-T651 and AA 1200-H19 using tapered tool”, *International Journal on Interactive Design and Manufacturing*, doi: 10.1007/s12008-023-01329-1.

Backhouse, A. and Baddoo, N. (2021), “Recent developments of stainless steels in structural applications”, *Ce/Papers*, doi: 10.1002/cepa.1560.

Baddoo, N.R. (2008), “Stainless steel in construction: A review of research, applications, challenges and opportunities”, *Journal of Constructional Steel Research*, Vol. 64 No. 11, pp. 1199–1206, doi: 10.1016/j.jcsr.2008.07.011.

Badji, R., Bouabdallah, M., Bacroix, B., Kahloun, C., Belkessa, B. and Maza, H. (2008), “Phase transformation and mechanical behavior in annealed 2205 duplex stainless steel welds”, *Materials Characterization*, Vol. 59 No. 4, pp. 447–453, doi: 10.1016/j.matchar.2007.03.004.

Balachandran, G., Bhatia, M.L., Ballal, N.B. and Krishna Rao, P. (2000), “Processing nickel free high nitrogen austenitic stainless steels through conventional electroslag remelting process”, *ISIJ International*, doi: 10.2355/isijinternational.40.478.

Balasubramanian, V., Varahamoorthy, R., Ramachandran, C.S. and Muralidharan, C.

(2009), “Selection of welding process for hardfacing on carbon steels based on quantitative and qualitative factors”, *International Journal of Advanced Manufacturing Technology*, doi: 10.1007/s00170-008-1406-8.

Banovic, S.W., DuPont, J.N. and Marder, A.R. (2001), “Dilution control in gas-tungsten-arc welds involving superaustenitic stainless steels and nickel-based alloys”, *Metallurgical and Materials Transactions B: Process Metallurgy and Materials Processing Science*, doi: 10.1007/s11663-001-0104-9.

Barbosa, C. and Abud, I. (2013), “Recent Developments on Martensitic Stainless Steels for Oil and Gas Production”, *Recent Patents on Corrosion Science*, Vol. 3 No. 1, doi: 10.2174/22106839112029990004.

Bateni, M.R., Szpunar, J.A., Wang, X. and Li, D.Y. (2006), “Wear and corrosion wear of medium carbon steel and 304 stainless steel”, *Wear*, Vol. 260 No. 1–2, doi: 10.1016/j.wear.2004.12.037.

Behm, V., Höfemann, M., Hatscher, A., Springer, A., Kaierle, S., Hein, D., Otto, M., *et al.* (2014), “Investigations on laser beam welding dissimilar material combinations of austenitic high manganese (FeMn) and ferrite steels”, *Physics Procedia*, doi: 10.1016/j.phpro.2014.08.049.

Bellezze, T., Giuliani, G. and Roventi, G. (2018), “Study of stainless steels corrosion in a strong acid mixture. Part 1: cyclic potentiodynamic polarization curves examined by means of an analytical method”, *Corrosion Science*, doi: 10.1016/j.corsci.2017.10.012.

Bitondo, C., Bossio, A., Monetta, T., Curioni, M. and Bellucci, F. (2014), “The effect of annealing on the corrosion behaviour of 444 stainless steel for drinking water applications”, *Corrosion Science*, Elsevier Ltd, Vol. 87, pp. 6–10, doi: 10.1016/j.corsci.2014.06.025.

Borgioli, F. (2020), “From austenitic stainless steel to expanded austenite-s phase: Formation, characteristics and properties of an elusive metastable phase”, *Metals*,

doi: 10.3390/met10020187.

Boumerzoug, Z. (2021), “A Review: Welding by Laser Beam of Dissimilar Metals”, *Aspects in Mining & Mineral Science*, doi: 10.31031/amms.2021.08.000683.

Brnic, J., Turkalj, G., Canadija, M., Lanc, D. and Krscanski, S. (2011), “Martensitic stainless steel AISI 420 - Mechanical properties, creep and fracture toughness”, *Mechanics of Time-Dependent Materials*, Vol. 15 No. 4, doi: 10.1007/s11043-011-9137-x.

Cashell, K.A. and Baddoo, N.R. (2014), “Ferritic stainless steels in structural applications”, *Thin-Walled Structures*, doi: 10.1016/j.tws.2014.03.014.

Ceschini, L. and Minak, G. (2008), “Fatigue behaviour of low temperature carburised AISI 316L austenitic stainless steel”, *Surface and Coatings Technology*, Vol. 202 No. 9, doi: 10.1016/j.surfcoat.2007.07.066.

Chahal, R. and Sharma, P. (2022), “A REVIEW ON SUBMERGED ARC WELDING”, *International Research Journal of Engineering and Technology*.

Chan, K.W. and Tjong, S.C. (2014), “Effect of secondary phase precipitation on the corrosion behavior of duplex stainless steels”, *Materials*, doi: 10.3390/ma7075268.

Chandra-ambhorn, S., Chauiphan, W., Sukwattana, N.C., Pudkhunthod, N. and Komkham, S. (2012), “Plasma arc welding between AISI 304 and AISI 201 stainless steels using a technique of mixing nitrogen in shielding gas”, *Advanced Materials Research*, Vol. 538–541, pp. 1464–1468, doi: 10.4028/www.scientific.net/AMR.538-541.1464.

Charles, J. (2008), “Duplex stainless steels, a review after DSS’07 held in Grado”, *Revue de Metallurgie. Cahiers D’Informations Techniques*, Vol. 105 No. 3, doi: 10.1051/metal:2008028.

Chen, C.J., Yan, K., Qin, L., Zhang, M., Wang, X., Zou, T. and Hu, Z. (2017), “Effect of Heat Treatment on Microstructure and Mechanical Properties of Laser Additively

Manufactured AISI H13 Tool Steel", *Journal of Materials Engineering and Performance*, doi: 10.1007/s11665-017-2992-0.

Chen, Y., Yang, B., Zhou, Y., Wu, Y. and Zhu, H. (2020), "Evaluation of pitting corrosion in duplex stainless steel Fe20Cr9Ni for nuclear power application", *Acta Materialia*, Vol. 197, doi: 10.1016/j.actamat.2020.07.046.

Choubey, A. and Jatti, V.S. (2014), "Influence of heat input on mechanical properties and microstructure of austenitic 202 grade stainless steel weldments", *WSEAS Transactions on Applied and Theoretical Mechanics*.

Chuaiphan, W. and Srijaroenpramong, L. (2012), "Effect of filler alloy on microstructure, mechanical and corrosion behaviour of dissimilar weldment between AISI 201 stainless steel and low carbon steel sheets produced by a gas tungsten arc welding", *Advanced Materials Research*, Vol. 581–582, doi: 10.4028/www.scientific.net/AMR.581-582.808.

Coniglio, N. and Cross, C.E. (2013), "Initiation and growth mechanisms for weld solidification cracking", *International Materials Reviews*, doi: 10.1179/1743280413Y.0000000020.

Covert, R. a. and Tuthill, A.H. (2000), "Stainless Steels : An Introduction to Their Metallurgy and Corrosion Resistance", *Dairy, Food and Environmental Sanitation*, Vol. 20 No. 7.

Dadfar, M., Fathi, M.H., Karimzadeh, F., Dadfar, M.R. and Saatchi, A. (2007), "Effect of TIG welding on corrosion behavior of 316L stainless steel", *Materials Letters*, Vol. 61 No. 11–12, pp. 2343–2346, doi: 10.1016/j.matlet.2006.09.008.

Derazkola, H.A., Gil, E.G., Murillo-Marrodán, A. and Méresse, D. (2021), "Review on dynamic recrystallization of martensitic stainless steels during hot deformation: Part i—experimental study", *Metals*, doi: 10.3390/met11040572.

Devakumar, D. and Jabaraj, D. (2014), "Research on Gas Tungsten Arc Welding of

Stainless Steel–An Overview", *International Journal of Scientific & Engineering Research*, Vol. 5 No. 1.

Deyev, G. and Deyev, D. (2005), *Surface Phenomena in Fusion Welding Processes*, *Surface Phenomena in Fusion Welding Processes*, doi: 10.1201/9781420036299.

Donahue, J.R., Lass, A.B. and Burns, J.T. (2017), "The interaction of corrosion fatigue and stress-corrosion cracking in a precipitation-hardened martensitic stainless steel", *Npj Materials Degradation*, doi: 10.1038/s41529-017-0013-2.

Dong, Z., Li, Y., Lee, B., Babkin, A. and Chang, Y. (2022), "Research status of welding technology of ferritic stainless steel", *International Journal of Advanced Manufacturing Technology*, doi: 10.1007/s00170-021-08128-6.

Esmailzadeh, S., Aliofkhazraei, M. and Sarlak, H. (2018), "Interpretation of Cyclic Potentiodynamic Polarization Test Results for Study of Corrosion Behavior of Metals: A Review", *Protection of Metals and Physical Chemistry of Surfaces*, doi: 10.1134/S207020511805026X.

Francis, R. and Byrne, G. (2021), "Duplex stainless steels—alloys for the 21st century", *Metals*, doi: 10.3390/met11050836.

Fu, H., Min, J., Zhao, H., Xu, Y., Hu, P., Peng, J. and Dong, H. (2019), "Improved mechanical properties of aluminum modified ultra-pure 429 ferritic stainless steels after welding", *Materials Science and Engineering: A*, Vol. 749, doi: 10.1016/j.msea.2019.01.106.

Gardner, L. (2019), "Stability and design of stainless steel structures – Review and outlook", *Thin-Walled Structures*, doi: 10.1016/j.tws.2019.04.019.

Gardner, L., Insausti, A., Ng, K.T. and Ashraf, M. (2010), "Elevated temperature material properties of stainless steel alloys", *Journal of Constructional Steel Research*, doi: 10.1016/j.jcsr.2009.12.016.

Ghassemieh, E. (2011), "Materials in Automotive Application, State of the Art and

Prospects", *New Trends and Developments in Automotive Industry*, doi: 10.5772/13286.

Gholami, M., Hoseinpoor, M. and Moayed, M.H. (2015), "A statistical study on the effect of annealing temperature on pitting corrosion resistance of 2205 duplex stainless steel", *Corrosion Science*, doi: 10.1016/j.corsci.2015.01.054.

Goode, K.R., Asteriadou, K., Robbins, P.T. and Fryer, P.J. (2013), "Fouling and cleaning studies in the food and beverage industry classified by cleaning type", *Comprehensive Reviews in Food Science and Food Safety*, Vol. 12 No. 2, doi: 10.1111/1541-4337.12000.

Goyal, S., Sandhya, R., Valsan, M. and Bhanu Sankara Rao, K. (2009), "The effect of thermal ageing on low cycle fatigue behaviour of 316 stainless steel welds", *International Journal of Fatigue*, Vol. 31 No. 3, doi: 10.1016/j.ijfatigue.2008.07.006.

Guiraldenq, P. and Hardouin Duparc, O. (2017), "The genesis of the Schaeffler diagram in the history of stainless steel", *Metallurgical Research and Technology*, Vol. 114 No. 6, doi: 10.1051/metal/2017059.

Haftlang, F., Asghari-Rad, P., Moon, J., Zargaran, A., Lee, K.A., Hong, S.J. and Kim, H.S. (2021), "Simultaneous effects of deformation-induced plasticity and precipitation hardening in metastable non-equiatomic FeNiCoMnTiSi ferrous medium-entropy alloy at room and liquid nitrogen temperatures", *Scripta Materialia*, Vol. 202, doi: 10.1016/j.scriptamat.2021.114013.

Haider, S.F., Quazi, M.M., Bhatti, J., Nasir Bashir, M. and Ali, I. (2019), "Effect of Shielded Metal Arc Welding (SMAW) parameters on mechanical properties of low-carbon, mild and stainless-steel welded joints: A review", *Journal of Advances in Technology and Engineering Research*, doi: 10.20474/jater-5.5.1.

Hasan, M.A., Yan, K., Lim, S., Akiyama, M. and Frangopol, D.M. (2020), "LCC-based identification of geographical locations suitable for using stainless steel rebars in

reinforced concrete girder bridges", *Structure and Infrastructure Engineering*, Vol. 16 No. 9, doi: 10.1080/15732479.2019.1703758.

Hilbert, L.R., Bagge-Ravn, D., Kold, J. and Gram, L. (2003), "Influence of surface roughness of stainless steel on microbial adhesion and corrosion resistance", *International Biodeterioration and Biodegradation*, Vol. 52 No. 3, doi: 10.1016/S0964-8305(03)00104-5.

Hochanadel, P.W., Lienert, T.J., Martinez, J.N., Martinez, R.J. and Johnson, M.Q. (2011), "Weld solidification cracking in 304 to 304l stainless steel", *Hot Cracking Phenomena in Welds III*, doi: 10.1007/978-3-642-16864-2_9.

Hossein Nedjad, S., Yildiz, M. and Saboori, A. (2023), "Solidification behaviour of austenitic stainless steels during welding and directed energy deposition", *Science and Technology of Welding and Joining*, doi: 10.1080/13621718.2022.2115664.

Huang, C.X., Yang, G., Gao, Y.L., Wu, S.D. and Zhang, Z.F. (2008), "Influence of processing temperature on the microstructures and tensile properties of 304L stainless steel by ECAP", *Materials Science and Engineering: A*, Vol. 485 No. 1–2, doi: 10.1016/j.msea.2007.08.067.

Ibrahim, I.A., Mohamat, S.A., Amir, A. and Ghalib, A. (2012), "The effect of Gas Metal Arc Welding (GMAW) processes on different welding parameters", *Procedia Engineering*, Vol. 41, doi: 10.1016/j.proeng.2012.07.342.

Ibrahim, M.A.M., Abd El Rehim, S.S. and Hamza, M.M. (2009), "Corrosion behavior of some austenitic stainless steels in chloride environments", *Materials Chemistry and Physics*, Vol. 115 No. 1, doi: 10.1016/j.matchemphys.2008.11.016.

"Introduction to Surface Engineering for Corrosion and Wear Resistance". (2020), *Surface Engineering for Corrosion and Wear Resistance*, doi: 10.31399/asm.tb.secwr.t68350001.

Joseph, A., Rai, S.K., Jayakumar, T. and Murugan, N. (2005), "Evaluation of residual

stresses in dissimilar weld joints", *International Journal of Pressure Vessels and Piping*, doi: 10.1016/j.ijpvp.2005.03.006.

K Srivastava, A. and Sharma, A. (2017), "Advances in Joining and Welding Technologies for Automotive and Electronic Applications", *American Journal of Materials Engineering and Technology*, doi: 10.12691/materials-5-1-2.

Kah, P., Suoranta, R. and Martikainen, J. (2013), "Advanced gas metal arc welding processes", *International Journal of Advanced Manufacturing Technology*, Vol. 67 No. 1–4, doi: 10.1007/s00170-012-4513-5.

Kahar, D.S.D. (2017), "Duplex Stainless Steels-An overview", *International Journal of Engineering Research and Applications*, doi: 10.9790/9622-0704042736.

Kang, B.Y., Prasad, Y.K.D.V., Kang, M.J., Kim, H.J. and Kim, I.S. (2009), "The effect of alternate supply of shielding gases in austenite stainless steel GTA welding", *Journal of Materials Processing Technology*, Vol. 209 No. 10, doi: 10.1016/j.jmatprotec.2008.11.035.

Kang, G. and Luo, H. (2020), "Review on fatigue life prediction models of welded joint", *Acta Mechanica Sinica/Lixue Xuebao*, doi: 10.1007/s10409-020-00957-0.

Kannan, T. and Murugan, N. (2006), "Effect of flux cored arc welding process parameters on duplex stainless steel clad quality", *Journal of Materials Processing Technology*, Vol. 176 No. 1–3, doi: 10.1016/j.jmatprotec.2006.03.157.

Karci, F., Kaçar, R. and Gündüz, S. (2009), "The effect of process parameter on the properties of spot welded cold deformed AISI304 grade austenitic stainless steel", *Journal of Materials Processing Technology*, Vol. 209 No. 8, doi: 10.1016/j.jmatprotec.2008.09.030.

Karlsson, L. (2012), "Welding duplex stainless steels - A review of current recommendations", *Welding in the World*, Vol. 56 No. 5–6, doi: 10.1007/bf03321351.

Kashiwar, A., Vennela, N.P., Kamath, S.L. and Khatirkar, R.K. (2012), "Effect of solution annealing temperature on precipitation in 2205 duplex stainless steel", *Materials Characterization*, doi: 10.1016/j.matchar.2012.09.008.

Keskitalo, M., Sundqvist, J., Mäntyjärvi, K., Powell, J. and Kaplan, A.F.H. (2015), "The Influence of Shielding Gas and Heat Input on the Mechanical Properties of Laser Welds in Ferritic Stainless Steel", *Physics Procedia*, Vol. 78, doi: 10.1016/j.phpro.2015.11.032.

Khan, M.M.A., Romoli, L., Fiaschi, M., Dini, G. and Sarri, F. (2012), "Laser beam welding of dissimilar stainless steels in a fillet joint configuration", *Journal of Materials Processing Technology*, Vol. 212 No. 4, pp. 856–867, doi: 10.1016/j.jmatprotec.2011.11.011.

Kim, D., Chung, W. and Shin, B.H. (2023), "Effects of the Volume Fraction of the Secondary Phase after Solution Annealing on Electrochemical Properties of Super Duplex Stainless Steel UNS S32750", *Metals*, doi: 10.3390/met13050957.

Kim, Y.H., Kim, K.Y. and Lee, Y.D. (2004), "Nitrogen-alloyed, metastable austenitic stainless steel for automotive structural applications", *Materials and Manufacturing Processes*, doi: 10.1081/AMP-120027498.

Kratochvil, M.J., Seymour, A.J., Li, T.L., Paşca, S.P., Kuo, C.J. and Heilshorn, S.C. (2019), "Engineered materials for organoid systems", *Nature Reviews Materials*, doi: 10.1038/s41578-019-0129-9.

Kumar, R., Ramesh Mevada, N., Rathore, S., Agarwal, N., Rajput, V. and Barad, A.S. (2017), "Experimental Investigation and Optimization of TIG Welding Parameters on Aluminum 6061 Alloy Using Firefly Algorithm", *IOP Conference Series: Materials Science and Engineering*, doi: 10.1088/1757-899x/225/1/012153.

Kumar, R.R., Singh, R.K., Anoop, C.R., Das, R., Narayana Murty, S.V.S., Thomas Tharian, K. and Alex, A. (2022), "Influence of Filler Metal on the Microstructure and Mechanical Properties of 316Ti–15-5 PH Stainless Steel Weld Joints", *Journal*

of Materials Engineering and Performance, Vol. 31 No. 12, doi: 10.1007/s11665-022-07000-2.

Kumar, S., Chaudhari, G.P., Nath, S.K. and Basu, B. (2012), "Effect of preheat temperature on weldability of martensitic stainless steel", *Materials and Manufacturing Processes*, Vol. 27 No. 12, doi: 10.1080/10426914.2012.700150.

Kumar, S. and Shahi, A.S. (2011), "Effect of heat input on the microstructure and mechanical properties of gas tungsten arc welded AISI 304 stainless steel joints", *Materials and Design*, Vol. 32 No. 6, pp. 3617–3623, doi: 10.1016/j.matdes.2011.02.017.

Kurtis, K.E. (2015), "Innovations in cement-based materials: Addressing sustainability in structural and infrastructure applications", *MRS Bulletin*, Vol. 40 No. 12, doi: 10.1557/mrs.2015.279.

Kutelu, B.J., Seidu, S.O., Eghabor, G.I. and Ibitoye, A.I. (2018), "Review of GTAW Welding Parameters", *Journal of Minerals and Materials Characterization and Engineering*, doi: 10.4236/jmmce.2018.65039.

Kutty, T.R.G. and Ganguly, C. (1992), "Indentation technique for evaluation of hot hardness and creep of SS 316 end-plug welds of nuclear, fuel pins", *Journal of Materials Science*, doi: 10.1007/BF01197640.

Lakshminarayanan, A.K. and Balasubramanian, V. (2012), "Assessment of sensitization resistance of AISI 409M grade ferritic stainless steel joints using Modified Strauss test", *Materials and Design*, Vol. 39, doi: 10.1016/j.matdes.2012.02.038.

Lakshminarayanan, A.K., Balasubramanian, V. and Madhusudhan Reddy, G. (2012), "On the fatigue behaviour of electron beam and gas tungsten arc weldments of 409M grade ferritic stainless steel", *Materials and Design*, doi: 10.1016/j.matdes.2011.10.010.

Lakshminarayanan, A.K., Shanmugam, K. and Balasubramanian, V. (2009), "Effect of

Autogenous Arc Welding Processes on Tensile and Impact Properties of Ferritic Stainless Steel Joints", *Journal of Iron and Steel Research International*, Gangtie Yanjiu Xuebao, Vol. 16 No. 1, pp. 62–68, doi: 10.1016/S1006-706X(09)60012-1.

Lee, K.J., Chun, M.S., Kim, M.H. and Lee, J.M. (2009), "A new constitutive model of austenitic stainless steel for cryogenic applications", *Computational Materials Science*, doi: 10.1016/j.commatsci.2009.06.003.

Li, L., Du, Z., Sheng, X., Zhao, M., Song, L., Han, B. and Li, X. (2022), "Comparative analysis of GTAW+SMAW and GTAW welded joints of duplex stainless steel 2205 pipe", *International Journal of Pressure Vessels and Piping*, doi: 10.1016/j.ijpvp.2022.104748.

Li, N., Yan, H., Wang, X., Xia, L., Zhu, Y., Li, Y. and Jiang, Z. (2023), "Effect of Copper on Microstructure and Corrosion Resistance of Hot Rolled 301 Stainless Steel", *Metals*, doi: 10.3390/met13010170.

de Lima-Neto, P., Farias, J.P., Herculano, L.F.G., de Miranda, H.C., Araújo, W.S., Jorcin, J.B. and Pébère, N. (2008), "Determination of the sensitized zone extension in welded AISI 304 stainless steel using non-destructive electrochemical techniques", *Corrosion Science*, doi: 10.1016/j.corsci.2007.07.014.

Lippold, J.C. (2014), *Welding Metallurgy and Weldability*, *Welding Metallurgy and Weldability*, Vol. 9781118230701, doi: 10.1002/9781118960332.

Liu, B., Jin, W., Lu, A., Liu, K., Wang, C. and Mi, G. (2020), "Optimal design for dual laser beam butt welding process parameter using artificial neural networks and genetic algorithm for SUS316L austenitic stainless steel", *Optics and Laser Technology*, doi: 10.1016/j.optlastec.2019.106027.

Liu, S., Yang, Y., Cao, Y. and Xie, N. (2013), "A summary on the research of GRA models", *Grey Systems*, doi: 10.1108/20439371311293651.

Liu, X., Liu, L., Sui, F., Bi, H., Chang, E. and Li, M. (2020), "Influence of Cu on the

microstructure and corrosion resistance of cold-rolled type 204 stainless steels", *Journal of Solid State Electrochemistry*, Vol. 24 No. 5, doi: 10.1007/s10008-020-04614-1.

Liu, Z.M., Cui, S.L., Luo, Z., Zhang, C.Z., Wang, Z.M. and Zhang, Y.C. (2016), "Plasma arc welding: Process variants and its recent developments of sensing, controlling and modeling", *Journal of Manufacturing Processes*, doi: 10.1016/j.jmapro.2016.04.004.

Lo, K.H., Shek, C.H. and Lai, J.K.L. (2009a), "Recent developments in stainless steels", *Materials Science and Engineering R: Reports*, doi: 10.1016/j.mser.2009.03.001.

Lo, K.H., Shek, C.H. and Lai, J.K.L. (2009b), "Recent developments in stainless steels", *Materials Science and Engineering R: Reports*, Elsevier BV, 29 May, doi: 10.1016/j.mser.2009.03.001.

Lot, R.T. (2013), "Pitting corrosion evaluation of austenitic stainless steel type 304 in acid chloride media", *Journal of Materials and Environmental Science*, Vol. 4 No. 4.

Lu, S., Fujii, H. and Nogi, K. (2009), "Arc ignitability, bead protection and weld shape variations for He-Ar-O2 shielded GTA welding on SUS304 stainless steel", *Journal of Materials Processing Technology*, Vol. 209 No. 3, doi: 10.1016/j.jmatprotec.2008.03.043.

Mandal, P., Kumar Chanda, U. and Roy, S. (2018), "A review of corrosion resistance method on stainless steel bipolar plate", *Materials Today: Proceedings*, Vol. 5, doi: 10.1016/j.matpr.2018.06.111.

Miller Welds. (2018), "Guidelines For Gas Metal Arc Welding (GMAW)", *Miller Electric Mfg. LLC*.

Mohanty, A., Gangopadhyay, S. and Thakur, A. (2016), "On Applicability of Multilayer Coated Tool in Dry Machining of Aerospace Grade Stainless Steel", *Materials and*

Manufacturing Processes, doi: 10.1080/10426914.2015.1070413.

Morita, T., Hirano, Y., Asakura, K., Kumakiri, T., Ikenaga, M. and Kagaya, C. (2012), "Effects of plasma carburizing and DLC coating on friction-wear characteristics, mechanical properties and fatigue strength of stainless steel", *Materials Science and Engineering A*, Vol. 558, doi: 10.1016/j.msea.2012.08.011.

Moteshakker, A. and Danaee, I. (2016), "Microstructure and Corrosion Resistance of Dissimilar Weld-Joints between Duplex Stainless Steel 2205 and Austenitic Stainless Steel 316L", *Journal of Materials Science and Technology*, doi: 10.1016/j.jmst.2015.11.021.

Moura, V.S., Lima, L.D., Pardal, J.M., Kina, A.Y., Corte, R.R.A. and Tavares, S.S.M. (2008), "Influence of microstructure on the corrosion resistance of the duplex stainless steel UNS S31803", *Materials Characterization*, doi: 10.1016/j.matchar.2007.09.002.

Mourad, M.M., Saudi, H.A., Eissa, M.M., Hassaan, M.Y. and Abdel-Latif M, A. (2021), "Modified austenitic stainless-steel alloys for sheilding nuclear reactors", *Progress in Nuclear Energy*, Vol. 142, doi: 10.1016/j.pnucene.2021.104009.

Muwila, A. and Papo, M.J. (2007), "A more corrosion resistant Hercules^{TM} alloy", *Journal of the Southern African Institute of Mining and Metallurgy*.

Nage, D.D., Raja, V.S. and Raman, R. (2006), "Effect of nitrogen addition on the microstructure and mechanical behavior of 317L and 904L austenitic stainless steel welds", *Journal of Materials Science*, Vol. 41 No. 7, doi: 10.1007/s10853-006-3150-5.

Nassour, A., Bose, W.W. and Spinelli, D. (2001), "Creep properties of austenitic stainless-steel weld metals", *Journal of Materials Engineering and Performance*, doi: 10.1361/105994901770344566.

Norrish, J. (2017), "Recent gas metal arc welding (GMAW) process developments: the

implications related to international fabrication standards", *Welding in the World*, doi: 10.1007/s40194-017-0463-8.

O'Brien, A. (2011), "Welding Handbook, Volume 4 - Materials and Applications, Part 1 (9th Edition)", *Welding Handbook, Volume 4 - Materials and Applications, Part 1 (9th Edition)*.

Obeid, O., Leslie, A.J. and Olabi, A.G. (2022), "Influence of girth welding material on thermal and residual stress fields in welded lined pipes", *International Journal of Pressure Vessels and Piping*, Vol. 200, doi: 10.1016/j.ijpvp.2022.104777.

Omar, M. and Soltan, H. (2020), "A framework for welding process selection", *SN Applied Sciences*, doi: 10.1007/s42452-020-2144-2.

P. Chauhan and P. Panchal. (2016), "A Review on Activated Gas Tungsten Arc Welding (A-GTAW) 1", *International Journal of Scientific Development and Research*.

Pandey, P.K., Rathi, R. and Verma, J. (2022), "Recent Trends in Weldability and Corrosion Behavior of Low Nickel Stainless Steels", *Lecture Notes in Mechanical Engineering*, doi: 10.1007/978-981-16-3135-1_21.

Pandey, P.K., Singh, M., Rathi, R. and Verma, J. (2023), "Analysis and optimization of welding techniques for austenitic stainless steel using grey relational analysis", *International Journal on Interactive Design and Manufacturing*, doi: 10.1007/s12008-023-01445-y.

Park, J.H. and Kang, Y. (2017), "Inclusions in Stainless Steels − A Review", *Steel Research International*, doi: 10.1002/srin.201700130.

Peguet, L., Malki, B. and Baroux, B. (2007), "Influence of cold working on the pitting corrosion resistance of stainless steels", *Corrosion Science*, doi: 10.1016/j.corsci.2006.08.021.

Pistorius, P.C. and Du Toit, M. (n.d.). *LOW-NICKEL AUSTENITIC STAINLESS STEELS: METALLURGICAL CONSTRAINTS*.

Plaut, R.L., Herrera, C., Escriba, D.M., Rios, P.R. and Padilha, A.F. (2007), "A Short review on wrought austenitic stainless steels at high temperatures: Processing, microstructure, properties and performance", *Materials Research*, doi: 10.1590/S1516-14392007000400021.

Potgieter, J.H., Adams, F. V, Maledi, N., Van Der Merwe, J. and Olubambi, P.A. (2012), *CORROSION RESISTANCE OF TYPE 444 FERRITIC STAINLESS STEEL IN ACIDIC CHLORIDE MEDIA*, *Journal Of Chemistry And Material Sciences*, Vol. 2.

Price, D., Morgan, P. and Morris, P. (2014), "Harry Brearley stainless steel centenary conference and exhibition, June 2013", *Ironmaking and Steelmaking*, doi: 10.1179/0301923314Z.000000000288.

Raj, S. and Biswas, P. (2022), "Mechanical and microstructural characterizations of friction stir welded dissimilar butt joints of Inconel 718 and AISI 204Cu austenitic stainless steel", *Materials Characterization*, Vol. 185, doi: 10.1016/j.matchar.2022.111763.

Rathi, R., Khanduja, D. and Sharma, S.K. (2017), "A fuzzy-MADM based approach for prioritising Six Sigma projects in the Indian auto sector", *International Journal of Management Science and Engineering Management*, doi: 10.1080/17509653.2016.1154486.

Ravitej, S. V., Murthy, M. and Krishnappa, M. (2018), "Review paper on optimization of process parameters in turning Custom 465® precipitation hardened stainless steel", *Materials Today: Proceedings*, Vol. 5, doi: 10.1016/j.matpr.2018.01.066.

Rezaei, M.A. and Naffakh-Moosavy, H. (2018), "The effect of pre-cold treatment on microstructure, weldability and mechanical properties in laser welding of superalloys", *Journal of Manufacturing Processes*, doi: 10.1016/j.jmapro.2018.06.018.

Rossi, B. (2014), "Discussion on the use of stainless steel in constructions in view of sustainability", *Thin-Walled Structures*, Vol. 83, doi: 10.1016/j.tws.2014.01.021.

Rückert, G., Huneau, B. and Marya, S. (2007), "Optimizing the design of silica coating for productivity gains during the TIG welding of 304L stainless steel", *Materials and Design*, Vol. 28 No. 9, doi: 10.1016/j.matdes.2006.09.021.

Saha Podder, A. and Bhanja, A. (2013), "Applications of stainless steel in automobile industry", *Advanced Materials Research*, Vol. 794, doi: 10.4028/www.scientific.net/AMR.794.731.

Saha, S. and Das, S. (2018), "Investigation on the Effect of Activating Flux on Tungsten Inert Gas Welding of Austenitic Stainless Steel Using AC Polarity", *Indian Welding Journal*, Vol. 51 No. 2, doi: 10.22486/iwj.v51i2.170313.

Sahoo, A. and Tripathy, S. (2019), "Development in plasma arc welding process: A review", *Materials Today: Proceedings*, Vol. 41, doi: 10.1016/j.matpr.2020.09.562.

Sahu, J.K., Krupp, U., Ghosh, R.N. and Christ, H.J. (2009), "Effect of 475 °C embrittlement on the mechanical properties of duplex stainless steel", *Materials Science and Engineering: A*, doi: 10.1016/j.msea.2009.01.039.

Sakthivel, T., Vasudevan, M., Laha, K., Parameswaran, P., Chandravathi, K.S., Mathew, M.D. and Bhaduri, A.K. (2011), "Comparison of creep rupture behaviour of type 316L(N) austenitic stainless steel joints welded by TIG and activated TIG welding processes", *Materials Science and Engineering A*, doi: 10.1016/j.msea.2011.05.052.

Samanta, S.K., Mitra, S.K. and Pal, T.K. (2008), "Microstructure and oxidation characteristics of laser and GTAW weldments in austenitic stainless steels", *Journal of Materials Engineering and Performance*, doi: 10.1007/s11665-008-9235-3.

Sánchez-Cabrera, V.M., Rubio-González, C., Ruíz-Vela, J.I. and Ramírez-Baltazar, C. (2007), "Effect of preheating temperature and filler metal type on the microstructure, fracture toughness and fatigue crack growth of stainless steel welded joints", *Materials Science and Engineering: A*, Vol. 452–453, doi: 10.1016/j.msea.2006.10.161.

Sanders, D.G. (2004), “Reinforced ceramic dies for superplastic forming operations”, *Journal of Materials Engineering and Performance*, Vol. 13, doi: 10.1361/10599490421376.

Sarkari Khorrami, M., Mostafaei, M.A., Pouraliakbar, H. and Kokabi, A.H. (2014), “Study on microstructure and mechanical characteristics of low-carbon steel and ferritic stainless steel joints”, *Materials Science and Engineering A*, Elsevier BV, Vol. 608, pp. 35–45, doi: 10.1016/j.msea.2014.04.065.

Sarolkar, A. and Kolhe, K. (2017), “A Review of (GTAW) Gas Tungsten Arc Welding and its Parameters for Joining Aluminium Alloy”, *Internation Journal for Science and Advance Research In Technology*.

Sathiya, P., Aravindan, S. and Noorul Haq, A. (2007), “Effect of friction welding parameters on mechanical and metallurgical properties of ferritic stainless steel”, *International Journal of Advanced Manufacturing Technology*, Vol. 31 No. 11–12, doi: 10.1007/s00170-005-0285-5.

Schmitt, J.H. and Iung, T. (2018), “New developments of advanced high-strength steels for automotive applications”, *Comptes Rendus Physique*, doi: 10.1016/j.crhy.2018.11.004.

Schulz, Z., Whitcraft, P. and Wachowiak, D. (2014), “Availability and economics of using duplex stainless steels”, *NACE - International Corrosion Conference Series*.

Şenol, M. and Çam, G. (2023), “Investigation into microstructures and properties of AISI 430 ferritic steel butt joints fabricated by GMAW”, *International Journal of Pressure Vessels and Piping*, doi: 10.1016/j.ijpvp.2023.104926.

Siddall, J.N. (2019), “WELDING, BRAZING, AND SOLDERING”, *Mechanical Design*, doi: 10.3138/9781487579890-121.

Silva, C.C., Farias, J.P., Miranda, H.C., Guimarães, R.F., Menezes, J.W.A. and Neto, M.A.M. (2008), “Microstructural characterization of the HAZ in AISI 444 ferritic

stainless steel welds", *Materials Characterization*, Vol. 59 No. 5, pp. 528–533, doi: 10.1016/j.matchar.2007.03.011.

Singh, M. and Rathi, R. (2022), "Empirical Investigation of Lean Six Sigma Enablers and Barriers in Indian MSMEs by Using Multi-Criteria Decision Making Approach", *EMJ - Engineering Management Journal*, Taylor and Francis Ltd., Vol. 34 No. 3, pp. 475–496, doi: 10.1080/10429247.2021.1952020.

Singh, M., Rathi, R. and Singh Kaswan, M. (2022), "Capacity utilization in industrial sector: a structured review and implications for future research", *World Journal of Engineering*, doi: 10.1108/WJE-09-2020-0447.

Šmíd, M., Kuběna, I., Jambor, M. and Fintová, S. (2021), "Effect of solution annealing on low cycle fatigue of 304L stainless steel", *Materials Science and Engineering: A*, Vol. 824, p. 141807, doi: https://doi.org/10.1016/j.msea.2021.141807.

Sohrabi, M.J., Naghizadeh, M. and Mirzadeh, H. (2020), "Deformation-induced martensite in austenitic stainless steels: A review", *Archives of Civil and Mechanical Engineering*, Springer Science and Business Media Deutschland GmbH, 1 December, doi: 10.1007/s43452-020-00130-1.

Srikanth, B., Goutham, R., Badri Narayan, R., Ramprasath, A., Gopinath, K.P. and Sankaranarayanan, A.R. (2017), "Recent advancements in supporting materials for immobilised photocatalytic applications in waste water treatment", *Journal of Environmental Management*, doi: 10.1016/j.jenvman.2017.05.063.

Tadepalli, L.D., Gosala, A.M., Kondamuru, L., Bairi, S.C., Subbiah, R. and Singh, S.K. (2019), "A review on effects of nitriding of AISI409 ferritic stainless steel", *Materials Today: Proceedings*, Vol. 26, doi: 10.1016/j.matpr.2020.01.299.

Taiwade, R. V., Shukla, R., Vashishtha, H., Ingle, A. V. and Dayal, R.K. (2013), "Effect of grain size on degree of sensitization of chrome-manganese stainless steel", *ISIJ International*, doi: 10.2355/isijinternational.53.2206.

Talha, M., Behera, C.K. and Sinha, O.P. (2013), "A review on nickel-free nitrogen containing austenitic stainless steels for biomedical applications", *Materials Science and Engineering C*, doi: 10.1016/j.msec.2013.06.002.

Tan, H., Jiang, Y., Deng, B., Sun, T., Xu, J. and Li, J. (2009), "Effect of annealing temperature on the pitting corrosion resistance of super duplex stainless steel UNS S32750", *Materials Characterization*, doi: 10.1016/j.matchar.2009.04.009.

Tavares, S.S.M., Pardal, J.M., Lima, L.D., Bastos, I.N., Nascimento, A.M. and de Souza, J.A. (2007), "Characterization of microstructure, chemical composition, corrosion resistance and toughness of a multipass weld joint of superduplex stainless steel UNS S32750", *Materials Characterization*, Vol. 58 No. 7, doi: 10.1016/j.matchar.2006.07.006.

Tavares, S.S.M., de Souza, J.A., Herculano, L.F.G., de Abreu, H.F.G. and de Souza, C.M. (2008), "Microstructural, magnetic and mechanical property changes in an AISI 444 stainless steel aged in the 560 °C to 800 °C range", *Materials Characterization*, Vol. 59 No. 2, pp. 112–116, doi: 10.1016/j.matchar.2006.11.002.

Tembhurkar, C., Kataria, R., Ambade, S., Verma, J., Sharma, A. and Sarkar, S. (2021), "Effect of Fillers and Autogenous Welding on Dissimilar Welded 316L Austenitic and 430 Ferritic Stainless Steels", *Journal of Materials Engineering and Performance*, doi: 10.1007/s11665-020-05395-4.

Teodorescu, M., Bercea, M. and Morariu, S. (2019), "Biomaterials of PVA and PVP in medical and pharmaceutical applications: Perspectives and challenges", *Biotechnology Advances*, doi: 10.1016/j.biotechadv.2018.11.008.

"The history of stainless steel". (2011), *Choice Reviews Online*, Vol. 48 No. 07, doi: 10.5860/choice.48-3837.

Thirumalaikumarasamy, D., Shanmugam, K. and Balasubramanian, V. (2014), "Comparison of the corrosion behaviour of AZ31B magnesium alloy under immersion test and potentiodynamic polarization test in NaCl solution", *Journal of*

Magnesium and Alloys, doi: 10.1016/j.jma.2014.01.004.

Thomas, M., Prakash, R. V., Ganesh Sundara Raman, S. and Vasudevan, M. (2018), "High Temperature Fatigue Crack Growth Rate Studies in Stainless Steel 316L(N) Welds Processed by A-TIG and MP-TIG Welding.", *MATEC Web of Conferences*, Vol. 165, doi: 10.1051/matecconf/201816521014.

Du Toit, M., Van Rooyen, G.T. and Smith, D. (2007), "An overview of the heat-affected zone sensitization and stress corrosion cracking behaviour of 12 % chromium type 1.4003 ferritic stainless steel", *Welding in the World*, Vol. 51 No. 9–10, doi: 10.1007/BF03266599.

Turnbull, A. and Griffiths, A. (2003), "Corrosion and cracking of weldable 13 wt-%Cr martensitic stainless steels for application in the oil and gas industry", *Corrosion Engineering Science and Technology*, doi: 10.1179/147842203225001432.

Vashishtha, H., Taiwade, R. V., Sharma, S. and Patil, A.P. (2017), "Effect of welding processes on microstructural and mechanical properties of dissimilar weldments between conventional austenitic and high nitrogen austenitic stainless steels", *Journal of Manufacturing Processes*, doi: 10.1016/j.jmapro.2016.10.008.

Vashishtha, H., Taiwade, R.V., Khatirkar, R.K., Ingle, A.V. and Dayal, R.K. (2014), "Welding behaviour of low nickel chrome-manganese stainless steel", *ISIJ International*, Vol. 54 No. 6, doi: 10.2355/isijinternational.54.1361.

Vasudevan, M. (2017), "Effect of A-TIG Welding Process on the Weld Attributes of Type 304LN and 316LN Stainless Steels", *Journal of Materials Engineering and Performance*, Vol. 26 No. 3, doi: 10.1007/s11665-017-2517-x.

Venkatraman, M., Pavitra, K., Jana, V. and Kachwala, T. (2013), "Manufacturing and critical applications of stainless steel- an overview", *Advanced Materials Research*, Vol. 794, doi: 10.4028/www.scientific.net/AMR.794.163.

Verma, J. and Taiwade, R.V. (2016), "Dissimilar welding behavior of 22% Cr series

stainless steel with 316L and its corrosion resistance in modified aggressive environment", *Journal of Manufacturing Processes*, Elsevier Ltd, Vol. 24, pp. 1–10, doi: 10.1016/j.jmapro.2016.07.001.

Verma, J. and Taiwade, R.V. (2017), "Effect of welding processes and conditions on the microstructure, mechanical properties and corrosion resistance of duplex stainless steel weldments—A review", *Journal of Manufacturing Processes*, Elsevier Ltd, 1 January, doi: 10.1016/j.jmapro.2016.11.003.

Vimal, K.E.K., Vinodh, S. and Raja, A. (2015), "Modelling, assessment and deployment of strategies for ensuring sustainable shielded metal arc welding process - A case study", *Journal of Cleaner Production*, Vol. 93, doi: 10.1016/j.jclepro.2015.01.049.

Vinoth Jebaraj, A., Ajaykumar, L., Deepak, C.R. and Aditya, K.V.V. (2017), "Weldability, machinability and surfacing of commercial duplex stainless steel AISI2205 for marine applications – A recent review", *Journal of Advanced Research*, doi: 10.1016/j.jare.2017.01.002.

Vinoth Jebaraj, A., Sampath Kumar, T. and Manikandan, M. (2018), "Investigation of Structure Property Relationship of the Dissimilar Weld Between Austenitic Stainless Steel 316L and Duplex Stainless Steel 2205", *Transactions of the Indian Institute of Metals*, doi: 10.1007/s12666-018-1392-y.

Wang, H., Wang, K., Wang, W., Huang, L., Peng, P. and Yu, H. (2019), "Microstructure and mechanical properties of dissimilar friction stir welded type 304 austenitic stainless steel to Q235 low carbon steel", *Materials Characterization*, Vol. 155, doi: 10.1016/j.matchar.2019.109803.

Wang, L., Dong, C. fang, Man, C., Hu, Y. bo, Yu, Q. and Li, X. gang. (2021), "Effect of microstructure on corrosion behavior of high strength martensite steel—A literature review", *International Journal of Minerals, Metallurgy and Materials*, doi: 10.1007/s12613-020-2242-6.

Węglowski, M.S., Błacha, S. and Phillips, A. (2016), "Electron beam welding -

Techniques and trends - Review", *Vacuum*, Vol. 130, doi: 10.1016/j.vacuum.2016.05.004.

Welding, A.R.C. (2003), "Guidelines To Gas Tungsten Arc Welding", *Current*.

"Welding metallurgy and weldability of stainless steels". (2005), *Choice Reviews Online*, Vol. 43 No. 04, doi: 10.5860/choice.43-2230.

Woo, I. and Kikuchi, Y. (2002), "Weldability of high nitrogen stainless steel", *ISIJ International*, doi: 10.2355/isijinternational.42.1334.

Wu, C.S., Wang, L., Ren, W.J. and Zhang, X.Y. (2014), "Plasma arc welding: Process, sensing, control and modeling", *Journal of Manufacturing Processes*, Vol. 16 No. 1, doi: 10.1016/j.jmapro.2013.06.004.

Wu, W., Hu, S. and Shen, J. (2015), "Microstructure, mechanical properties and corrosion behavior of laser welded dissimilar joints between ferritic stainless steel and carbon steel", *Materials and Design*, Elsevier Ltd, Vol. 65, pp. 855–861, doi: 10.1016/j.matdes.2014.09.064.

Yadav, G., Seth, D. and Desai, T.N. (2018), "Application of hybrid framework to facilitate lean six sigma implementation: a manufacturing company case experience", *Production Planning and Control*, doi: 10.1080/09537287.2017.1402134.

Yan, H., Bi, H., Li, X. and Xu, Z. (2009a), "Precipitation and mechanical properties of Nb-modified ferritic stainless steel during isothermal aging", *Materials Characterization*, Vol. 60 No. 3, doi: 10.1016/j.matchar.2008.09.001.

Yan, H., Bi, H., Li, X. and Xu, Z. (2009b), "Effect of two-step cold rolling and annealing on texture, grain boundary character distribution and r-value of Nb + Ti stabilized ferritic stainless steel", *Materials Characterization*, Vol. 60 No. 1, doi: 10.1016/j.matchar.2008.05.006.

Yan, X.F., Hassanein, M.F., Wang, F. and He, M.N. (2021), "Behaviour and design of

high-strength concrete-filled rectangular ferritic stainless steel tubular (CFFSST) short columns subjected to axial compression", *Engineering Structures*, doi: 10.1016/j.engstruct.2021.112611.

Yunlian, Q., Ju, D., Quan, H. and Liying, Z. (2000), "Electron beam welding, laser beam welding and gas tungsten arc welding of titanium sheet", *Materials Science and Engineering: A*, Vol. 280 No. 1, doi: 10.1016/S0921-5093(99)00662-0.

Zhang, W., Jiang, W., Zhao, X. and Tu, S.T. (2018), "Fatigue life of a dissimilar welded joint considering the weld residual stress: Experimental and finite element simulation", *International Journal of Fatigue*, Vol. 109, doi: 10.1016/j.ijfatigue.2018.01.002.

Zhu, Z., Ma, X., Wang, C., Mi, G. and Zheng, S. (2020), "The metallurgical behaviors and crystallographic characteristic on macro deformation mechanism of 316 L laser-MIG hybrid welded joint", *Materials and Design*, doi: 10.1016/j.matdes.2020.108893.

PUBLICATIONS

1) Pandey, P.K., Singh, M., Rathi, R. and Verma, J., 2023. Analysis and optimization of welding techniques for austenitic stainless steel using grey relational analysis. *International Journal on Interactive Design and Manufacturing (IJIDeM)*, pp.1-9. (Indexing: ESCI, Impact factor: 2.1)
2) Pandey, P., Rathi, R., Singh, M. and Verma, J., 2024. Experimental analysis on microstructure, mechanical properties, and corrosion behavior of TIG welded AISI 444 ferritic stainless steels. *Engineering Solid Mechanics*, *12*(1), pp.93-102. (Indexing: SCOPUS, SJR: 0.40)
3) Pandey, P.K., Rathi, R. and Verma, J., 2023, September. Welding behavior of dissimilar joints of stainless steel: A metadata study. In *AIP Conference Proceedings* (Vol. 2800, No. 1). AIP Publishing. (Indexing: SCOPUS, SJR: 0.16)
4) Pandey, P.K., Rathi, R. and Verma, J., 2022. Recent trends in weldability and corrosion behavior of low nickel stainless steels. In *Recent Trends in Industrial and Production Engineering: Select Proceedings of ICAST 2020* (pp. 193-203). Springer Singapore. (Indexing: SCOPUS)
5) Pandey, P.K., Singh, M., Rathi, R. and Verma, J., 2024. "Comparative investigations on microstructure evolution, mechanical properties, and corrosion behavior of welded joints of Low Nickel Stainless steels AISI444 and J204 Cu", *International Journal on Interactive Design and Manufacturing (IJIDeM)*, (Indexing: ESCI, Impact factor: 2.1)

APPENDIX

Questionnaire: Expert Opinion to Rate Welding Techniques for Austenitic Stainless Steel

1. **Name of the Participant:** _____
2. **Designation:** _____
3. **Organization Name:** _____
4. **Location:** _____
5. **Work Experience:** _____

Welding Techniques/ Alternatives	Selection Criteria						
	Sound Weld	HAZ	Weld Suitability in Various Positions	Joint Configuration	Equipment Portability	Weld Penetration	Capital Cost
SMAW							
FCAW							
GMAW							
SAW							
EBW							
PAW							
TIG							
LBW							

Scale

5 = Highly Significant

4 = Significant

3 = Neutral

2 = Less Significant

1 = Not Significant

SMAW = Shielded Metal Arc Welding

FCAW = Flux-Cored Arc Welding

GMAW = Gas Metal Arc Welding

SAW = Submerged Arc Welding

EBW = Electron Beam Welding

PAW = Plasma Arc Welding

TIG = Tungsten Inert Gas Welding

LBW = Laser Beam Welding

HAZ = Heat Affected Zone